AN ABSTRACT OF THE DISSERTATION OF

Roberta P. M. Fernandes for the degree of Doctor of Philosophy in Pharmacy presented on March 11, 2005.
Title: Studies on 1-Deoxy-D-Xylulose 5-Phosphate Reductoisomerase from *Synechocystis sp.* PCC6803: Characterization of Mutants and Inhibitors.

Abstract approved:

Redacted for privacy

Philip J. Proteau

In recent years, the methyl erythritol phosphate (MEP) pathway to isoprenoids has been the subject of intensive research. The interest is because isoprenoids have important roles in many cellular processes essential for the survival of several pathogenic organisms, making the inhibition of this pathway an attractive target for the drug discovery. The second enzyme in the MEP pathway is 1-deoxy-D-xylulose 5-phosphate reductoisomerase (DXR). DXR is a promising target for the development of new antibiotics, antimalarials and herbicides. The overall objective of this research was a better understanding of DXR by using site-directed mutagenesis guided by crystal structure analysis and inhibition studies.

One set of mutants was designed to expand the selectivity of DXR. An analog of DXP, 1,2-dideoxy-D-threo-3-hexulose 6-phosphate (1-methyl-DXP or Me-DXP), that differs from DXP by having an ethyl ketone, rather than a methyl ketone, was reported to be a weak competitive inhibitor. Using the x-ray crystal structures of DXR as a guide, a highly conserved tryptophan residue in the flexible loop was identified as a potential steric block to the use of this analog as a substrate. Four mutants of *Synechocystis sp.* PCC6803 DXR, named W204F, W204L, W204V and W204A, were prepared and characterized. The W204F mutant was found to utilize the analog Me-DXP as a substrate.

The roles of amino acids residues shown to be in the DXR active site in the available *E. coli* crystal structures were also studied. Mutants at the positions D152,

S153, E154, H155, M206 and E233, were prepared. The kinetic characterization of these mutants showed that the amino acid substitution, conservative or not, in these residues reduced the DXR catalytic activity, confirming that these are key amino acids responsible for the DXR catalytic efficiency.

Inhibition studies of the *E. coli* DXR by fosmidomycin in the presence of Co^{2+}, Mg^{2+} and Mn^{2+} showed that this inhibition is not dependent on a specific divalent cation. Inhibition of the *Synechocystis sp.* PCC6803 DXR by fosmidomycin and its hydroxamate and FR 900098 analogs was conducted showing that these compound are potent inhibitors of this enzyme. Fosmidomycin and FR900098 have inhibition constants in the low nM range. In addition the patterns of the progress curves for fosmidomycin, its hydroxamate analog and FR900098 were shown to be prototypical for slow, tight-binding inhibitors, as was seen for these inhibitors with the *E. coli* enzyme.

Studies on 1-Deoxy-D-Xylulose 5-Phosphate Reductoisomerase from *Synechocystis sp.* PCC6803: Characterization of Mutants and Inhibitors.

by

Roberta P. M. Fernandes

A DISSERTATION

submitted to

Oregon State University

in partial fulfillment of
the requirements for the
degree of

Doctor of Philosophy

Presented March 11, 2005

Commencement June 2005

Doctor of Philosophy dissertation of Roberta P. M. Fernandes presented on March 11, 2005

APPROVED:

Redacted for privacy

Major Professor, representing Pharmacy

Redacted for privacy

Dean of the College of Pharmacy

Redacted for privacy

Dean of Graduate School

I understand that my dissertation will become part of the permanent collection of Oregon State University libraries. My signature below authorizes release of my dissertation to any reader upon request.

Redacted for privacy

Roberta P. M. Fernandes, Author

ACKNOWLEDGEMENTS

First of all, I am really grateful to my major advisor Dr. Phil Proteau for supporting me throughout this project. I am truly fortunate to have found an advisor who has taken so much interest in my research and academic dealing. I am indebted to him for all his effort and advice. I also want to thanks Dr. Mark Zabriskie for his help in many parts of my research. Dr. Mike Schimerlik is appreciated for his help in the inhibitors experiment. I also would like to thank Dr. Bill Gerwick and Dr. Taifo Mahmud for being part of my committee and Dr. Jeffrey Greenwood for being my graduate council representative. I would like to thanks the National Institutes of Health for funding this research, Conselho Nacional de Desenvolvimento Cientifico e Tecnologico (CNPq-Brazil) for my scholarship and Federal University of Sergipe for allowing me to come to OSU and financial support.

Thanks to all my colleagues David Blanchard, Donjung Kim, Qingmei Yao, Shiny Phaosiri, Younhi Woo, Gerwick's and Mahmud's lab members for their friendship. Dr. Xihou Yin and Laura Grochowski are thanked for being great lab partners, for the useful discussion everyday in the lab and their friendship. The College of Pharmacy staff is thanked for their technical support.

I would like to express my gratitude to my mother Maria, my parents in law Vera and Porfirio, and all my family for their support and always believing in me. Thanks to all the great friends I have met here in Corvallis. I want give a special thank you for my father Roberto that could not be here to see me getting this degree but always supported me and was proud of my accomplishments.

Above of all I would like to express my most sincere appreciation to my husband Marcelo for his continuous love, patient and support. A very special thanks for my son João, whose love and joy have given me the strength to pursue this degree.

CONTRIBUTION OF AUTHORS

Dr. Chanokporn Phaosiri performed the synthesis of 1-Me-DXP, synthesis of the ethylerythritol triacetate standard, and identified the turnover product described in Chapter Two. Ms. Qingmei Yao conducted the NMR analysis for the X5P experiment in Chapter Two.

TABLE OF CONTENTS

TABLE OF CONTENTS

LIST OF FIGURES

LIST OF FIGURES (continued)

LIST OF FIGURES (continued)

LIST OF FIGURES (continued)

LIST OF TABLES

LIST OF ABREVIATIONS

Ala	Alanine
ATP	Adenosine triphosphate
CDP	Cytidine diphosphate
CDP-ME	4-Diphosphocytidyl-2*C*-methylerythritol
CoA	Coenzyme A
CTP	Cytidine triphosphate
DMAPP	Dimethylallyl diphosphate
DTT	Dithiothreitol
DXP	1-Deoxy-D-xylulose-5-phosphate
DXR	1-Deoxy-D-xylulose 5-phosphate reductoisomerase
EST	Expressed sequence tag
FPP	Farnesyl diphosphate
G3P	D-glyceraldehyde 3-phosphate
GC/MS	Gas chromatography/ mass spectrometry
GGPP	Geranylgeranyl diphosphate
GPP	Geranyl diphosphate
His	Histidine
HMB-PP	1-Hydroxy-2-methyl-2-(E)-butenyl-4-diphosphate
HMG-CoA	3-Hydroxy-3-methylglutaryl-CoA
IPP	Isopentenyl diphosphate
IPTG	Isopropyl-β-D-thiogalactopyranose
kDa	Kilo daltons
Leu	Leucine
MecPP	2*C*-methyl-D-erythritol 2,4-cyclodiphosphate
Me-DXP	1-Methyl-DXP
MVA	Mevalonate
MVAPP	Mevalonic acid 5-diphosphate
NADPH	Reduced nicotinamide adenine dinucleotide phosphate
NMR	Nuclear magnetic resonance
ORF	Open reading frame
PMA	Phosphomolybdic acid
Ru5P	D-ribulose 5-phosphate
SDS-PAGE	Sodium dodecyl sulfate-polyacrylamide gel electrophoresis
TLC	Thin-layer chromatography
TPP	Thiamin diphosphate
Trp	Tryptophan
Val	Valine
X5P	D-xylulose 5-phosphate

LIST OF SCHEMES

Studies on 1-Deoxy-D-Xylulose 5-Phosphate reductoisomerase from *Synechocystis sp* PCC6803: Characterization of mutants and inhibitors

CHAPTER ONE

Biosynthesis of Isoprenoids

1. Isoprenoid Natural Products

Isoprenoids constitute the largest family of natural products with more than 35,000 naturally occurring compounds reported.[1] Isoprenoids, also known as terpenoids, are widespread among living organisms.[2] They represent a wide variety of essential molecules, such as plant hormones (gibberellins, abscisic acid), photosynthetic pigments (carotenoids and the phytyl side chain of chlorophyll), electron carriers (ubiquinone, plastoquinone), mediators of polysaccharide assembly (dolichol phosphate and bactoprenol phosphate), modification of proteins involved in membrane targeting and cycle regulation (prenylated proteins), steroid hormones, bile acids, and structural components of membranes (hopanoids and sterols).[3,4] These compounds are metabolically important for the survival of the organisms and are called primary metabolites (Figure 1.1).

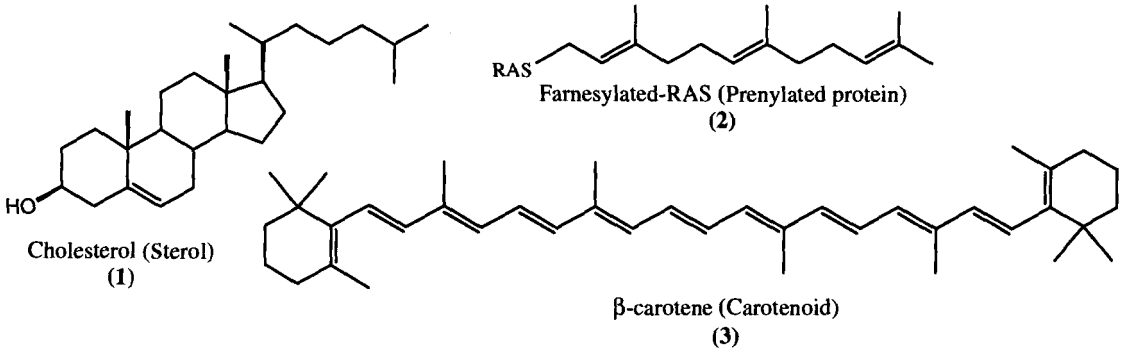

Figure 1.1. Examples of isoprenoid primary metabolites.

The isoprenoids with the most diverse structures are not essential for the organisms and may be considered secondary metabolites. Examples of these classes of

compounds include, mono-, sesqui- di- and triterpenes from plants, essential oils and resins, antibiotics, antitumor and antioxidants agents (Figure 1.2).[5,6] This last class of isoprenoids is especially abundant and diverse in plants.[3,7,8] These isoprenoid secondary metabolites are specific for a plant species and they play roles in communication and defense, for instance, as antibiotics (trichothecin), defense against pathogen attack (phytoalexins), repellents (camphor) and attractants for pollinators (geraniol (**4**)).[3,9] Other secondary metabolites do not have a known function for the plant, but they are medically useful. For example paclitaxel or Taxol® (**5**)[10] and artemesinin (**6**)[11] are antitumor and antimalarial agents, respectively.

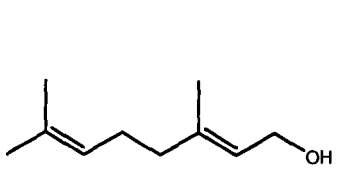

Geraniol
(**4**)

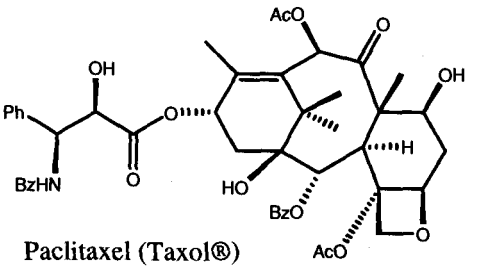

Paclitaxel (Taxol®)
(**5**)

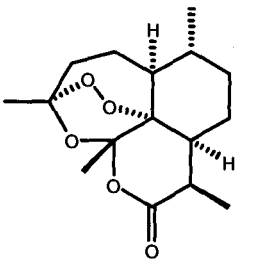

Artemesinin
(**6**)

Figure 1.2. Examples of isoprenoid secondary metabolites.

2. Isoprenoids biosynthesis

Despite their diversity of function and structure, isoprenoids are synthesized by condensations of two common five-carbon precursors, isopentenyl diphosphate (IPP) and its isomer, dimethylallyl diphosphate (DMAPP). IPP and DMAPP are also known as the biological isoprene units. Isoprene itself is the simplest isoprenoid known. An enzyme named isoprene synthase catalyzes the magnesium ion-dependent elimination of diphosphate from DMAPP to form isoprene (2-methyl-1,3-butadiene).[12,13,14]

Enzymes named prenyltransferases perform the condensation of DMAPP (**7**) and IPP (**8**) to generate the variable chain length products (Figure 1.3). These prenyltransferases are homodimers of 70-80 KDa that require either Mg^{2+} or Mn^{2+} for activity. The divalent metal ion binds the diphosphate of the allylic cosubstrate, to

make it a better leaving group, in the ionization step. This ionization leads to formation of a charge-stabilized allylic carbocation. Electrophilic addition to the double-bond of IPP generates a new carbocation intermediate that, after trans-elimination of a proton yields a new prenyl diphosphate five carbons larger.[3]

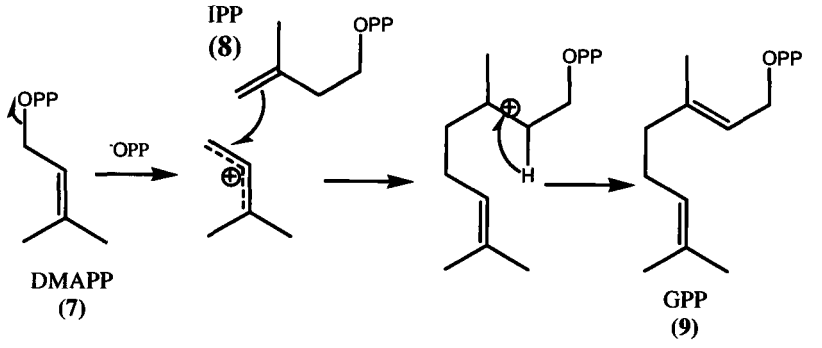

Figure 1.3. Prenyltransferase mechanism.

The first condensation of IPP and DMAPP generates geranyl diphosphate (**9**) (GPP; C10). The addition of one more IPP unit provides farnesyl diphosphate (FPP, C15), which can accept one more IPP unit generating geranylgeranyl diphosphate (GGPP; C20). The number of IPP units added, cyclization reactions, rearrangements and further oxidation of the carbon skeletons are responsible for the enormous diversity of structure.[8]

The most common isoprenoid derivatives are oxygenated, such as alcohols, epoxides, aldehydes, ketones, acids and lactones, but halogen-, sulfur-, and nitrogen-containing forms and composite structures (e.g. esters, glycosides, isoprenoid alkaloids and prenylated aromatics) have been described.[15] The biosynthesis of isoprenoids (Figure 1.4) can be conveniently divided into four major processes.[3] The first step involves the formation of IPP and DMAPP. Then prenyltransferases perform condensations of IPP and DMAPP, forming the C10, C15 and C20 isoprenoids as described above. In a third step the C10 intermediate can be used as side chain of monoterpenoids, while C15 and C20 isoprenoids may self-condense to form the C30 and C40, respectively. The C30 and C40 condensation products squalene and phytoene are the precursors of sterols and carotenoids, respectively. The C10, C15,

and C20 intermediates may also undergo cyclization by enzymes called Terpene cyclases or synthases to create the basic parent skeleton of the various terpenoid families. Finally, other transformations such as oxidations, reductions, isomerizations, conjugation with proteins, aromatic compounds and alkaloids, are carried out to form unique isoprenoids. Isoprenoids are classified according to the number of units (IPP and/or DMAPP) they contain: hemiterpenes (one unit) monoterpenes (two units), sesquiterpenes (three units), diterpenes (four units), sesterterpenes (five units), triterpenes (six units), tetraterpenes (eight units), and polyterpenes (more than eight units).

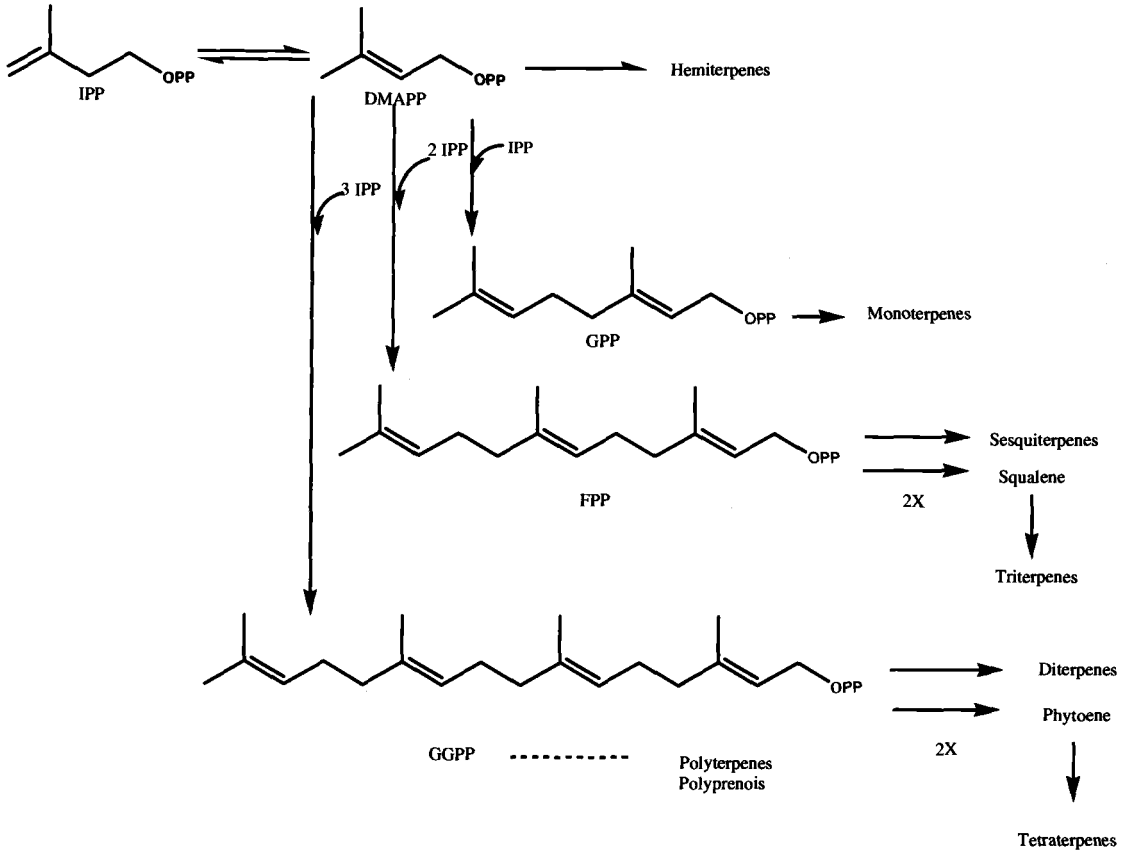

Figure 1.4. Overview of the isoprenoid skeleton biosynthesis.[3]

3. *The mevalonate pathway for biosynthesis of IPP*

Studies by Bloch, Cornforth and Lynen aimed at understanding cholesterol biosynthesis established that mevalonate (MVA) is the precursor of IPP and DMAPP

in yeast and animal cells. [9, 16] Incorporation of labeled MVA into various isoprenoids confirmed MVA as aprecursor of these compounds. Because many isoprenoids are biologically important, the biosynthesis of these compounds was the subject of extensive research. The MVA pathway (Figure 1.5) starts with the formation of acetoacetyl-CoA (**10**) by the condensation of two molecules of acetyl-CoA (**11**).

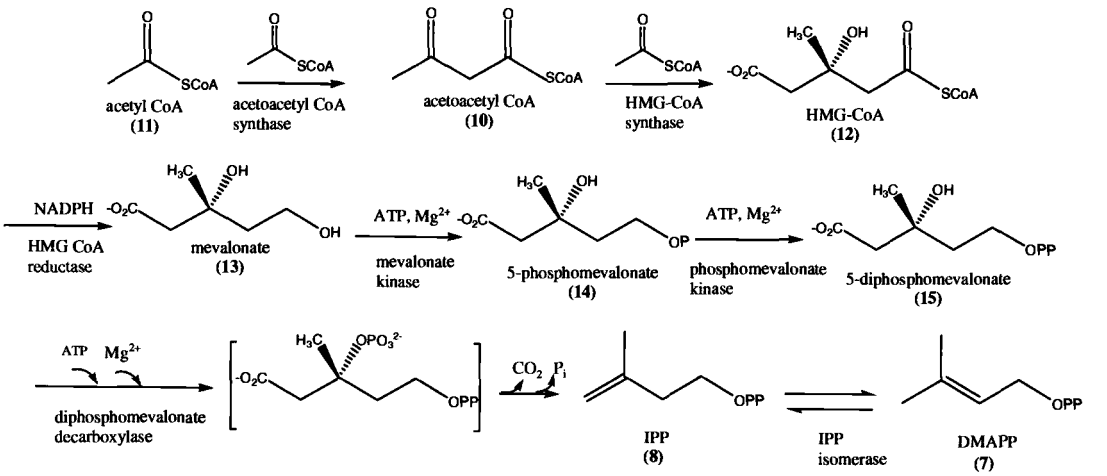

Figure 1.5. The mevalonate pathway to IPP.

The first step is catalyzed by the enzyme acetoacetyl-CoA synthase. The second step, addition of one more acetyl-CoA to form 3-hydroxy-3-methylglutaryl-CoA (**12**) (HMG-CoA), is mediated by the enzyme hydroxymethylglutaryl-CoA synthase [EC 2.3.3.10]. The next step is a reduction of the thioester of HMG-CoA providing mevalonate (**13**). This step is catalyzed by HMG-CoA reductase [EC 1.1.1.34], which uses NADPH as the reductant. Mevalonic acid is the first committed intermediate for this pathway and HMG-CoA reductase is a key regulatory enzyme controlling isoprenoid metabolism in mammals and fungi.[17] Two subsequent phosphorylations involving ATP-dependent kinases are the next steps. Mevalonate kinase [EC 2.7.1.36] phosphorylates MVA to produce mevalonate 5-phosphate (**14**), then phosphomevalonate kinase [EC 2.7.4.2] phosphorylates mevalonate 5-phosphate providing mevalonic acid 5-diphosphate (**15**) (MVAPP). MVAPP is decarboxylated yielding IPP. This last step is catalyzed by another ATP-dependent enzyme, MVAPP

decarboxylase.[18,19] DMAPP (**7**) is derived from IPP (**8**) by the action of an IPP isomerase enzyme [EC 5.3.3.2].[5]

The most studied enzyme of the MVA pathway is HMG-CoA reductase. This enzyme is highly regulated and is responsible for the regulation of cholesterol biosynthesis.[17] Mevinolin, a metabolite isolated from *Aspergillus terreus*, and its natural analogs are potent and highly specific competitive inhibitors of HMG-CoA reductases from animals, microorganisms and plants.[20,21] Detailed studies of the inhibition and regulation of this enzyme led to the development of successful drugs used to lower cholesterol, such as lovastatin (Mevacor®) and simvastatin (Zocor®).[22]

4. The discovery of the MEP pathway

The mevalonate pathway was universally accepted to be responsible for the biosynthesis of IPP and DMAPP in all organisms for many years. Until around 1990 all biosynthetic labeling studies of the isoprenoid biosynthesis were conducted with isotopes of mevalonate and acetate. In some cases, the incorporation levels in these experiments were very low. Many explanations were given, the main one being that the labeled compounds could not get into the cells due to permeability barriers.

Inhibition studies using mevinolin, an inhibitor of the MVA pathway, also provided inconsistencies with the MVA pathway. This compound was found to efficiently inhibit formation of the cytosolic isoprenoids in plants, sterols and ubiquinone, while the production of plastid isoprenoids such as phytol, carotenoids and plastoquinone was not inhibited. [21,23,24] These studies confirmed the formation of cytosolic isoprenoids by the mevalonate pathway, but suggested that the plastid isoprenoids could be synthesized by a different pathway. In addition mevinolin did not inhibit the growth of *E. coli*.[25] Another result inconsistent with the operation of the mevalonate pathway was the inability of isolated plastids from mustard to make IPP from MVA.[26]

This evidence against the mevalonate pathway stimulated the search for another pathway for isoprenoid biosynthesis. The existence of a MVA-independent pathway for IPP and DMAPP biosynthesis was reported independently by two

different research groups in the early 1990's. The search by Rohmer and co-workers for a new pathway for isoprenoid biosynthesis started with chemical and biochemical studies on bacterial hopanoids.[27] Although these triterpenoids are not widespread in bacteria, they are present in higher concentrations than quinones in the bacterium *Zymomonas mobilis* and also are stable, readily isolatable and suited to stable-isotope incorporation studies, so several experiments were focused on hopanoids. Research in plants and *E. coli* by the laboratory of Arigoni also led to this new pathway.[28] Both of these groups found isotope patterns in the experiments that could not be explained by the MVA pathway.

Further experiments involving the incorporation of ^{13}C-labelled glucose, acetate, pyruvate or erythrose in hopanoids, performed by Rohmer and coworkers[27] using the bacteria *E. coli*, *Zymomonas mobilis*, *Methylobacterium fujisawaense* and *Alicyclobacillus acidoterrestris* allowed the determination of the origin of the carbons atoms used in this new pathway. The labeling pattern found in hopanoids was in accordance with pyruvate as precursor of the C2 subunit and a triose phosphate derivative, probably from dihydroxyacetone phosphate, as precursor of the C3 subunit. Confirmation of pyruvate as the C2 subunit and the finding that glyceraldehyde 3-phosphate was the C3 subunit also was provided by labeling experiments. Incorporation of ^{13}C-labeled glycerol or pyruvate into the ubiquinone of *E. coli* mutants lacking enzymes of the triose phosphate metabolism and of (U-$^{13}C_6$)glucose in *Z. mobilis* hopanoids were consistent with a condensation of a C2 unit derived from pyruvate and a triose phosphate, glyceraldehyde phosphate, to form a 1-deoxypentulose 5-phosphate, probably 1-deoxyxylulose 5-phosphate.[29] Efficient incorporation of deuterium labeled 1-deoxy-D-xylulose into the ubiquinone side chain had already been observed.[30] Later, the incorporation of deoxyxylulose, ^{13}C and ^{2}H-labelled, into isoprenoids from *Catharanthus roseus*[28], *Mentha x piperita*[31], *E. coli* [32], and other higher plants and red algae[33] was reported.

These studies established that the new pathway for the biosynthesis of IPP and DMAPP starts with the condensation of pyruvate and glyceraldehyde 3-phosphate producing 1-deoxy-D-xylulose 5-phosphate (DXP).[28, 29] The non-mevalonate pathway, mevalonate independent pathway, triose phosphate/pyruvate pathway and

deoxyxylulose pathway have all been used as names for the new pathway. The methylerythritol 4-phosphate (MEP) pathway, however, has been recommended as the preferred name for the pathway. MEP is the first intermediate in the pathway and naming the pathway in this manner follows the procedence for the MVA pathway, which was named after its committed intermediate, mevalonate.[34]

5. The MEP pathway

Because the reaction for the synthesis of DXP is a condensation that requires thiamine diphosphate (TPP), it was thought that the gene encoding this enzyme could share sequence motifs with pyruvate decarboxylating enzymes such as the E1 component of the pyruvate dehydrogenase complex or transketolases.[35,36] Bioinformatics screening of the *E. coli* genome detected only one additional ORF with a high percentage of amino acids identical or similar to those of transketolase of *E. coli* K-12.

The biochemical characterization of this ORF showed that it could catalyze the synthesis of DXP (**16**) from pyruvate (**17**) and glyceraldehyde 3-phosphate (**18**).[35] The gene encoding the enzyme was then named *dxs* and the protein DXP synthase [DXS, EC 2.2.1.7] (Figure 1.6).

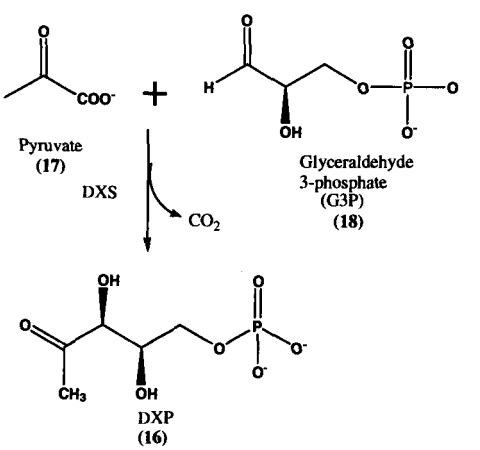

Figure 1.6. The reaction catalyzed by the enzyme DXP synthase (DXS).

The *dxs* sequence was used to search for DXP synthase genes in other organisms. This search showed that the *dxs* gene is widespread in bacteria (Gram-positive, Gram-negative and cyanobacteria) and plants (*A. thaliana*, rice, pine). The DXP synthase genes of several of these organisms have been cloned and expressed for biochemical characterization.[35,36,37,38,39]

Studies of the *E. coli* DXP synthase exploring substrate binding and kinetics provided evidence for an ordered kinetic mechanism where the binding of the second substrate (G3P) is required for the formation of a catalytically competent enzyme-substrate complex.[40] Besides D-glyceraldehyde 3-phosphate, DXP synthase from *E. coli* can use other sugar phosphates as well as short-chain aldehydes as acceptor substrates. Hydroxypyruvate and 2-oxobutyrate are also accepted in place of pyruvate.[41] It has been established that DXP synthase is an enzyme that is not specific for the methylerythritol phosphate pathway (Figure 1.7). DXP is also the precursor of the thiazole moiety of thiamine diphosphate (**19**) (vitamin B1) and of the pyridine ring of pyridoxal phosphate (**20**) (vitamin B6).[42,43,44]

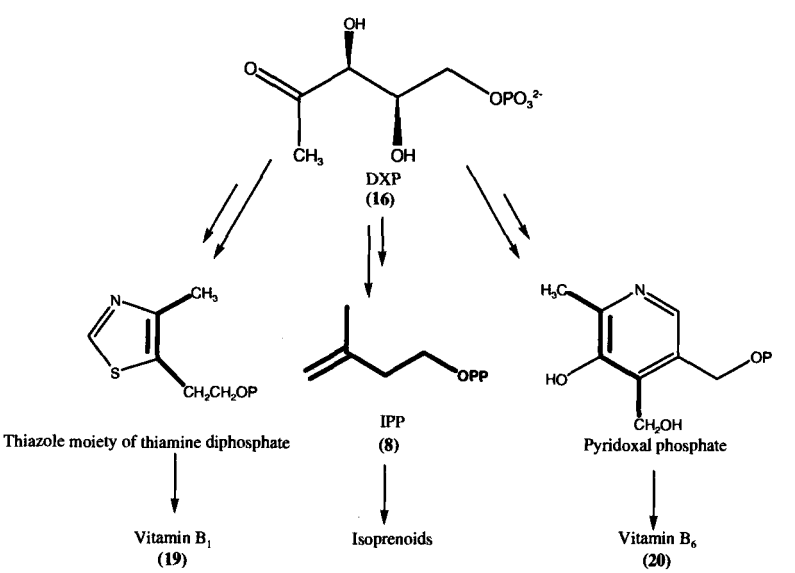

Figure 1.7. DXP as a common precursor of thiamine, pyridoxal and isoprenoids.[35] The carbons from DXP are highlighted.

The studies on the second enzyme of the MEP pathway started with the work of Kuzuyama and co-workers[45] using *E. coli.* Earlier experiments had shown that 2-*C*-

methylerythritol was taken up by *E. coli* cells and utilized as a precursor of the side chain of ubiquinone.[46,47] Based on this result it was assumed that an intramolecular rearrangement of DXP would provide 2-*C*-methylerythrose 4-phosphate, which could be reduced to 2-*C*-methylerythritol 4-phosphate (MEP). By this mechanism it was thought that two enzymes, an isomerase and a reductase, were involved in the MEP biosynthesis. To further investigate this mechanism and isolate the gene encoding the enzyme or enzymes catalyzing MEP biosynthesis, mutants with a block in the MEP pathway between the DXP and MEP were selected. These mutants could grow only in the presence of the free-alcohol of MEP and after complementation studies with an *E. coli* library they found a gene that complemented IPP biosynthesis in the blocked mutants.[45] Only one gene, *yae*M, was identified. All the mutants that needed ME to grow had the *yae*M gene deficient. The gene *yae*M was overexpressed and the resulting protein was proved to catalyze the rearrangement of MEP to 2-*C*-methylerythrose 4-phosphate (**21**) and the reduction to provide MEP (**22**) (Figure 1.8).[48] The enzyme was named 1-deoxy-D-xylulose 5-phosphate reductoisomerase [DXR; EC 1.1.1.267].[48] The gene *yae*M was renamed *dxr*. More recent studies have also referred to *dxr* as *isp*C and DXR as MEP synthase.[49,50]

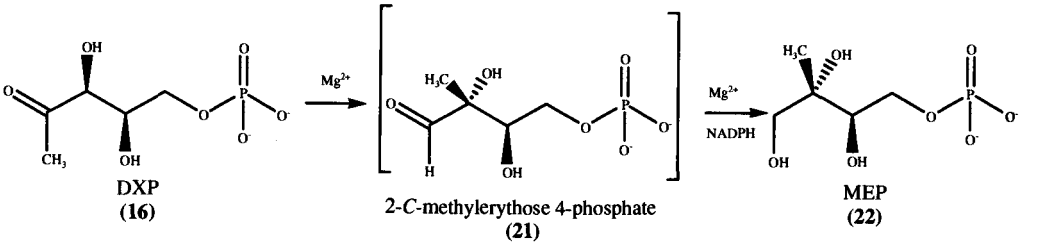

Figure 1.8. The DXR reaction to convert DXP to MEP.

DXR proteins, homologous to the *E. coli* enzyme, were soon shown to be present in several organisms including bacteria such as *Pseudomonas aeruginosa*[39], *Streptomyces coelicolor*[38], and *Zymomonas mobilis*[51], the cyanobacteria *Synechocystis sp.* PCC6803[52] and *Synechococcus leopoliensis*[53], the plants *Arabidopsis thaliana*[54], tomato[55] and *Mentha piperita*[56] and the protozoan that causes malaria, *Plasmodium falciparum* .[57]

The *dxr* genes from several of these organisms have been cloned and the DXR proteins characterized.[38,50-52,58,59] At the present, DXRs from bacteria have been studied extensively with respect to their mechanism, biochemical properties and inhibition. X-ray crystallographic structures have also been determined for the *E. coli* and *Zymomonas mobilis* DXRs. This step of the MEP pathway will be discussed in detail in Chapters 2-4.

The genes encoding enzymes involved in steps downstream of the DXR enzyme were elucidated using a multidisciplinary approach that combined organic chemistry, microbial genetics, biochemistry, molecular biology and bioinformatics. The fast identification of the genes involved in the MEP pathway, in both bacteria and plants, was possible using genetic tools such as the availability of full genome sequences and expressed sequence tag (EST) collections.[34]

The search for the gene encoding the enzyme for the third step in the MEP pathway was guided by the finding that 4-diphosphocytidyl-2*C*-methylerythritol (CDP-ME) is the product of the incubation of MEP and radiolabeled CTP. A database search with the term "cytidine diphosphate" (CDP) and "pyrophosphorylase" identified a gene that specifies a bifunctional ribulose 5-phosphate reductase/CDP-ribitol pyrophosphorylase. A similar and unannoted gene (*ygb*P) from *Haemophilus influenzae* was also identified. Subsequent searches with this gene uncovered several similar genes from various organisms.[60] The occurrence of putative *ygb*P homologs was correlated with the occurrence of the MEP pathway. The *ygb*P genes from *E. coli*, *Streptomyces coelicolor* and *Arabidopsis thaliana* were overexpressed and the proteins were shown to catalyze the formation of CDP-ME (**23**) from MEP (**22**) and CTP[38,60,61] (Figure 1.9).

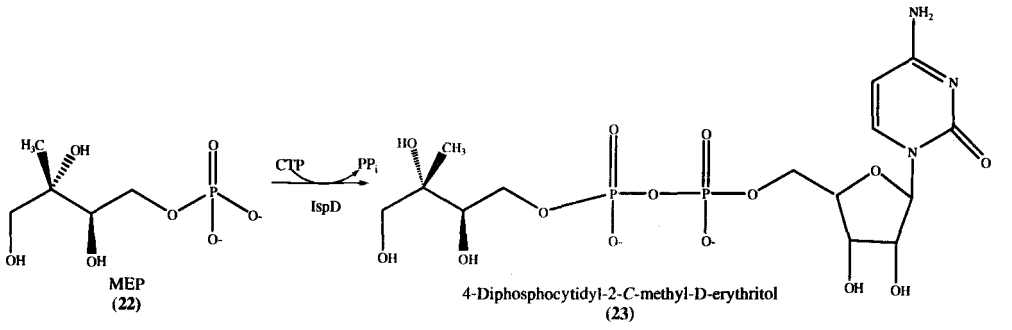

Figure 1.9. Cytidylation of MEP generating 4-diphosphocytidyl-2*C*-methylerythritol.

Once the function of the gene product was confirmed to be involved in the MEP pathway, the *ygb*P gene was renamed *isp*D. The protein encoded by the *isp*D gene was named 4-diphosphocytidyl-2C-methylerythritol synthase or 4-diphosphocytidyl-2C-methylerythritol cytidyltransferase [EC 2.7.7.60]. The three-dimensional structures of the *E. coli* CDP-ME synthase enzyme complexed with both substrate ($CTP.Mg^{2+}$) and product ($CDP\text{-}ME.Mg^{2+}$) provided the first structural information for an enzyme in the MEP pathway.[62]

The next step in the MEP pathway is phosphorylation of 4-diphosphocytidyl-2*C*-methyl-D-erythritol (CDP-ME). The gene encoding the enzyme involved in this step was identified by a bioinformatics search for additional genes following the same distribution as the genes previously identified for the MEP pathway. An unannotated *E. coli* gene named *ych*B was found. Overexpression and purification of this gene from *E. coli* and tomato produced a protein able to catalyze an ATP-dependent phosphorylation of 4-diphosphocytidyl-2*C*-methyl-D-erythritol **(23)** producing 4-diphosphocytidyl-2*C*-methyl-D-erythritol 2-phosphate **(24)**[63,64,65] (Figure 1.10).

The product 4-diphosphocytidyl-2*C*-methyl-*D*-erythritol 2-phosphate was shown to be incorporated into carotenoids by isolated chromoplasts leaving no doubt that it is an intermediate in the MEP pathway to isoprenoids.[63] The *ych*B gene was renamed *isp*E and the encoded protein was 4-diphosphocytidyl-2*C*-methyl-*D*-erythritol (CDP-ME) kinase (EC 2.7.1.148). A crystal structure of the CDP-ME kinase from *E. coli* was solved in a ternary complex with 4-diphosphocytidyl-2*C*-methyl-D-erythritol and a nonhydrolyzable ATP analog.[66]

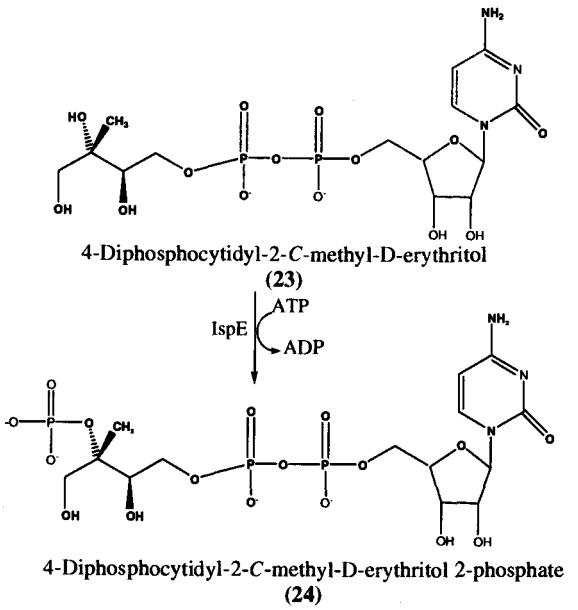

Figure 1.10. Phosphorylation of CDP-ME to produce 4-diphosphocytidyl-2C-methyl-D-erythritol 2-phosphate.

Following the phosphorylation of 4-diphosphocytidyl-2*C*-methyl-*D*-erythritol by the CDP-ME kinase is a cyclization reaction that produces 2*C*-methyl-D-erythritol 2,4-cyclodiphosphate (**25**) (Figure 1.11). Bioinformatics analysis of the genes of the MEP pathway showed that the *isp*D gene of *E. coli* appears to be cotranscribed with an unannotated reading frame, *ygb*B. Putative orthologs of these two genes were also linked on the chromosomes of 21 other bacteria that contain putative orthologs of *dxs, dxr, ispE*.[67] Using the same biochemical approach used to validate other genes proposed to be in the MEP pathway, the *ygb*B gene was cloned, overexpressed and the purified protein was used in enzymatic assays with 4-diphosphocytidyl-2*C*-methyl-D-erythritol as substrate. Nuclear magnetic resonance (NMR) analysis of the reaction product confirmed the formation of 2*C*-methyl-*D*-erythritol 2,4-cyclodiphosphate by the YgbB protein.[67] Further confirmation of the 2*C*-methyl-D-erythritol 2,4-cyclodiphosphate (MecPP) as an intermediate of isoprenoid biosynthesis came from studies using isolated chromoplasts of *Capsicum annuum* and *Narcissus pseudonarcissus*.[68] The chromoplasts were able to catalyze the conversion of MEP into MecPP in a process that displays saturation kinetics and moreover the product of this reaction is further processed efficiently into phytoene, a plant isoprenoid. The

*ygb*B gene was renamed *isp*F and the protein named 2*C*-methyl-D-erythritol 2,4-cyclodiphosphate synthase (MECDP synthase) [EC 4.6.1.12].

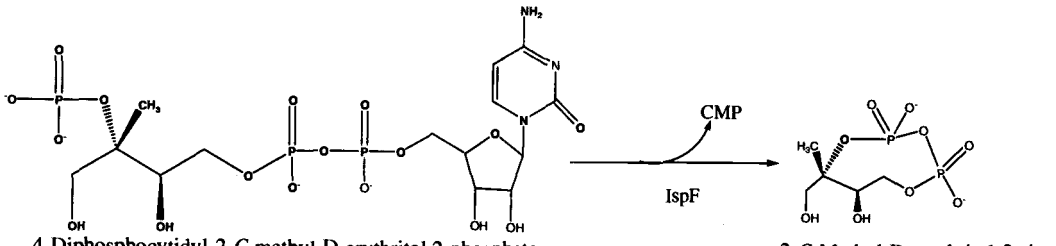

4-Diphosphocytidyl-2-*C*-methyl-D-erythritol 2-phosphate
(24)

2-*C*-Methyl-D-erythritol-2, 4-cyclodiphosphate
(25)

Figure 1.11. Cyclization to form 2*C*-methyl-D-erythritol 2,4-cyclodiphosphate.

The last two steps in the MEP pathway were identified by two different but complementary approaches. First, in the genomic approach 28 organisms completely sequenced and with known occurrence of the MEP pathway were chosen and then genes with the same pattern of occurrence were identified.[69] Only two genes, named *lyt*B and *gcp*E, with unknown function and with co-occurrence to the other genes for the MEP pathway were identified. The involvement of these two genes in the MEP pathway was studied in an *E. coli* strain engineered for the synthesis of IPP and DMAPP from MVA. This strain is viable only when the culture medium is supplemented with MVA. Disruption of these two genes in this *E. coli* strain produces mutants that are not viable, but can be rescued by addition of MVA in the culture medium.[70,71,72] In the functional approach accumulation of the isoprenoid end products was examined. The *lyt*b genes from *Synechocystis*[69] and from the plant *Adonis aestivalis* were overexpressed in an *E. coli* strain engineered to produce the carotenoids β-carotene and zeaxanthin, and lycopene, a pink-colored isoprenoid compound. The amounts of lycopene produced in the liquid cultures were 1.5-fold higher than in the control, suggesting a role of *lyt*B in the MEP pathway.

The role of *gcp*E in the MEP pathway was studied by the aid of a recombinant *E. coli* strain overexpressing *xyl*B (a kinase that phosphorylates D-xylulose), *isp*CDEF and *gcp*E.[73] Formation of 1-hydroxy-2-methyl-2-(E)-butenyl-4-diphosphate (**26**) (HMB-PP) from MecPP was observed only when *gcp*E was overexpressed (Figure

1.12). Subsequent attempts to transform MecPP into 1-hydroxy-2-methyl-2-(E)-butenyl-4-diphosphate (HMB-PP) in vitro with purified GcpE were unsuccessful[74], but the activity could be restored by addition of a crude cell extract from a *gcp*E-deficient mutant of *E. coli*. The *gcp*E gene was renamed *isp*G and the protein IspG.[73]

The metabolic role of the protein LytB was studied following the same approach used for GcpE. The engineered *E. coli* strain overexpressing *xyl*B and *isp*CDEFG and *lyt*B produced a 5:1 mixture of IPP and DMAPP[75] (Figure 1.12). The substrate for this reaction is HMB-PP (**26**). This compound had been shown to accumulate in a *lyt*B deficient strain able to use the MVA pathway.[76] The *lyt*B gene was renamed *isp*H.

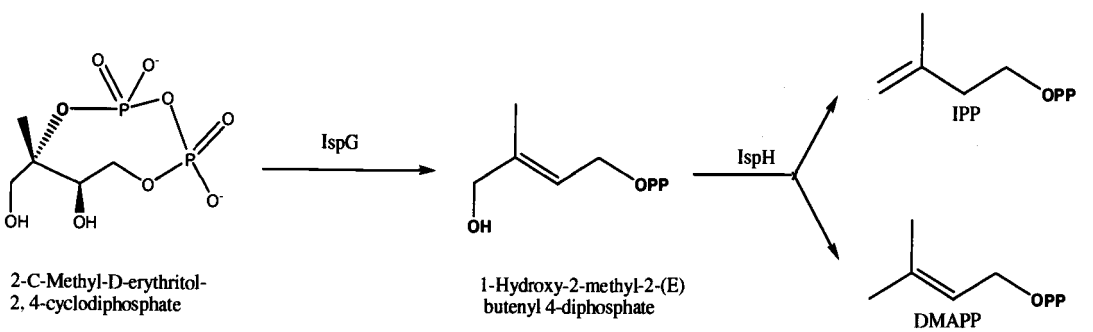

Figure 1.12. Last two steps of the MEP pathway.

The proteins IspG and IspH have common characteristics. These proteins have been shown to have a $[4Fe\text{-}4S]^{2+}$ cluster that mediates electron transfer and then requires a reducing system such as flavodoxin, flavodoxin reductase and NADPH for catalysis. This explained unsuccessful attempts to assay these proteins in the presence of oxygen. When the enzymatic reactions are conducted under oxygen free conditions and are activated by a reducing agent, catalysis is observed. [74,77,78]

An overview of the entire MEP pathway is presented in Figure 1.13. After the discovery of all of the steps of the pathway, mechanistic studies for the individual steps are being conducted. [59,74,79]

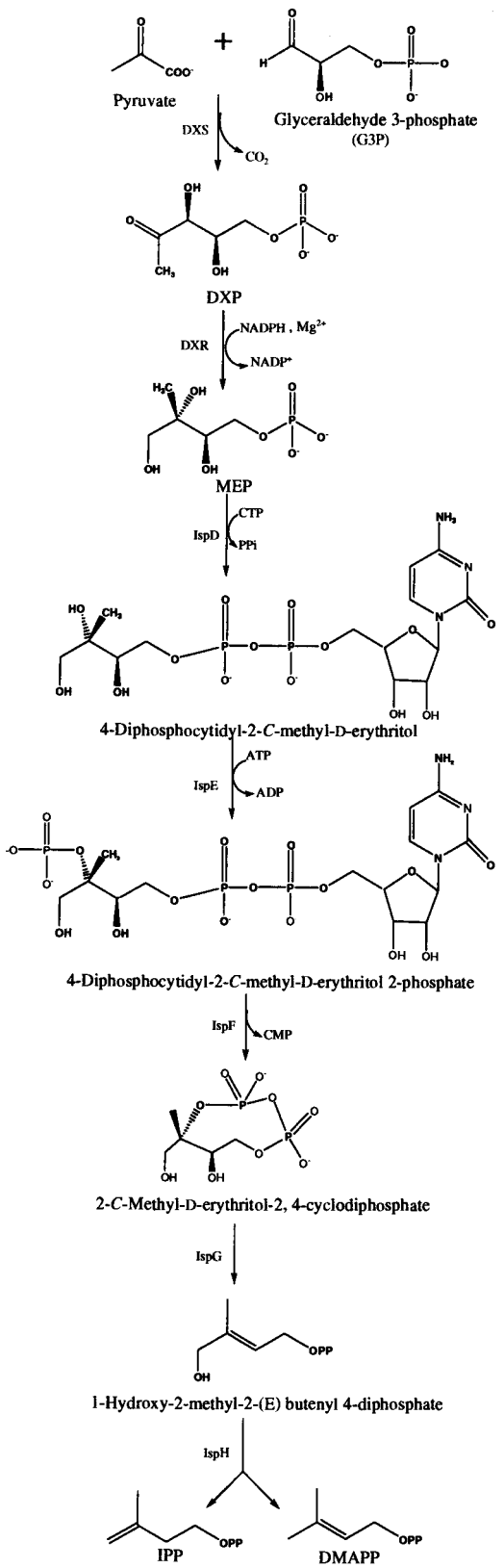

Figure 1.13. Overview of the MEP pathway.

6. Distribution of the isoprenoid biosynthesis pathways

The distribution of the two pathways for biosynthesis of IPP and DMAPP in bacteria is now well established. The completely sequenced genomes of about 150 microbial species provided a detailed description of the occurrence of the MVA- and MEP-pathways in microorganisms. Most of the eubacteria contain exclusively genes for the MEP pathway.[80] Exceptions to this are *Borrelia burgdorferi* and *Staphylococcus aureus* that contain only genes for the mevalonate pathway and *Listeria monozytogenes* that contains complete sets of both MVA and MEP pathway genes. A noteworthy exception to the bacteria cited above is a small group of actinomycetes that employ both pathways.[81] In *Streptomyces* species the primary metabolites are formed by the MEP pahway, while the MVA pathway is used to make secondary metabolites.[82] In all archaeal genomes sequenced, genes for the MVA pathway, but not for the MEP pathway, are found.[83]

In higher plants, both pathways are involved in the biosynthesis of the active isoprene unit. Over the course of evolution, plants have maintained the MVA pathway and acquired the MEP pathway from the cyanobacterial ancestor of plastids.[84] Today it is well established that the MVA pathway operates in the cytoplasm, making isoprenoids such as sterols and the side chain of mitochondrial ubiquinone, while the MEP pathway operates in the plastids being responsible by the biosynthesis of isoprene, carotenoids, abscisic acid and the side chains of chlorophylls and plastoquinone.[28,33,85] Although this subcellular compartmentation allows both pathways to operate independently, there is evidence that they cooperate in the biosynthesis of certain metabolites. Sesquiterpenes produced by chamomile were shown to be assembled by two isoprene units from the MVA pathway and one from the MEP pathway.[86] A small amount (1-2%) of ginkgolides produced by the MEP pathway, is also formed from mevalonic acid.[87] Conversely Arigoni and co-workers[28] showed that some 1-deoxy-D-xylulose-5-phosphate could be diverted to sterols. These reports suggest that IPP or IPP-derived products can be exchanged in both directions through the plastid membranes. Further studies in *Arabidopsis thaliana* and tobacco cell cultures probed this interaction using specific inhibitors for each pathway and analysis of the isoprenoid metabolites after inhibition.[88,89,90] The interaction

between the MEP and MVA-pathways was also studied at the transcriptional level using microarrays.[88] Genes involved in sterol, chlorophyll and carotenoid metabolism were analyzed after inhibition with fosmidomycin, an inhibitor of the MEP pathway, and lovastatin, an inhibitor of the MVA-pathway. Interestingly, the expression of these genes did not change significantly compared with control levels, although differential accumulation of the metabolites was observed. These results suggest that posttranscriptional processes may be involved in regulating flux through isoprenoid metabolic pathways.

The distribution of the pathways in algae has been studied by isotope incorporation experiments. Isoprenoid biosynthesis was investigated in the following green algae: *Scenedesmus obliquus*,[91] *Chlorella fusca*, and *Chlamydomonas reinhardtii*.[92] The biosynthetic studies were carried out with the algae growing heterotrophically on ^{13}C-labelled glucose and acetate. The ^{13}C-labelling pattern of all plastidic isoprenoids (prenyl side chains of chlorophylls and plastoquinone, and the carotenoids β-carotene and lutein), as well as of the non-plastidic cytoplasmic sterols, were not consistent with the MVA pathway but showed a very similar pattern of labelling to those of bacterial isoprenoids synthesized by the MEP pathway. These results indicated that the MEP pathway is responsible for the biosynthesis of all isoprenoids in green algae. In contrast to the green algae, the red algae possess both pathways for isoprenoid biosynthesis.[92] Incorporation of ^{13}C-glucose into the isoprenoids of *Cyanidium caldarium* and the Chrysophyte *Ochromonas danica* was similar to the labelling patterns observed in plants. Sterols were labeled via the MVA-pathway, while phytol showed labelling that suggested the MEP pathway. The green algae possibly spread the MEP pathway to others organisms through an endosymbiotic event. One example is *Euglena gracilis,* a phytoflagellate that is thought to have obtained its chloroplasts from a secondary endosymbiotic event in which a green algae was putatively engulfed. The MEP pathway was shown to contribute to carotenoid biosynthesis in this organism.[93] Incubation experiments where [5,5-$^{2}H_2$]-deoxyxylulose (DX) was supplemented to the culture medium showed a high level incorporation of DX in both β-carotene and diadinoxanthin. Phytol was also labeled by DX but to a much lesser extent than for the carotenoids and the labeling pattern

suggested that DX was catabolized, presumably to acetate before incorporation into phytol. The completely sequenced genomes of animal and yeast have complete sets of the MVA pathway genes and the ones for the MEP pathways are absent (National Center for Biotechnology website).

7. The MEP pathway as a target for drugs

The development of resistance against current antibiotics by human pathogens has been reported to be rapid and progressing. This problem, coupled with the poor rate of the discovery of new antibiotics is cause for concern. Aside from linezolide (Zyvox®), the last new class of antibiotic to reach the US market was 30 years ago.[94] Although some success in overcoming resistance has been achieved through modification of the existing classes, the development of new antibiotics is a matter of urgency.[94] The MEP pathway shows characteristics that are desirable for the development of new drugs, such as it is essential for the growth of relevant pathogens and it is absent in mammals.

Plants, algae, protozoa and bacteria use the MEP pathway for synthesis of isoprenoids, but animals and fungi lack this pathway. Because the MEP pathway is not present in humans, the enzymes in this pathway have been considered ideal targets for new drugs. Due to the absence of the MEP pathway in mammals it is believed that any inhibitors of this pathway should have low toxicity in humans. The bacterial species that use the MEP pathway include the causal agents for diverse and serious human diseases including leprosy (*M. leprae*), bacterial meningitis (*Haemophilus influenzae* and *Neisseria meningitis*), various gastrointestinal (*Campylobacter jejuni*, *Vibrium cholerae* and *Salmonella species*) and sexually transmitted infections (*Chlamydia trachomatis*, *N. gonorrhoeae* and *Treponema pallidum*), tuberculosis (*M. tuberculosis*) and certain types of pneumonia (*Klebsiella pneumoniae*).[95,96] The MEP pathway also appears to be present in *Yersinia pestis*, *Francisella tularensis* and *Bacillus anthracis*, three bacteria used as biological warfare agents.[95] The presence of the MEP pathway in these bacteria makes it an interesting alternative target for new antibacterial drugs. Moreover, disruption of any of the steps of the MEP pathway results in a lethal phenotype, showing that this pathway is essential for bacterial viability.[45,97]

Malaria, in developing tropical countries, is the cause of 1.5-2.7 million deaths per year.[98] The appearance of *Plasmodium* species resistant to the available drugs to treat this disease makes the search for new drugs a priority in malaria research. Protozoa such as *Plasmodim falciparum*, the causative agent of malaria, *Plasmodium vivax* and *Toxoplasma gondii* also contain the genes for the MEP pathway for isoprenoid biosynthesis. Enzymes in the MEP pathway, therefore, also provide a new target for development of drugs to treat the disease caused by these protozoa.

The first compound described to inhibit the MEP pathway was fosmidomycin, also known as FR-31564 or 3-(N-formyl-N-hydroxyamino) propylphosphonic acid[99,100,101,102] (Figure 1.14). This compound was shown to strongly inhibit the DXR enzyme and thus validated the MEP pathway as a target to development of new drugs.[103]

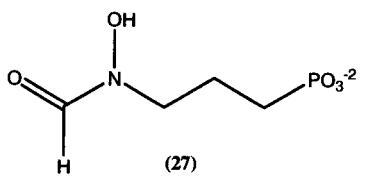

(27)

Figure 1.14. Fosmidomycin structure

DXR is a promising target for the development of new drugs such as antibiotics, antimalarials and herbicides. The overall objective of this project was a better understanding of the DXR enzyme. The role of amino acids in the active site of DXR will be studied to expand the knowledge already accumulated about DXR. We will report the use of site-directed mutagenesis, guided by crystal structure analysis, to produce a series of DXR mutants. One set of mutants was designed to expand the selectivity of DXR. Kinetic characterization of other DXR mutants at the active site was also conducted. Inhibition of DXR by fosmidomycin and other inhibitors related to this compound will also be presented. The information obtained allows us to more fully understand the roles of DXR active site residues.

8. References

(1) Rohdich, F.; Bacher, A.; Eisenreich, W. "Perspectives in anti-infective drug design. The late steps in the biosynthesis of the universal terpenoid precursors, isopentenyl diphosphate and dimethylallyl diphosphate". *Bioorg. Chem.* **2004**, *32*, 292-308.

(2) Sacchettini, J. C.; Poulter, C. D. "Creating isoprenoid diversity". *Science* **1997**, *277*, 1788-1789.

(3) McGarvey, D. J.; Croteau, R. "Terpenoid metabolism". *Plant Cell* **1995**, *7*, 1015-1026.

(4) Rohmer, M. "The discovery of a mevalonate-independent pathway for isoprenoid biosynthesis in bacteria, algae and higher plants". *Nat. Prod. Rep.* **1999**, *16*, 565-574.

(5) Kuzuyama, T.; Seto, H. "Diversity of the biosynthesis of the isoprene units". *Nat. Prod. Rep.* **2003**, *20*, 171-183.

(6) Ramos-Valdivia, A. C.; van der Heijden, R.; Verpoorte, R. "Isopentenyl diphosphate isomerase: a core enzyme in isoprenoid biosynthesis. A review of its biochemistry and function". *Nat. Prod. Rep.* **1997**, *14*, 591-603.

(7) Chappell, J. "Biochemistry and molecular biology of the isoprenoid biosynthetic pathway in plants". *Annu. Rev. Plant Physiol. Plant Mol. Biol.* **1995**, *46*, 521-527.

(8) Croteau, R. K., T.M.; Lewis, N.G. Natural Products (Secondary Metabolites). *Biochemistry & Molecular Biology of Plants*; American Society of Plant Physiologists, 2000; pp 1250-1268.

(9) Bach, T. J. "Some new aspects of isoprenoid biosynthesis in plants--a review". *Lipids* **1995**, *30*, 191-202.

(10) Vyas, D. M.; Kadow, J. F. "Paclitaxel: a unique tubulin interacting anticancer agent". *Prog. Med. Chem.* **1995**, *32 289-337.*

(11) Klayman, D. L. "Qinghaosu (artemisinin): an antimalarial drug from China". *Science* **1985**, *228*, 1049-1055.

(12) Silver, G. M.; Fall, R. "Enzymatic synthesis of isoprene from dimethylallyl diphosphate in Aspen leaf extracts." *Plant Physiol.* **1991**, *97*, 1588-1591.

(13) Silver, G. M.; Fall, R. "Characterization of aspen isoprene synthase, an enzyme responsible for leaf isoprene emission to the atmosphere." *J. Biol. Chem.* **1995**, *270*, 13010-13016.

(14) Miller, B.; Oschinski, C.; Zimmer, W. "First isolation of an isoprene synthase gene from poplar and successful expression of the gene in *Escherichia coli*". *Planta* **2001**, *213*, 483-487.

(15) Kleinig, H. "The role of plastids in isoprenoid biosynthesis". *Annu. Rev. Plant Physiol. Plant Mol. Biol.* **1989**, *40*, 39-59.

(16) Bloch, K. "Sterol molecule: structure, biosynthesis, and function". *Steroids* **1992**, *57*, 378-383.

(17) Goldstein, J. L.; Brown, M. S. "Regulation of the mevalonate pathway". *Nature* **1990**, *343*, 425-430.

(18) Dewick, P. M. "The biosynthesis of C5-C25 terpenoid compounds". *Nat. Prod. Rep.* **1997**, *14*, 111-144.

(19) Dewick, P. M. "The biosynthesis of C5-C25 terpenoid compounds". *Nat. Prod. Rep.* **1999**, *19*, 97-130.

(20) Alberts, A. W.; Chen, J.; Kuron, G.; Hunt, V.; Huff, J. et al. "Mevinolin: a highly potent competitive inhibitor of hydroxymethylglutaryl-coenzyme A reductase and a cholesterol-lowering agent". *Proc. Natl. Acad. Sci. U S A* **1980**, *77*, 3957-3961.

(21) Bach, T. J.; Lichtenthaler, H. K. "Mechanisms of inhibition by mevinolin (MK 803) of microsome-bound radish and of partially purified yeast HMG-CoA reductase (EC.1.1.1.34)". *Z. Naturforsch. [C]* **1983**, *38*, 212-219.

(22) Slater, E. E.; MacDonald, J. S. "Mechanism of action and biological profile of HMG CoA reductase inhibitors. A new therapeutic alternative". *Drugs* **1988**, *36*, 72-82.

(23) Bach, T. J.; Lichtenthaler, H. K. "Mevinolin: a highly specific inhibitor of microsomal 3-hydroxy-3-methylglutaryl-coenzyme A reductase of radish plants". *Z. Naturforsch. [C]* **1982**, *37*, 46-50.

(24) Bach, T. J. L., H.K "Inhibition by mevinolin of plant growth, sterol formation and pigment accumulation". *Physiol. Plant* **1983**, *59*, 50-60.

(25) Zhou, D.; White, R. H. "Early steps of isoprenoid biosynthesis in *Escherichia coli*". *Biochem. J.* **1991**, *273*, 627-634.

(26) Lutke-Brinkhaus, F. K., H. "Formation of isopentenyl diphosphate via mevalonate does not occur within etioplasts and etiochloroplasts of mustard (Sinapis alba L.) seedlings". *Planta* **1987**, *171*, 406-411.

(27) Rohmer, M.; Knani, M.; Simonin, P.; Sutter, B.; Sahm, H. "Isoprenoid biosynthesis in bacteria: a novel pathway for the early steps leading to isopentenyl diphosphate". *Biochem. J.* **1993**, *295*, 517-524.

(28) Arigoni, D.; Sagner, S.; Latzel, C.; Eisenreich, W.; Bacher, A. et al. "Terpenoid biosynthesis from 1-deoxy-D-xylulose in higher plants by intramolecular skeletal rearrangement". *Proc. Natl. Acad. Sci. U S A* **1997**, *94*, 10600-10605.

(29) Rohmer, M. S., M.; Horbach, S.; Bringer-Meyer, S.; Sahm, H. "Glyceraldehyde 3-phosphate and pyruvate as precursors of isoprenic units in an alternative non-mevalonate pathway for terpenoid biosynthesis". *J. Am. Chem. Soc.* **1996**, *118*, 2564-2566.

(30) Broers, S. T. J.; Eidgenossische Technische Hochschule: Zurich, 1994.

(31) Lange, B. M.; Wildung, M. R.; McCaskill, D.; Croteau, R. "A family of transketolases that directs isoprenoid biosynthesis via a mevalonate-independent pathway". *Proc. Natl. Acad. Sci. U S A* **1998**, *95*, 2100-2104.

(32) Putra, S. R.; Disch, A.; Bravo, J. M.; M., R. "Distribution of mevalonate and glyceraldehyde 3-phosphate/pyruvate routes for isoprenoid biosynthesis in some gram-negative bacteria and mycobacteria". *FEMS Microbiol. Lett.* **1998**, *164*, 169-175.

(33) Schwender, J.; Zeidler, J.; Gröner, R.; Müller, C.; Focke, M. et al. "Incorporation of 1-deoxy-D-xylulose into isoprene and phytol by higher plants and algae". *FEBS Lett.* **1997**, *414*, 129-134.

(34) Rodríguez-Concepción, M.; Boronat, A. "Elucidation of the methylerythritol phosphate pathway for isoprenoid biosynthesis in bacteria and plastids. A metabolic milestone achieved through genomics". *Plant Physiol.* **2002**, *130*, 1079-1089.

(35) Sprenger, G. A.; Schörken, U.; Wiegert, T.; Grolle, S.; de Graaf, A. A. et al. "Identification of a thiamin-dependent synthase in *Escherichia coli* required for the formation of the 1-deoxy-D-xylulose 5-phosphate precursor to isoprenoids, thiamine, and pyridoxal". *Proc. Natl. Acad. Sci. U S A* **1997**, *94*, 12857-12862.

(36) Lois, L. M.; Campos, N.; Putra, S. R.; Danielsen, K.; Rohmer, M. et al. "Cloning and characterization of a gene from *Escherichia coli* encoding a transketolase-like enzyme that catalyzes the synthesis of D-1-deoxyxylulose 5-phosphate, a common precursor for isoprenoid, thiamine, and pyridoxal biosynthesis". *Proc. Natl. Acad. Sci. U S A* **1998**, *95*, 2105-2110.

(37) Hahn, F. M.; Eubanks, L. M.; Testa, C. A.; Blagg, B. S.; Baker, J. A. et al. "1-Deoxy-D-xylulose 5-phosphate synthase, the gene product of open reading frame (ORF) 2816 and ORF 2895 in *Rhodobacter capsulatus*". *J. Bacteriol.* **2001**, *183*, 1-11.

(38) Cane, D. E.; Chow, C.; Lillo, A.; Kang, I. "Molecular cloning, expression and characterization of the first three genes in the mevalonate-independent isoprenoid pathway in *Streptomyces coelicolor*". *Bioorg. Med. Chem.* **2001**, *9*, 1467-1477.

(39) Altincicek, B.; Hintz, M.; Sanderbrand, S.; Wiesner, J.; Beck, E. et al. "Tools for discovery of inhibitors of the 1-deoxy-D-xylulose 5-phosphate (DXP) synthase and DXP reductoisomerase: an approach with enzymes from the pathogenic bacterium *Pseudomonas aeruginosa*". *FEMS Microbiol. Lett.* **2000**, *190*, 329-333.

(40) Eubanks, L. M.; Poulter, C. D. "Rhodobacter capsulatus 1-deoxy-D-xylulose 5-phosphate synthase: steady-state kinetics and substrate binding". *Biochemistry* **2003**, *42*, 1140-1149.

(41) Schurmann, M. S., M.; Sprenger, G. A. "Fructose 6-phosphate aldolase and 1-deoxy-D-xylulose 5-phosphate synthase from *Escherichia coli* as tolls in enzymatic synthesis of 1-deoxysugars". *J.Mol.Catal. B: Enzym.* **2002**, *19-20*, 247.252.

(42) Hill, R. E.; Himmeldirk, K.; Kennedy, I. A.; Pauloski, R. M.; Sayer, B. G. et al. "The biogenetic anatomy of vitamin B6. A 13C NMR investigation of the biosynthesis of pyridoxol in *Escherichia coli*". *J. Biol. Chem.* **1996**, *271*, 30426-30435.

(43) Drewke, C.; Leistner, E. "Biosynthesis of vitamin B6 and structurally related derivatives". *Vitam. Horm.* **2001**, *61*, 121-155.

(44) Laber, B.; Maurer, W.; Scharf, S.; Stepusin, K.; Schmidt, F. S. "Vitamin B6 biosynthesis: formation of pyridoxine 5'-phosphate from 4-(phosphohydroxy)-L-threonine and 1-deoxy-D-xylulose-5-phosphate by PdxA and PdxJ protein". *FEBS Lett.* **1999**, *449*, 45-48.

(45) Kuzuyama, T.; Takahashi, S.; Seto, H. "Construction and characterization of *Escherichia coli* disruptants defective in the yaeM gene". *Biosci. Biotechnol. Biochem.* **1999**, *63*, 776-778.

(46) Duvold, T. C., P.; Bravo, J. M.; Rhomer, M. "Incorporation of 2-C-methyl-D-erythritol, a putative C-5 intermediate precursor in the mevalonate-independent pathway, into ubiquinone and menaquinone of *Escherichia coli*". *Tetrahedron Lett.* **1997**, *38*, 6181-6184.

(47) Duvold, T. B., J. M.; Pale-Grodemange, C.; Rhomer, M. "Biosynthesis of 2-C-methyl-D-erythritol, a putative C-5 intermediate in the mevalonate independent pathway for isoprenoid biosynthesis". *Tetrahedron Lett.* **1997**, *38*, 4769-4772.

(48) Takahashi, S.; Kuzuyama, T.; Watanabe, H.; Seto, H. "A 1-deoxy-D-xylulose 5-phosphate reductoisomerase catalyzing the formation of 2-C-methyl-D-erythritol 4-phosphate in an alternative nonmevalonate pathway for terpenoid biosynthesis". *Proc. Natl. Acad. Sci. U S A* **1998**, *95*, 9879-9884.

(49) Steinbacher, S.; Kaiser, J.; Eisenreich, W.; Huber, R.; Bacher, A. et al. "Structural basis of fosmidomycin action revealed by the complex with 2-C-methyl-D-erythritol 4-phosphate synthase (IspC). Implications for the catalytic mechanism and anti-malaria drug development". *J. Biol. Chem.* **2003**, *278*, 18401-18407.

(50) Koppisch, A. T.; Fox, D. T.; Blagg, B. S.; Poulter, C. D. "*E. coli* MEP synthase: steady-state kinetic analysis and substrate binding". *Biochemistry* **2002**, *41*, 236-243.

(51) Grolle, S.; Bringer-Meyer, S.; Sahm, H. "Isolation of the dxr gene of *Zymomonas mobilis* and characterization of the 1-deoxy-D-xylulose 5-phosphate reductoisomerase". *FEMS Microbiol. Lett.* **2000**, *191*, 131-137.

(52) Yin, X.; Proteau, P. J. "Characterization of native and histidine-tagged deoxyxylulose 5-phosphate reductoisomerase from the cyanobacterium *Synechocystis* sp. PCC6803". *Biochim. Biophys. Acta* **2003**, *1652*, 75-81.

(53) Miller, B.; Heuser, T.; Zimmer, W. "Functional involvement of a deoxy-D-xylulose 5-phosphate reductoisomerase gene harboring locus of *Synechococcus leopoliensis* in isoprenoid biosynthesis". *FEBS Lett.* **2000**, *481*, 221-226.

(54) Mueller, C.; Schwender, J.; Zeidler, J.; K., L. H. "Properties and inhibition of the first two enzymes of the non-mevalonate pathway of isoprenoid biosynthesis". *Biochem. Soc. Trans* **2000**, *28*, 792-793.

(55) Rodríguez-Concepción, M.; Ahumada, I.; Diez-Juez, E.; Sauret-Güeto, S.; Lois, L. M. et al. "1-Deoxy-D-xylulose 5-phosphate reductoisomerase and plastid isoprenoid biosynthesis during tomato fruit ripening". *Plant J.* **2001**, *27*, 213-222.

(56) Lange, B. M.; Croteau, R. "Isoprenoid biosynthesis via a mevalonate-independent pathway in plants: cloning and heterologous expression of 1-deoxy-D-xylulose-5-phosphate reductoisomerase from peppermint". *Arch. Biochem. Biophys.* **1999**, *365*, 170-174.

(57) Jomaa, H.; Wiesner, J.; Sanderbrand, S.; Altincicek, B.; Weidemeyer, C. et al. "Inhibitors of the nonmevalonate pathway of isoprenoid biosynthesis as antimalarial drugs". *Science* **1999**, *285*, 1573-1576.

(58) Argyrou, A.; Blanchard, J. S. "Kinetic and chemical mechanism of *Mycobacterium tuberculosis* 1-deoxy-D-xylulose-5-phosphate isomeroreductase". *Biochemistry* **2004**, *43*, 4375-4384.

(59) Hoeffler, J. F.; Tritsch, D.; Grosdemange-Billiard, C.; Rohmer, M. "Isoprenoid biosynthesis via the methylerythritol phosphate pathway. Mechanistic investigations of the 1-deoxy-D-xylulose 5-phosphate reductoisomerase". *Eur. J. Biochem.* **2002**, *269*, 4446-4457.

(60) Rohdich, F.; Wungsintaweekul, J.; Fellermeier, M.; Sagner, S.; Herz, S. et al. "Cytidine 5'-triphosphate-dependent biosynthesis of isoprenoids: YgbP protein of *Escherichia coli* catalyzes the formation of 4-diphosphocytidyl-2-C-methylerythritol". *Proc. Natl. Acad. Sci. U S A* **1999**, *96*, 11758-11763.

(61) Rohdich, F.; Wungsintaweekul, J.; Eisenreich, W.; Richter, G.; Schuhr, C. A. et al. "Biosynthesis of terpenoids: 4-diphosphocytidyl-2C-methyl-D-erythritol synthase of *Arabidopsis thaliana*". *Proc. Natl. Acad. Sci. U S A* **2000**, *97*, 6451-6456.

(62) Richard, S. B.; Bowman, M. E.; Kwiatkowski, W.; Kang, I.; Chow, C. et al. "Structure of 4-diphosphocytidyl-2-C- methylerythritol synthetase involved in mevalonate- independent isoprenoid biosynthesis". *Nat. Struct. Biol.* **2001**, *8*, 641-648.

(63) Lüttgen, H.; Rohdich, F.; Herz, S.; Wungsintaweekul, J.; Hecht, S. et al. "Biosynthesis of terpenoids: YchB protein of *Escherichia coli* phosphorylates the 2-hydroxy group of 4-diphosphocytidyl-2C-methyl-D-erythritol". *Proc. Natl. Acad. Sci. U S A* **2000**, *97*, 1062-1067.

(64) Rohmer, M.; Grosdemange-Billiard, C.; Seemann, M.; Tritsch, D. "Isoprenoid biosynthesis as a novel target for antibacterial and antiparasitic drugs". *Curr. Opin. Investig. Drugs* **2004**, *5*, 154-162.

(65) Rohdich, F.; Wungsintaweekul, J.; Luttgen, H.; Fischer, M.; Eisenreich, W. et al. "Biosynthesis of terpenoids: 4-diphosphocytidyl-2-C-methyl-D-erythritol kinase from tomato". *Proc. Natl. Acad. Sci. U S A* **2000**, *97*, 8251-8256.

(66) Miallau, L.; Alphey, M. S.; Kemp, L. E.; Leonard, G. A.; McSweeney, S. M. et al. "Biosynthesis of isoprenoids: crystal structure of 4-diphosphocytidyl-2C-methyl-D-erythritol kinase". *Proc. Natl. Acad. Sci. U S A* **2003**, *100*, 9173-9178.

(67) Herz, S.; Wungsintaweekul, J.; Schuhr, C. A.; Hecht, S.; Luttgen, H. et al. "Biosynthesis of terpenoids: YgbB protein converts 4-diphosphocytidyl-2C-methyl-D-erythritol 2-phosphate to 2*C*-methyl-D-erythritol 2,4-cyclodiphosphate". *Proc. Natl. Acad. Sci. U S A* **2000**, *97*, 2486-2490.

(68) Fellermeier, M.; Raschke, M.; Sagner, S.; Wungsintaweekul, J.; Schuhr, C. A. et al. "Studies on the nonmevalonate pathway of terpene biosynthesis. The role of 2*C*-methyl-D-erythritol 2,4-cyclodiphosphate in plants". *Eur. J. Biochem.* **2001**, *268*, 6302-6310.

(69) Cunningham, F. X., Jr.; Lafond, T. P.; Gantt, E. "Evidence of a role for LytB in the nonmevalonate pathway of isoprenoid biosynthesis". *J. Bacteriol.* **2000**, *182*, 5841-5848.

(70) Campos, N.; Rodríguez-Concepción, M.; Seemann, M.; Rohmer, M.; Boronat, A. "Identification of gcpE as a novel gene of the 2-C-methyl-D-erythritol 4-phosphate pathway for isoprenoid biosynthesis in *Escherichia coli*". *FEBS Lett.* **2001**, *488*, 170-173.

(71) Altincicek, B.; Kollas, A. K.; Sanderbrand, S.; Wiesner, J.; Hintz, M. et al. "GcpE is involved in the 2-C-methyl-D-erythritol 4-phosphate pathway of isoprenoid biosynthesis in *Escherichia coli*". *J. Bacteriol.* **2001**, *183*, 2411-2416.

(72) Altincicek, B.; Kollas, A.; Eberl, M.; Wiesner, J.; Sanderbrand, S. et al. "LytB, a novel gene of the 2-C-methyl-D-erythritol 4-phosphate pathway of isoprenoid biosynthesis in *Escherichia coli*". *FEBS Lett.* **2001**, *499*, 37-40.

(73) Hecht, S.; Eisenreich, W.; Adam, P.; Amslinger, S.; Kis, K. et al. "Studies on the nonmevalonate pathway to terpenes: the role of the GcpE (IspG) protein". *Proc. Natl. Acad. Sci. U S A* **2001**, *98*, 14837-14842.

(74) Rohdich, F.; Zepeck, F.; Adam, P.; Hecht, S.; Kaiser, J. et al. "The deoxyxylulose phosphate pathway of isoprenoid biosynthesis: studies on the mechanisms of the reactions catalyzed by IspG and IspH protein". *Proc. Natl. Acad. Sci. U S A* **2003**, *100*, 1586-1591.

(75) Rohdich, F.; Hecht, S.; Gärtner, K.; Adam, P.; Krieger, C. et al. "Studies on the nonmevalonate terpene biosynthetic pathway: metabolic role of IspH (LytB) protein". *Proc. Natl. Acad. Sci. U S A* **2002**, *99*, 1158-1163.

(76) Hintz, M.; Reichenberg, A.; Altincicek, B.; Bahr, U.; Gschwind, R. M. et al. "Identification of (E)-4-hydroxy-3-methyl-but-2-enyl pyrophosphate as a major activator for human gammadelta T cells in *Escherichia coli*". *FEBS Lett.* **2001**, *509*, 317-322.

(77) Seemann, M.; Bui, B. T.; Wolff, M.; Tritsch, D.; Campos, N. et al. "Isoprenoid biosynthesis through the methylerythritol phosphate pathway: the (E)-4-hydroxy-3-methylbut-2-enyl diphosphate synthase (GcpE) is a [4Fe-4S] protein". *Angew. Chem. Int. Ed. Engl.* **2002**, *41*, 4337-4339.

(78) Wolff, M.; Seemann, M.; Tse Sum Bui, B.; Frapart, Y.; Tritsch, D. et al. "Isoprenoid biosynthesis via the methylerythritol phosphate pathway: the (E)-4-hydroxy-3-methylbut-2-enyl diphosphate reductase (LytB/IspH) from *Escherichia coli* is a [4Fe-4S] protein". *FEBS Lett.* **2003**, *541*, 115-120.

(79) Richard, S. B.; Ferrer, J. L.; Bowman, M. E.; Lillo, A. M.; Tetzlaff, C. N. et al. "Structure and mechanism of 2-*C*-methyl-D-erythritol 2,4-cyclodiphosphate synthase. An enzyme in the mevalonate-independent isoprenoid biosynthetic pathway". *J. Biol. Chem.* **2002**, *277*, 8667-8672.

(80) Eisenreich, W.; Schwarz, M.; Cartayrade, A.; Arigoni, D.; Zenk, M. H. et al. "The deoxyxylulose phosphate pathway of terpenoid biosynthesis in plants and microorganisms". *Chem. Biol.* **1998**, *5*, R221-233.

(81) Kawasaki, T.; Kuzuyama, T.; Furihata, K.; Itoh, N.; Seto, H. et al. "A relationship between the mevalonate pathway and isoprenoid production in actinomycetes". *J. Antibiotic.* **2003**, *56*, 957-966.

(82) Kuzuyama, T. "Mevalonate and nonmevalonate pathways for the biosynthesis of isoprene units". *Biosci. Biotechnol. Biochem.* **2002**, *66*, 1619-1627.

(83) Smit, A.; Mushegian, A. "Biosynthesis of isoprenoids via mevalonate in Archaea: the lost pathway". *Genome Res.* **2000**, *10(*1468-1484.

(84) Lange, B. M.; Rujan, T.; Martin, W.; Croteau, R. "Isoprenoid biosynthesis: the evolution of two ancient and distinct pathways across genomes". *Proc. Natl. Acad. Sci. U S A* **2000**, *97*, 13172-13177.

(85) Lichtenthaler, H. K.; Schwender, J.; Disch, A.; Rohmer, M. "Biosynthesis of isoprenoids in higher plant chloroplasts proceeds via a mevalonate-independent pathway". *FEBS Lett.* **1997**, *400*, 271-274.

(86) Adam, K. P.; Thiel, R.; J, Z. "Incorporation of 1-[1-(13)C]Deoxy-D-xylulose in chamomile sesquiterpenes". *Arch. Biochem. Biophys.* **1999**, *369*, 127-132.

(87) Schwarz, M. A., D. Ginkgolide biosynthesis. *Comprehensive Natural Products Chemistry: Isoprenoids including carotenoids and steroids*; Elsevier: Amsterdan, 1999; pp 367-401.

(88) Laule, O.; Fürholz, A.; Chang, H. S.; Zhu, T.; Wang, X. et al. "Crosstalk between cytosolic and plastidial pathways of isoprenoid biosynthesis in *Arabidopsis thaliana*". *Proc. Natl. Acad. Sci. U S A* **2003**, *100*, 6866-6871.

(89) Hemmerlin, A.; Hoeffler, J. F.; Meyer, O.; Tritsch, D.; Kagan, I. A. et al. "Cross-talk between the cytosolic mevalonate and the plastidial methylerythritol phosphate pathways in tobacco bright yellow-2 cells". *J. Biol. Chem.* **2003**, *278*, 26666-26676.

(90) Nagata, N.; Suzuki, M.; Yoshida, S.; Muranaka, T. "Mevalonic acid partially restores chloroplast and etioplast development in Arabidopsis lacking the non-mevalonate pathway". *Planta* **2002**, *216*, 345-350.

(91) Schwender, J.; Seemann, M.; Lichtenthaler, H. K.; Rohmer, M. "Biosynthesis of isoprenoids (carotenoids, sterols, prenyl side-chains of chlorophylls and plastoquinone) via a novel pyruvate/glyceraldehyde 3-phosphate non-mevalonate pathway in the green alga *Scenedesmus obliquus*". *Biochem. J.* **1996**, *316*, 73-80.

(92) Disch, A.; Schwender, J.; Müller, C.; Lichtenthaler, H. K.; M., R. "Distribution of the mevalonate and glyceraldehyde phosphate/pyruvate pathways for isoprenoid biosynthesis in unicellular algae and the cyanobacterium *Synechocystis* PCC 6714". *Biochem. J.* **1998**, *333*, 381-388.

(93) Kim, D.; Filtz, M. R.; Proteau, P. J. "The methylerythritol phosphate pathway contributes to carotenoid but not phytol biosynthesis in *Euglena gracilis*". *J. Nat. Prod.* **2004**, *67*, 1067-1069.

(94) White, R. J.; Margolis, P. S.; Trias, J.; Yuan, Z. "Targeting metalloenzymes: a strategy that works". *Curr. Opin. Pharmacol.* **2003**, *3*, 502-507.

(95) Testa, C. A.; Brown, M. J. "The methylerythritol phosphate pathway and its significance as a novel drug target". *Curr. Pharm. Biotechnol.* **2003**, *4*, 248-259.

(96) Boucher, Y.; Doolittle, W. F. "The role of lateral gene transfer in the evolution of isoprenoid biosynthesis pathways". *Mol. Microbiol.* **2000**, *37*, 703-716.

(97) Sauret-Güeto, S.; Ramos-Valdivia, A.; Ibáñez, E.; Boronat, A.; Rodríguez-Concepción, M. "Identification of lethal mutations in *Escherichia coli* genes encoding enzymes of the methylerythritol phosphate pathway". *Biochem Biophys. Res. Commun.* **2003**, *307*, 408-415.

(98) Wellems, T. E. "Plasmodium chloroquine resistance and the search for a replacement antimalarial drug". *Science* **2002**, *298*, 124-126.

(99) Kojo, H.; Shigi, Y.; Nishida, M. "FR-31564, a new phosphonic acid antibiotic: bacterial resistance and membrane permeability". *J. Antibiotic.* **1980**, *33*, 44-48.

(100) Kuroda, Y.; Okuhara, M.; Goto, T.; Okamoto, M.; Terano, H. et al. "Studies on new phosphonic acid antibiotics. IV. Structure determination of FR-33289, FR-31564 and FR-32863". *J. Antibiotic.* **1980**, *33*, 29-35.

(101) Mine, Y.; Kamimura, T.; Nonoyama, S.; Nishida, M.; Goto, S. et al. "In vitro and in vivo antibacterial activities of FR-31564, a new phosphonic acid antibiotic". *J. Antibiotic.* **1980**, *33*, 36-43.

(102) Neu, H. C.; Kamimura, T. "In vitro and in vivo antibacterial activity of FR-31564, a phosphonic acid antimicrobial agent". *Antimicrob. Agents Chemother.* **1981**, *19*, 1013-1023.

(103) Kuzuyama, T.; Seto, H.; Takahashi, S.; Shimizu, T. "Fosmidomycin, a specific inhibitor of 1-deoxy-D-xylulose 5-phosphate reductoisomerase in the nonmevalonate pathway for terpenoid biosynthesis." *Tetrahedron Lett.* **1998**, *39*, 7913-7916.

CHAPTER TWO

Me-DXP studies

1. Introduction

In recent years, the methylerythritol phosphate pathway to isoprenoids has been the subject of intensive research. The interest is because isoprenoids are essential for the survival of several pathogenic organisms, making the inhibition of this pathway an attractive target for the drug discovery.[1-4] The second enzyme in the methyl erythritol phosphate pathway is 1-deoxy-D-xylulose 5-phosphate reductoisomerase (DXR; EC 1.1.1.267), which catalyzes the intramolecular rearrangement of 1-deoxy-D-xylulose 5-phosphate (DXP) providing 2-*C*-methylerythrose 4-phosphate that is then reduced to 2-*C*-methyl-D-erythritol 4-phosphate (MEP) (Figure 2.1).[5] DXR is of particular interest because it is the molecular target of fosmidomycin, a new antimalarial drug.[6,7,8]

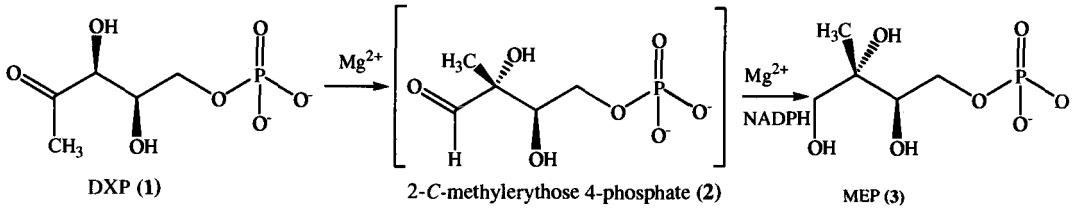

DXP (1) 2-*C*-methylerythose 4-phosphate (2) MEP (3)

Figure 2.1. DXR mediated conversion of DXP to MEP.

Due to its importance as a target not only for antimalarial drugs but also for antibacterial drugs, DXRs from several different organisms have been intensely studied. The effect of several metal ions on the DXR activity has been investigated and shown to be essential for the DXR activity. DXR showed in vitro activity in the presence of Mn^{2+}, Mg^{2+} and Co^{2+} but there was no activity, or very low activity, in the presence of other divalent ions such as Ca^{2+}, Zn^{2+}, Cu^{2+} and Fe^{2+}.[5, 9, 10] In vitro studies show that the highest k_{cat} value is obtained when Mn^{2+} is added to the reaction mixture in comparison to the addition of Mg^{2+} and Co^{2+} but the highest specificity constant (k_{cat}/K_m) was obtained for Co^{2+}.[11] Because higher levels of Mg^{2+} are present in the

cells, compared to Mn^{2+} and Co^{2+}, it is proposed to be physiologically relevant metal ion activator for DXR.[10,12] The physical parameters that give the maximal rate for the DXR reactions have also been determined. The optimal pH is between 7-8 and the optimal temperature is between 50-60 °C.[9,11]

Although much research has been conducted on DXR, the exact mechanism for forming the 2-*C*-methyl-erythrose 4-phosphate intermediate in the DXR reaction remains unknown. Three different mechanisms have been proposed: α-ketol rearrangement, retro-aldol/aldol and sequential 1,2-hydride and 1,2-methyl shifts (Figure 2.2).

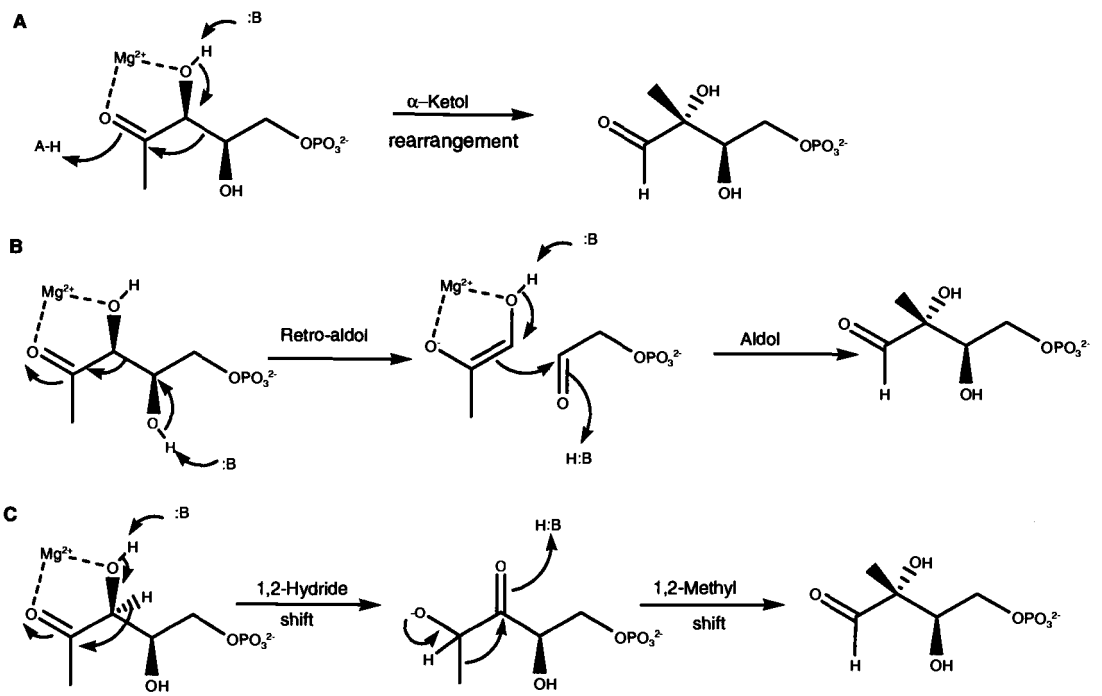

Figure 2.2. Proposed mechanisms for the rearrangement of DXP to the 2-*C*-methylerythrose 4-phosphate intermediate.[13]

One of the mechanisms, the sequential 1,2-hydride and 1,2-methyl shifts, can be eliminated based on labeling experiments.[10] Both of the other two mechanisms, an α-ketol rearrangement and the retro-aldol/aldol reactions, are possible. [10,14] Although the 2-*C*-methylerythrose 4-phosphate intermediate has never been isolated from the

DXR reaction, its chemically synthesized form has been shown to be converted into MEP by DXR.[14]

Kinetic studies with the *E. coli* DXR showed that the reaction obeys an ordered mechanism in which the NADPH binds to the enzyme before DXP, and $NADP^+$ is released after the discharge of MEP.[12] Separate isotope effect studies and product inhibition analysis using DXR from *Mycobacterium tuberculosis* suggested a random mechanism.[10] However, the authors also concede that the much lower K_m for NADPH, compared to DXP, could indicate a preferred order of binding similar to the *E. coli* enzyme.

Stereochemical experiments, using techniques such as NMR and isotope effect, with DXR proteins from *Synechocystis*,[15] *E. coli*,[16] *M. tuberculosis*,[10] and *Liriodendron tulipifera*,[17] a higher plant, revealed that the 4*S*-hydride is delivered from NADPH during the reduction step, which classifies DXR as a class B dehydrogenase. Other stereochemical issues were also reported. The C1 *pro*-S hydrogen of MEP derives from C3 of DXP and the C1 *pro*-R hydrogen comes from NADPH. Delivery of the NADPH hydride is to the *re* face of the aldehyde intermediate of the DXR reaction.[15]

The importance of DXR as a target for the development of antibacterial and antimalarial drugs and possibly for new herbicides, has stimulated detailed studies of this enzyme. Analogs of the DXR substrate DXP have been designed to aid in understanding the DXR mechanism and also to reveal the mode of DXP binding. Five DXP analogues have been synthesized and characterized using the *E. coli* DXR. The compounds (3*S*)-3-hydroxypentan-2-one 5-phosphate (**4**) and (4*S*)-4-hydroxypentan-2-one 5-phosphate (**5**), which lack the hydroxyl group at carbons four and three, respectively, were first designed to probe the DXR mechanism.[14] These compounds were not substrates for DXR, but were found to be reversible mixed-type inhibitors with K_i values of 120 and 800 μM. Three fluorinated analogues were also prepared with the same objective as the ones mentioned above. It was found that 3- and 4-fluoro-DXP (**6** and **7**) also are competitive inhibitors of DXR with similar K_is (444 and 733 μM) to the ones found for the deoxy analogs.[18] From these results it is clear that both hydroxyl groups are important for DXR catalysis and substrate binding. Two

DXP analogs can be used as alternate substrates by DXR, but they are less effective than the natural substrate DXP. The fluorinated analog 1-fluoro-DXP (8) showed a K_m of 100 μM compared with 61 μM to DXP under the same conditions.[18] Although the K_m for 1-fluoro-DXP was similar to the DXP, the catalytic efficiency (k_{cat}/K_m) for this compound was only 13 % of the one observed for DXP. (3*R*,4*S*)-3,4-Dihydroxy-5-oxohexylphosphonic acid (**9**), DXP_N, a methylene phosphonate, showed a 4-fold increase in the K_m compared to DXP. As observed for 1-fluoro-DXP a more pronounced decrease in the k_{cat}/K_m was observed for DXP_N, which was 2.5% of the one determined for DXP (Figure 2.3).[19]

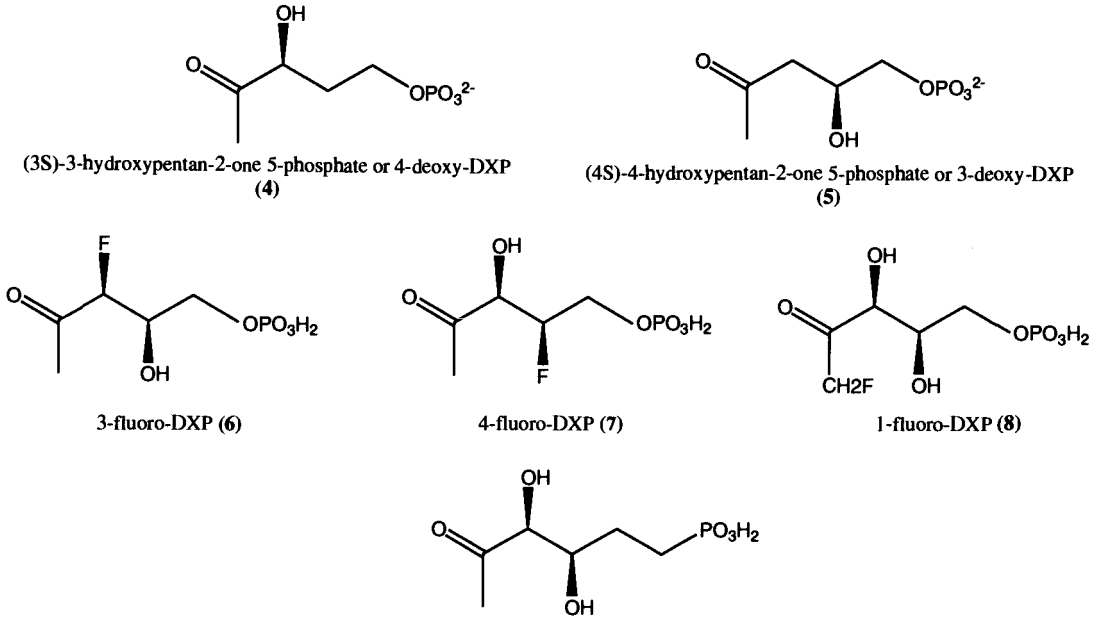

Figure 2.3. DXP analog structures.

In our laboratory six DXP analogs were prepared and tested as alternative substrates for the *Synechocystis sp.* PCC6803 DXR (Figure 2.4).[20] From the six compounds tested only one could be used as an alternative substrate for DXR, the deoxyxylulose phosphonate (**9**); the 4-deoxy and 3-deoxy DXP (**4** and **5**), DXP carboxamide (**10**) and 1-deoxy-L-ribulose 5-phosphate (**11**) are competitive inhibitors. Three of these compounds, 4-deoxy and 3-deoxy DXP (**4** and **5**) as inhibitors, and

deoxyxylulose phosphonate (**9**) as an alternate substrate, had been reported before in studies with the *E. coli* DXR.[14,19]

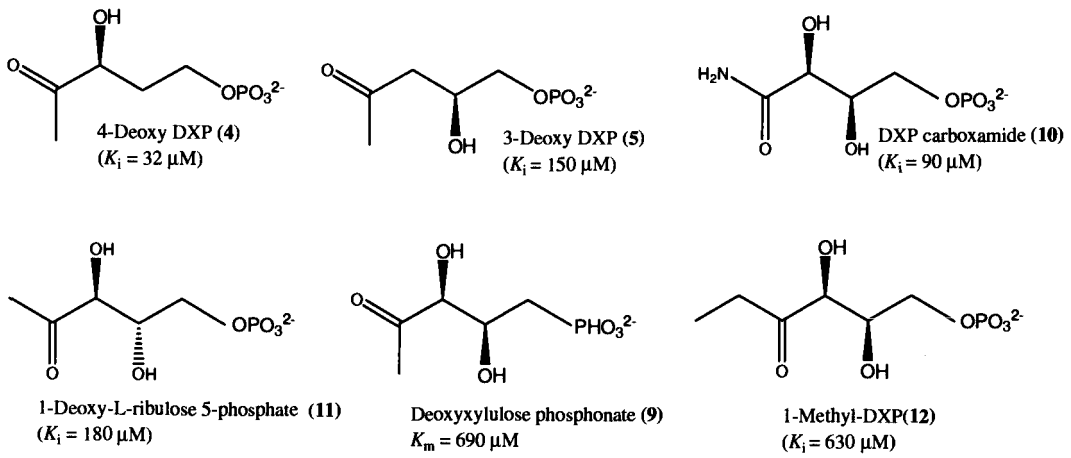

Figure 2.4. DXP analogs characterized using the *Synechocystis* DXR.

The compound 1,2-dideoxy-D-threo-3-hexulose 6-phosphate (**12**) (1-methyl-DXP or Me-DXP), that differs from DXP by having an ethyl ketone, rather than a methyl ketone (Figure 2.5) was of particular interest. Although this analog has a relatively minor structural change, it was not an alternate substrate, but acted as a weak competitive inhibitor with a K_i of 630 μM.

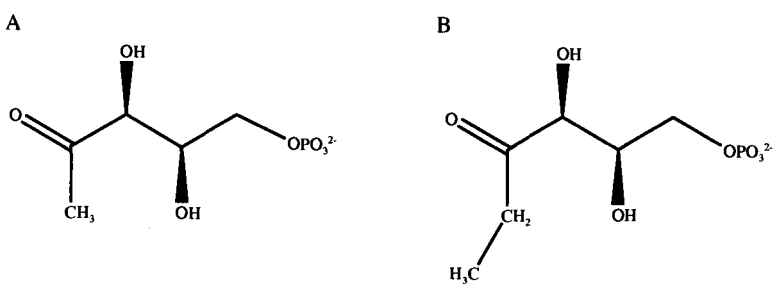

Figure 2.5. Comparison between the structures of DXP (A) and Me-DXP (B).

Two factors can contribute to the lack of turnover of Me-DXP by DXR. One would be steric limitations in the DXR active site in the vicinity of the methyl ketone moiety of DXP, preventing binding of Me-DXP in a mode favorable for catalysis. The

other factor would involve the rearrangement of Me-DXP. The DXR reaction consists of two steps (Figure 2.1), a rearrangement of the carbon backbone and a reduction. The product of the first step is a methylerythrose phosphate. The product of the rearrangement of Me-DXP will have an ethyl group instead of a methyl at C2 and thus steric hindrance may prevent the formation of this intermediate. When the DXR crystal structures became available, the possibility arose to uncover the structural basis for this lack of turnover. In this chapter we will report the use of site-directed mutagenesis guided by crystal structure analysis to produce a DXR mutant able to use the DXP analog Me-DXP, as a substrate.

2. Results

2.1. Strategy for identification of mutagenesis targets

Analysis of the *E. coli* DXR crystal structure data was used to identify the amino acid residue that might be the structural basis that prevents Me-DXP from being used as a substrate. At the start of this project, only the crystal structure of the *E. coli* DXR in the apo form, without cofactors, substrate or inhibitors, was available (PDB # 1K5H).[21] Analysis of this structure suggested that the leucine 130 and 222 residues might be interfering with Me-DXP binding. The mutants L130V, L130A and L222A were prepared and were found to not use Me-DXP as a substrate in concentrations up to 30 mM. Mutants L130A and L222A did not show any detectable activity (activity lower than 6×10^{-4} μmol min^{-1} mg^{-1}) with DXP. Mutant L130V showed no difference in the kinetic parameters for DXP and NADPH when compared with the wild-type DXR.

Shortly after the publication of the first crystal structure, a second one became available (PDB # 1JVS). In this structure NADPH was added to the crystallization buffer and crystals of DXR complexed with NADPH were obtained.[22] In addition to NADPH, a sulfate ion, from the crystallization buffer, was trapped in the DXR active site. Because DXP possesses a phosphate group the sulfate ion supposedly is occupying the phosphate binding site in DXR.

Using this second structure and Viewer-Pro protein visualization software, molecules of DXP, Me-DXP and the 2-*C*-methylerythrose 4-phosphate intermediate of the DXR reaction were placed in the putative active site of DXR (PDB # 1JVS). The sulfate ion was changed for phosphate, which served as the starting point to build the molecules of interest. Other information, such as the amino acids proposed to bind the metal ion and the position of NADPH, were also considered in the placement of the molecules in the DXR active site. Measurements were made to determine which amino acid side chain might be interacting with the extra carbon in the substrate analog. When DXP or Me-DXP was placed at the active site of the *E. coli* DXR crystal structure, it was difficult to detect any severe steric clashes with active site amino acid residues. However, when the 2-*C*-methylerythrose 4-phosphate intermediate was placed at the active site, it appeared as though the Trp^{212} indole ring might interact strongly with the methyl group of the intermediate (Figure 2.6). We hypothesized that the Trp^{212} may be an amino acid that prevents DXR from using Me-DXP as a substrate.

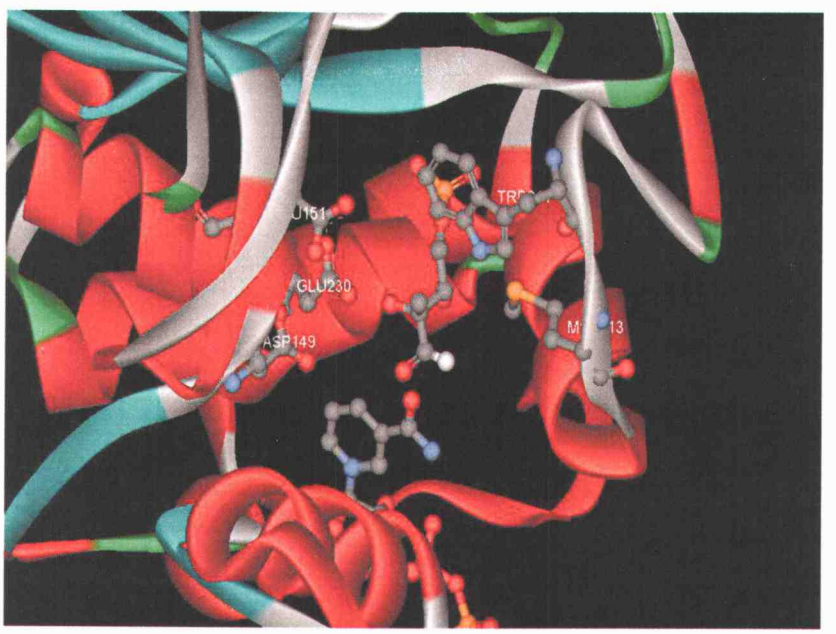

Figure 2.6. 2-*C*-methylerythrose 4-phosphate placed in the DXR active-site. The methyl group at C2 is pointing to the indole side chain of tryptophan 212 (*E. Coli* numbering).

At the later stage of our analysis a third crystal structure of DXR was published. As reported in this article, crystals of DXR were soaked with fosmidomycin and Mn^{2+} and a DXR complex with fosmidomycin and Mn^{2+} was solved.[23] In this structure the side chain of Trp^{212} is in the direct vicinity of fosmidomycin methylene chain. Although these data are consistent with our analysis, this structure needs to be considered carefully because it does not have NADPH bound. Studies with the *E. coli* DXR have shown that NADPH binds before DXP,[12] so the structure of fosmidomycin bound alone may not exactly reflect the binding mode of DXP.

Further information suggesting the overall importance of the Trp^{212} residue was provided by protein sequence alignments. Alignments of 62 deduced sequences for DXR of different organisms available in the Swiss-Prot database indicated that the Trp^{212} is invariant. This Trp^{212} was selected as target for mutagenesis. The DXR used in our laboratory is from the cyanobacterium *Synechocystis sp.* PCC6803 and was then used in this dissertation. The *E. coli* Trp^{212} corresponds to Trp^{204} in *Synechocystis* PCC6803 DXR.

2.2. Site-directed mutagenesis, mutant expression and purification

If the bulkiness of the indole ring of tryptophan prevents the turnover of Me-DXP, then a change to a less bulky side chain might allow the use of Me-DXP as substrate. In order to test this hypothesis, a series of Trp mutants was prepared, with each mutant having a progressively smaller sidechain: phenylalanine, leucine, valine, and alanine. Figure 2.7 shows a SDS-PAGE gel typical of the mutant expression. Each mutant was expressed in *E. coli* as a N-terminal 6x His-tagged protein at a level comparable with the wild-type enzyme.

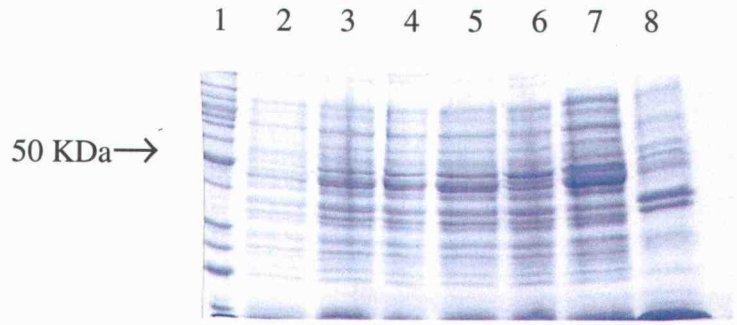

Figure 2.7. SDS-PAGE gel for overexpression of the mutant W204F mutant. The gel was stained with Coomassie Blue. Lane 1, molecular markers, lane 2, expression immediately before induction, lanes 3, 4, 5 whole cells from culture 3, 4 and 5 h after induction with L-arabinose, lane 6 (control culture) not induced, grown for 5 h, lane 7, supernatant from cells after 5 h induction, lane 8, pellet from cells after 5 h induction.

The recombinant proteins have a 6xHis tag at the N-terminus, which allowed the mutants to be purified by metal ion affinity chromatography using a Talon® resin. The talon resin contain Co^{2+} ions that will bind the His-tag in the DXR protein. A single step purification was sufficient to obtain highly purified proteins for the kinetic assays. Figure 2.8 shows the highly purified fractions that were combined and used for kinetic assays.

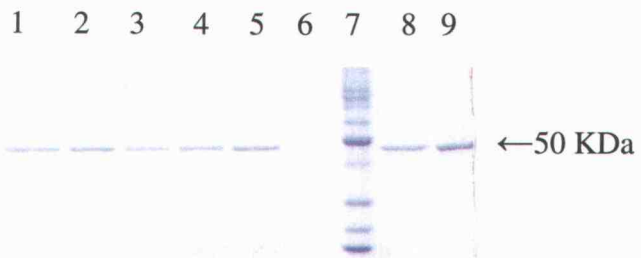

Figure 2.8. SDS-PAGE gel for part of the W204F purification. The gel was stained with Coomassie Blue. Lanes 1-5 and 8-9 represent fractions from the affinity chromatography purification. Lane 6, control (running buffer) and lane 7, molecular markers.

2.3. Comparison of kinetic parameters between the wild-type and DXR mutants when DXP was used as a substrate.

Kinetic parameters for the wild-type and the DXR mutants are summarized in Table 2.1. The K_m and k_{cat} values for each mutant were obtained using the natural substrates DXP and NADPH.

Table 2.1. Kinetic parameters for the wild-type and mutants of *Synechocystis* DXR.

DXR	K_m (μM)		k_{cat} (sec^{-1})	k_{cat}/K_m (sec^{-1} μM^{-1})
	DXP	NADPH		
Wild-type	210 ± 30	3.5 ± 0.3	17	0.1
W204F	420 ± 60	3.5 ± 1.3	10	0.024
W204L	2900 ± 400	24 ± 1	0.26	9.0×10^{-5}
W204V	5000 ± 500	ND	0.54	1.1×10^{-4}
W204A	12000 ± 2000	ND	0.16	1.3×10^{-5}

*ND = not determined.

As can be seen in Table 2.1, all four mutants showed detectable activity using DXP as substrate. The $K_{m(DXP)}$ values increased significantly as the size of the side-chain residue in the mutants decreased. The k_{cat} values decreased accordingly. Actually the k_{cat} was higher for the W204V than for the W204L mutant, although the k_{cat}/K_m is almost the same. The $K_{m(NADPH)}$ values were determined for the mutants W204F and W204L. A wild-type $K_{m(NADPH)}$ was observed for the Phe mutant and the increase for Leu mutant was 7-fold compared with the wild-type DXR. The $K_{m(NADPH)}$ was not determined for the W204V and W204A due to the high amount of DXP required to saturate these DXR mutants. These experiments provided a baseline for comparison with the Me-DXP substrate. The mutant W204F showed only a 2.5 fold increase in the K_m for DXP (Figure 2.9).

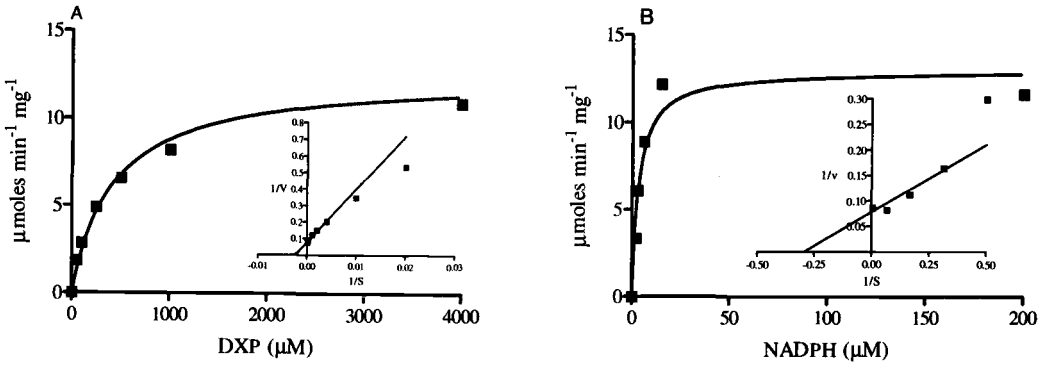

Figure 2.9. Hyperbolic curves and Lineweaver-Burk plots for determination of the kinetic parameters for DXP (A) and NADPH (B) for the mutant W204F.

The mutants with the aliphatic side chains substituting for Trp showed an increase in $K_{m(DXP)}$ with the decreasing size of the side chain (Figure 2.10). The highest K_m was observed for the mutant W204A, which had an approximately 700-fold increasing in the $K_{m\ (DXP)}$ in comparison to the wild-type, which indicates the importance of the bulky lipophilic side chain in this position. The k_{cat} and specificity constants of these aliphatic side chain mutants are much lower than for the wild-type DXR and the mutant W204F.

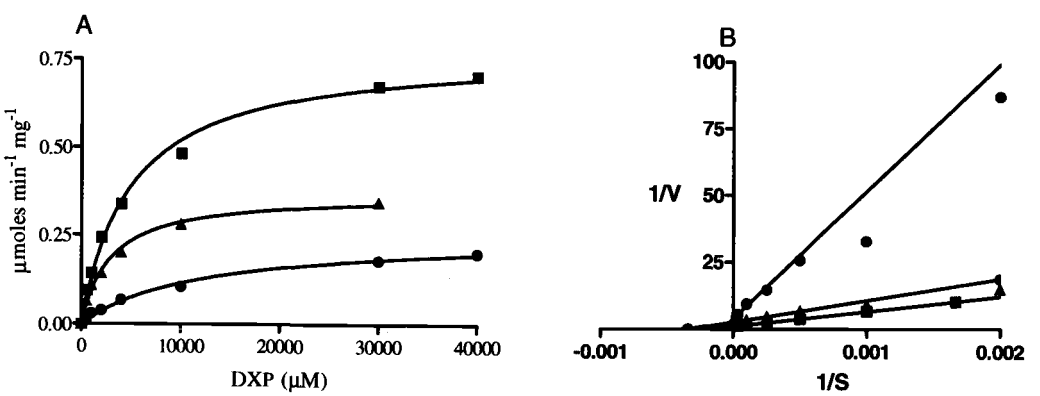

Figure 2.10. Hyperbolic curves (A) and Lineweaver-Burk (B) plots for determination of the kinetic parameters for the mutants W204L (■), W204V (▲) and (●) W204A, using DXP as substrate.

The K_m for NADPH was also determined for the mutant W204L (Table 2.1 and Figure 2.11). The K_m increased 7–fold when compared with the wild-type K_m. The K_m's for NADPH for the mutants W204V and W204A would likely also increase but they were not determined due to the requirement for high concentrations of DXP.

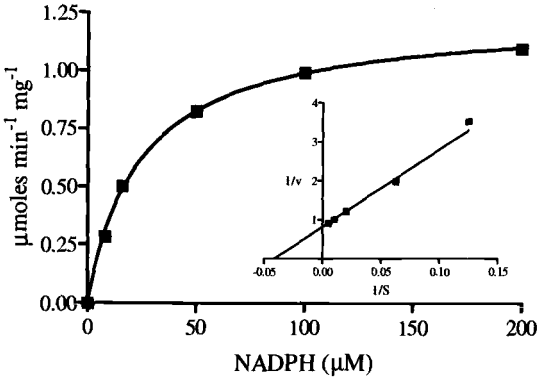

Figure 2.11. Hyperbolic curve and Lineweaver-Burk plot for determination of the K_m for NADPH using mutant W204L.

2.4. Me-DXP as a substrate for the W204 DXR mutants

When Me-DXP was used as a substrate in the standard assay for DXR in the presence of the W204F DXR mutant, oxidation of NADPH was observed, indicating DXR activity. The W204L mutant was also assayed with Me-DXP (**12**) as a sustrate, but it was only weakly active. Due to the high K_m for DXP for the valine and alanine mutants, they were not assayed with Me-DXP. To prove that the turnover product of the enzymatic activity is an ethylerythritol phosphate (**13**), Me-DXP was incubated with the mutant W204F DXR in a large scale reaction. The incubation product of the reaction was dephosphorylated and acetylated (Scheme 2.1) and purified for comparison with an authentic ethylerythritol triacetate standard using GC/MS and ^{1}H NMR.

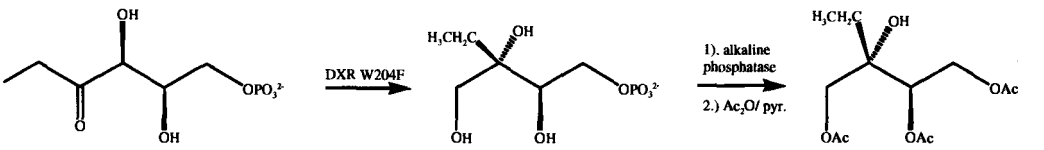

Me-DXP (12) 2-C-ethylerythritol 4-phosphate (13) Ethylerythritol triacetate (14)

Scheme 2.1. Conversion of Me-DXP into ethylerythritol phosphate and ethylerythritol triacetate.

The retention time and fragmentation pattern matched well with those of the synthetic standard. The authentic ethylerythritol triacetate eluted at an R_t of 26.01 min and the triacetate derivative from the enzymatic reaction eluted with an R_t of 26.24 min. Identical fragmentation patterns were observed for both the standard and the reaction product. In order to verify the identity of the reaction product, a co-injection of both samples showed a single higher intensity peak eluting at an R_t of 25.99 min. A ^1H NMR spectrum of the triacetate also verified the identity of the enzymatic product. The purification and identification of the ethylerythritol product were conducted by Dr. Chanokporn Phaosiri. These analyses established that the W204F mutant does convert Me-DXP into the corresponding 2-*C*-ethylerythritol 4-phosphate product.

2.5. Effect of the W204F mutation on binding of Me-DXP

To further characterize the activity of the W204F mutant, the K_m for Me-DXP was determined. Although the mutant W204F did not show a significant increase in the DXP K_m (3-fold increase), a much lower k_{cat} was observed in comparison to the value for this mutant in the presence of DXP (Table 2.2 and Figure 2.12). These results showed that although the mutant DXR can accept Me-DXP as a substrate, the turnover is much slower than with the natural substrate DXP.

Table 2.2. Comparison of the kinetic parameters of the W204F mutant of DXR using DXP and 1-methyl-DXP as substrates.

Substrate	Kinetic Parameters		
	K_m (μM)	k_{cat} (sec^{-1})	k_{cat}/K_m (sec^{-1} μM^{-1})
DXP	420 ± 60	10	0.024
1-Methyl-DXP	1300 ± 100	0.040	3.1×10^{-5}

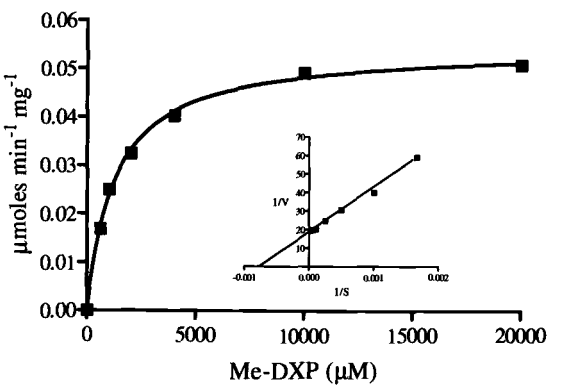

Figure 2.12. Hyperbolic curve and Lineweaver-Burk plot for determination of the K_m for Me-DXP using DXR mutant W204F.

2.6. D-xylulose 5-phosphate as a substrate for DXR

The sugar phosphate D-xylulose 5-phosphate (X5P) is an intermediate of the pentose phosphate pathway. Because the extra methyl group in the Me-DXP is similar in size to the C1 hydroxyl group of X5P, the residue Trp^{204} may also block the turnover of X5P. If this is true the mutant W204F would accept X5P as substrate while the wild-type DXR would not. To further investigate the role of Trp^{204} in the substrate specificity of DXR, attempts were made to assay X5P as a substrate to DXR.

Unfortunately, X5P is no longer available from commercial sources. X5P (**15**) can be produced by the epimerization of D-ribulose 5-phosphate (**16**, Ru5P) by the enzyme Ru5P epimerase (Figure 2.13). This approach, however, provides a mixture of

X5P and Ru5P. A control reaction using Ru5P as substrate for DXR showed that Ru5P is not a substrate for DXR.

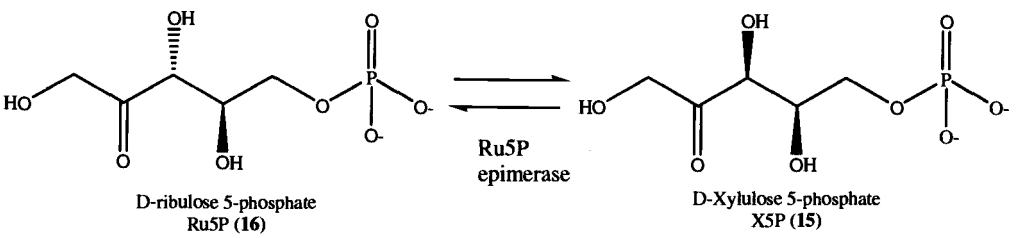

Figure 2.13. Formation of X5P by epimerization of Ru5P.

The experiment involved a coupled assay where first Ru5P is epimerized to produce X5P by the enzyme Ru5P epimerase, then X5P is used as a potential substrate for DXR. Because the DXR reaction requires NADPH, the assay was monitored by the decrease of absorbance at 340 nm. The enzyme assay with both wild-type DXR and the W204F mutant showed a decrease in the absorbance at 340 nm greater than in the control reaction where all components of the reaction but DXR was present. These results suggested that the X5P formed by the epimerase was used as substrate for DXR. The reaction time in the experiment above described was 30 min. The reaction was repeated using a longer incubation time, 2 hours instead of 30 min used in the experiment repeated above. A longer incubation time would provide higher amount of X5P and consequently higher amount of the product formed by action of DXR. A control reaction containing Ru5P, NADPH and DXR was also included. In this experiment the decrease of absorbance in the control reaction lacking DXR was 0.013/min, which is higher than the usual 0.003/min. The reaction control where Ru5P was used showed an increase in the absorbance, which was also observed in the coupled reaction (epimerase-DXR). Due to these conflicting results, another protocol for synthesis of X5P was used.

In another experiment an adaptation of the synthesis of DXP using DXP synthase was used for the synthesis of X5P.[24] Hydroxypyruvate had been shown to be accepted as an alternate substrate by the enzyme 1-deoxy-D-xylulose phosphate synthase, producing D-xylulose 5-phosphate (Figure 2.14). The relative activity of the

enzyme using hydroxypyruvate was 7% when compared with the activity with pyruvate.[25]

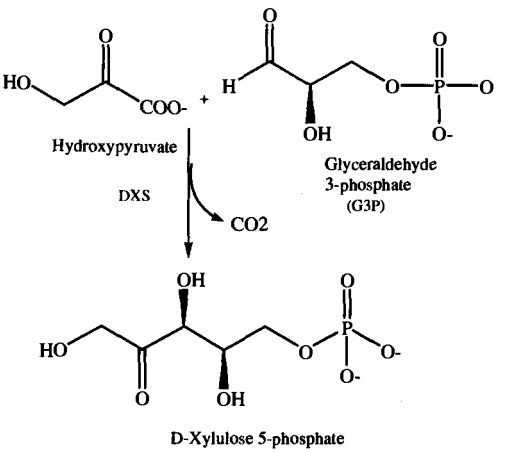

Figure 2.14. Synthesis of X5P by the enzyme 1-deoxy-D-xylulose 5-phosphate synthase.

The synthesis was monitored by assaying DXR using the reaction mixture as substrate. If X5P was being formed and it is a substrate for DXR a decrease in the absorbance should be observed. In these assays, as well assays conducted during the purification, the decrease of absorbance at 340nm was observed. After purification proton NMR analysis showed that X5P was present in the sample but it was in small amount and not pure. Because the NMR analysis showed that the X5P was not pure, it was not known if the substrate used by DXR was X5P. The synthesis was repeated and a different purification protocol was used. Using this alternative purification X5P could not be found in the purified fractions, although DXR activity was also observed during synthesis. Due to the difficult in the purification of X5P, this project was not further pursued. The evaluation of X5P as substrate for DXR needs to be the subject of further studies.

3. Discussion

The DXP analog Me-DXP, that differs from DXP by having an ethyl ketone, rather than a methyl ketone, was found to be a weak inhibitor of the enzyme instead of

an alternate substrate.[20] In order to understand the molecular basis for the lack of turnover of this compound, DXR crystal structures were analyzed in order to identify the amino acid side chain that might interfere with Me-DXP. When Me-DXP was placed in the DXR active site, no major steric clashes were observed. However when Me-DXP was replaced by the methylerythrose phosphate intermediate of the DXR reaction a severe interaction was observed. The indole moiety of Trp^{204} appeared to be in close proximity to the methyl group of the methylerythrose phosphate and may be a steric hindrance that prevents Me-DXP from being used as a substrate by DXR.

The amino acid Trp in the position 204 of *Synechocystis sp.* PCC6803 and 212 of *E. coli* is conserved in DXRs from various organisms and appears to be important for substrate binding. This Trp residue is part of the DXR flexible loop that is formed from residues 186 to 216 (*E. coli* numbering). The flexible loop also has other invariant residues such as His^{209} and Met^{214} and $Trp^{212}$and has been suggested to be essential for closing the loop over the active site, possibly forming a highly specific binding pocket.[21,23,26] The amino acid His^{209} in the Yajima structure makes a hydrogen bond with the sulfate ion. A similar bond is probably formed with the phosphate group of DXP, which can fix the substrate at the DXR active site, also assisting with closing the loop over the active site.

In the crystal structure analysis conducted in this experiment, Trp^{212} is believed to interact strongly with the methyl group of the methylerythrose intermediate. The methyl group of this intermediate has been suggested to play a crucial role in the binding of this sugar phosphate to the enzyme active site. The molecule that lacks this methyl group, D-erythrose 4-phosphate has been reported to be either a very poor substrate for DXR[12] or not to be a substrate or an inhibitor of the DXR.[14]

To investigate the hypothesis that the Trp^{204} is the steric impediment for the DXR not being able to use Me-DXP as a substrate, site-directed mutagenesis of this highly conserved Trp^{204} was undertaken. As tryptophan has a bulky side chain, the mutant W204F was constructed, which still has an aromatic side chain, but one that is smaller than tryptophan. Additional mutants with decreasing size of the aliphatic side chains, namely W204L, W204V and W204A, were also prepared. We hypothesized that these mutants might not only accept Me-DXP as substrate, but might also help

explain the molecular basis for this compound not being a substrate for the wild-type DXR and the importance of the Trp^{204} for DXR.

These mutants were expressed as soluble proteins in *E. coli* and subsequently purified. Substitution of Trp by Phe did not have a dramatic effect on substrate binding, yielding only a 2-fold increase in the K_m for DXP and no change in the K_m for NADPH. The mutant W204F was also able to convert Me-DXP to ethylerythritol phosphate proving that the Trp^{204} is a steric impediment for the wild-type DXR not to accept Me-DXP as a substrate.

The mutants W204L, W204V, and W204A, which have aliphatic side chains, showed an increase of 14-, 24- and 58-fold, respectively, in the K_m for DXP. This result suggests that an aromatic side chain in this position is important for substrate binding in DXR. A decrease in the specificity constant was observed for all of these mutants compared to the wild-type, especially for the mutant W204A, which presented a 7800-fold decrease in this value. This loss of activity strongly suggests that the aromatic side chain residue plays an important role in the binding of the DXP substrate to DXR.

This study illustrates how an x-ray crystal structure can play an important role in understanding enzyme substrate specificity. Although Me-DXP was used as a substrate, the much lower specificity constant for the mutant with Me-DXP relative to the wild-type enzyme with DXP illustrates that the new interaction between the phenyl ring of F204 and the ethyl group of the intermediate is not optimal for enzyme function. It seems reasonable that other factors are also important in discriminating substrates for this enzyme. One discriminating factor used by DXR might be a lower K_m for its natural substrate DXP than for other similar sugar phosphates present in the cells.

In conclusion, a DXR mutant was designed to accept a new substrate explaining the role of a key conserved amino acid residues for the proper functioning of the enzyme. The Trp^{204} residue present in the flexible loop has a role in the substrate binding, possibly making an important contact with the methyl group of the DXP substrate, as suggested by recent x-ray crystal data.[26]

4. Experimental procedures

4.1. General

Routine molecular biology procedures including DNA manipulation, growth and maintenance of *E. coli*, transformations and competent cell preparation were conducted according to standard techniques.[27] Restriction enzymes were used according to the manufacturer's protocols. QIAprep® spin miniprep kits (Qiagen) were used for plasmid purification.

4.2. Site-directed mutagenesis

Site-directed mutagenesis was performed using the QuikChange® mutagenesis kit from Stratagene with a pair of complementary mutagenic primers (Table 2.3). All mutations in the *dxr* gene were designed to introduce or eliminate a restriction endonuclease site, which was later used to screen the mutants. The mutated codons are in italics and the introduced or eliminated restriction site in each primer is underlined in Table 2.3. Primers were synthesized by MWG Biotech. Mutants were constructed in the pBAD-His*dxr* plasmid previously constructed as in Yin and Proteau.[9]

PCR was carried out in a total volume of 50 μL containing 50 ng of pBAD-His*dxr* template, 1X Quick change reaction buffer, 1 μL dNTP mix, 125 ng of each primer and 2.5 units of *Pfu Turbo* DNA polymerase. Following restriction of the parental plasmid strand that is methylated with *DpnI*, the PCR products were used to transform *E. coli* XLI-Blue supercompetent cells. Plasmids isolated from the resulting transformants were screened for the correct alteration in restrictions patterns using appropriate restriction endonucleases. The presence of each mutation and the absence of unwanted mutations in the plasmids with the correct restriction pattern were confirmed by automated dye terminator sequencing, which was conducted by the Center for Gene Research and Biotechnology, Oregon State University.

Table 2.3. Sequences of the primers used for site-directed mutagenesis.

Mutant	Primer	Sequence
W204A	sense	5'ACAGTACAGGATGCCCTTAAGCATCCCAAC*GCG*TCTATGGGAC 3'
	antisense	5'GTCCCATAGA*CGC*GTTGGGATGCTTAAGGGCATCCTGTACTGT 3'
W204F	sense	5'ACAGTACAGGATGCCCTTAAGCATCCCAAC*TTC*TCTATGGGAC 3'
	antisense	5'GTCCCATAGA*GAA*GTTGGGATGCTTAAGGGCATCCTGTACTGT 3'
W204L	sense	5'ACAGTACAGGATGCCCTTAAGCATCCCAAC*CTG*TCTATGGGAC 3'
	antisense	5'GTCCCATAGA*CAG*GTTGGGATGCTTAAGGGCATCCTGTACTGT 3'
W204V	sense	5'ACAGTACAGGATGCCCTTAAGCATCCCAAC*GTG*TCTATGGGAC 3'
	antisense	5'GTCCCATAGA*CAC*GTTGGGATGCTTAAGGGCATCCTGTACTGT 3'

Underlined is the introduced restriction site for *BspT* I.

4.3. Overexpression of dxr and DXR Purification

The *dxr* gene from *Synechocystis sp.* PCC6803 was previously cloned as reported.[9] The wild-type and mutants *dxr* plasmids were used to transform *E. coli* Top 10 competent cells for expression. One single colony of transformants carrying the wild-type or *dxr* mutants was grown overnight at 37 °C with shaking in LB medium supplemented with ampicillin (100 μg/mL). This seed culture (10 mL) was used to inoculate one liter of LB also supplemented with ampicillin (100 μg/mL). The cells were grown at 37 °C with shaking to an optical density at 600 nm of 0.4 –0.5 and then protein expression was induced with arabinose at a final concentration of 0.2 %. The culture was grown for an additional 4-5 hours at 37 °C.

Cells were harvested by centrifugation (3000 x *g*/10 min) and resuspended in Tris-HCl 50 mM pH 7.8, 0.3 M NaCl with 1 mg/mL of lysozyme. The solution was incubated on ice for 30 min and then lysed by sonication, on ice, in a Microson ultrasonic cell disruptor (8 x 1 min bursts at 5 watts output with 1 min cooling between bursts). Cellular debris were pelleted by centrifugation at 14000 x *g* for 30 min at 4 °C.

The soluble DXR was purified from the cleared lysate using cobalt affinity chromatography (Talon® resin, BD Bioscience). The batch/gravity flow column purification protocol was used according to the manufacturer's instructions. Following protein binding and washing with 20 mM imidazole, DXR was eluted by using increasing concentrations of imidazole in Tris-HCl pH 7.8, 0.3 M NaCl buffer (4 column volumes with 40 mM imidazole, 3 with 100 mM imidazole and 2 with 150 mM imidazole). Highly purified DXR was eluted using 100 mM imidazole.

The fractions containing DXR were verified by SDS-PAGE.[28] Fractions with highly purified DXR were pooled and concentrated with Centricon® Plus-20 concentrators from Millipore. Concentrated fractions (typically 3 mL) were dialyzed overnight at 4 °C against two changes of Tris-HCl 50 mM , 0.3 M NaCl pH 7.8 buffer. Total protein concentration was determined by using the Protein Assay Kit (Bio-Rad), based on the Bradford method.[29] DXR was stored at 4 °C and used within a few days. After use the remaining protein solution was stored at –20 °C with 20% glycerol.

4.4. DXP synthesis

DXP was enzymaticaly synthesized and purified as previously described.[24] The DXS enzyme was prepared as follows. The *dxs* gene from *E. coli* was previously cloned and overexpressed as described by Yin and Proteau.[9] The *E. coli* BL21 Gold competent cells were used for overexpression of *dxs*, which was induced by isopropyl-β-D-thiogalactopyranose (IPTG). Purification of DXS from 1 L of culture was conducted using anion exchange chromatography in a Sepharose high performance column as described before.[30]

Fructose 1-6-biphosphate (Sigma F4757, 25 mM, 406 mg), sodium pyruvate (Sigma P2256-5G, 50 mM, 220 mg), triose phosphate isomerase (Sigma T6258, 200 units), and rabbit muscle aldolase (Sigma A2714, 40 units), and 4 mg of purified DXS were added to 36 mL of buffer A (Tris-HCl 50 mM pH 7.5, $MgCl_2$ 5 mM, dithiothreitol (DTT) 1 mM and thiamine pyrophosphate (TPP) 0.5 mM) and incubated in a water bath at 37 °C. The production of DXP was checked every 8 hours using the DXR assay. After 16 hours, 4 mg of purified DXS, fructose 1,6-biphosphate (12.5

mM, 203 mg), and sodium pyruvate (25 mM, 110 mg) were added. After 48 hours the reaction was stopped by deproteinization using a Millipore Centricon® 20 column and centrifugation of 3000 rpm/20 min/4 °C. DXP was purified from the supernatant by precipitation using $BaCl_2$ and ethanol. After precipitation the pellets were dried overnight at room temperature. Excess of $BaCl_2$ was removed by gel filtration on a column of Sephadex G-10. Fractions containing DXP were detected by TLC. TLC was conducted on C18 silica plates using 6:3:1 of isopropanol/H_2O/ethyl acetate as the solvent system. The plates were developed using phosphomolybdic acid (PMA). Fractions containing DXP were combined and lyophilized. Ba^{2+} was exchanged for Na^{2+} using a Dowex-50 column. Fractions containing DXP (analyzed by TLC) were again combined and lyophilized. Proton and phosphorus NMR were used to confirm the presence and purity of DXP.[24] The DXP concentration was determined by phosphorus analysis [31] and dry weight.

4.5. Enzyme assays

The enzyme activity was assayed by monitoring the decrease in absorbance at 340 nm.[5] Routine assays to check mutant activity after expression were performed in a 1 mL mixture containing 50 mM Tris-HCl pH 7.8, 1 mM $MnCl_2$, 0.3 mM DXP and 0.2 mM NADPH. The reaction was initiated by adding the enzyme to the total assay mixture. The oxidation of NADPH was monitored at 37 °C in a Hitachi U-2000 Spectrophotometer, typically for four minutes. One unit of DXP reductoisomerase activity was defined as the amount of enzyme that caused the oxidation of 1 μmol NADPH per minute.

4.6. Kinetic studies

Using the standard DXR assay the kinetic parameters of the wild-type and mutant DXRs were determined for three substrates: DXP, Me-DXP and NADPH. Kinetic parameters were determined using between 5-7 varying concentration of these substrates, in triplicate. The concentrations ranges for DXP, Me-DXP and NADPH

were 50-40000 μM, 600-20000 μM and 2-200 μM. The amount of enzyme was adjusted to give an initial velocity for each substrate where the percentage of conversion of substrate at each concentration was less than 5%. Kinetic parameters were calculated by fitting the initial velocity versus substrate concentration to the Michaelis equation, v = (Vmax.[S])/(Km +[S]), using GraphPad Prism software.

4.7. Turnover product identification

Me-DXP was incubated with the W204F for 7 h to allow formation of enough product to be identified. Me-DXP (10 mg) was incubated with 1 mg of W204F DXR in Tris-HCl 50 mM pH 7.8, 1 mM $MnCl_2$, BSA 1mg/ml and 200 mM NADPH in a water bath at 37 °C for 7 hours. An aliquot of the reaction was checked for NADPH oxidation every 30 min. When the absorbance at 340 nm was 0.1, which occurred once, an additional 200 mM NADPH was added. After incubation, the reaction was terminated by adjusting the pH to 10 and alkaline phosphatase was added to cleave the phosphate group from the putative product. Proteins were precipitated with ethanol and the crude product solution was concentrated to dryness. The crude mixture was treated with acetic anhydride and pyridine overnight. The acetate derivative of the enzymatic product was purified by silica chromatography. The product was identified by GC/MS and proton NMR by comparison with an authentic standard.

4.8. 1-Me-DXP synthesis, synthesis of the ethylerythritol triacetate standard, and identification of the turnover product were conducted by Dr. Chanokporn Phaosiri.

4.9. D-xylulose 5-phosphate synthesis

The synthesis of X5P by epimerization of Ru5P was conducted on a small scale. Ru5P (Sigma R9875, 2 mg, 4 mM), Ru5P epimerase (Sigma R3251, 2 units), Tris-HCl 160 mM pH 7.5, $MgCl_2$ 5 mM in a total volume of 600 μL were incubated

at 37 °C.[32] After 30 min DXR was added to the reaction and the decrease of the absorbance at 340 nm was recorded for 30 min.

The synthesis of X5P using the enzyme 1-deoxy-D-xylulose synthase (DXS) was conducted as described for DXP[24] in section 4.4. The DXS enzyme was also prepared as described in section 4.4. Hydroxypyruvate lithium salt (Fluka 54913) was used instead of pyruvate.[25] Two different protocols were used for X5P purification. The first one was identical to DXP purification involving precipitation with $BaCl_2$ and ethanol as described in section 2.4.4. In the second procedure the synthesis reaction was first terminated by addition of acidic cation exchange resin (10 g of Dowex Ag 50W-X8, H^+ form). After dilution with 125 mL of water and degassing, the solution was passed through an anion exchange column (30 mL, AG 1-X8, formate form). After washing with 150 mL of water, 675 mL (23 column volume) of formic acid 1.3 N was used for elution (flow 1.7 mL/min).[33] The fractions were evaluated by TLC as described in the section 4.4.

5. References

(1) Rohdich, F.; Kis, K.; Bacher, A.; Eisenreich, W. "The non-mevalonate pathway of isoprenoids: genes, enzymes and intermediates". *Curr. Opin. Chem. Biol.* **2001**, *5*, 535-540.

(2) Lichtenthaler, H. K.; Zeidler, J.; Schwender, J.; Müller, C. "The non-mevalonate isoprenoid biosynthesis of plants as a test system for new herbicides and drugs against pathogenic bacteria and the malaria parasite". *Z. Naturforsch. [C]* **2000**, *55*, 305-313.

(3) Lichtenthaler, H. K. "Non-mevalonate isoprenoid biosynthesis: enzymes, genes and inhibitors". *Biochem. Soc. Trans.* **2000**, *28*, 785-789.

(4) Testa, C. A.; Brown, M. J. "The methylerythritol phosphate pathway and its significance as a novel drug target". *Curr. Pharm. Biotechnol.* **2003**, *4*, 248-259.

(5) Takahashi, S.; Kuzuyama, T.; Watanabe, H.; Seto, H. "A 1-deoxy-D-xylulose 5-phosphate reductoisomerase catalyzing the formation of 2-*C*-methyl-D-erythritol 4-phosphate in an alternative nonmevalonate pathway for terpenoid biosynthesis". *Proc. Natl. Acad. Sci. U S A* **1998**, *95*, 9879-9884.

(6) Borrmann, S.; Adegnika, A. A.; Matsiegui, P. B.; Issifou, S.; Schindler, A. et al. "Fosmidomycin-clindamycin for *Plasmodium falciparum* Infections in African children". *J. Infect. Dis.* **2004**, *189*, 901-908.

(7) Borrmann, S.; Issifou, S.; Esser, G.; Adegnika, A. A.; Ramharter, M. et al. "Fosmidomycin-clindamycin for the treatment of *Plasmodium falciparum* malaria". *J. Infect. Dis.* **2004**, *190*, 1534-1540.

(8) Missinou, M. A.; Borrmann, S.; Schindler, A.; Issifou, S.; Adegnika, A. A. et al. "Fosmidomycin for malaria". *Lancet* **2002**, *360*, 1941-1942.

(9) Yin, X.; Proteau, P. J. "Characterization of native and histidine-tagged deoxyxylulose 5-phosphate reductoisomerase from the cyanobacterium *Synechocystis sp.* PCC6803". *Biochim. Biophys. Acta* **2003**, *1652*, 75-81.

(10) Argyrou, A.; Blanchard, J. S. "Kinetic and chemical mechanism of *Mycobacterium tuberculosis* 1-deoxy-D-xylulose-5-phosphate isomeroreductase". *Biochemistry* **2004**, *43*, 4375-4384.

(11) Kuzuyama, T.; Takahashi, S.; Takagi, M.; Seto, H. "Characterization of 1-deoxy-D-xylulose 5-phosphate reductoisomerase, an enzyme involved in isopentenyl diphosphate biosynthesis, and identification of its catalytic amino acid residues". *J. Biol. Chem.* **2000**, *275*, 19928-19932.

(12) Koppisch, A. T.; Fox, D. T.; Blagg, B. S.; Poulter, C. D. "E. coli MEP synthase: steady-state kinetic analysis and substrate binding". *Biochemistry* **2002**, *41*, 236-243.

(13) Proteau, P. J. "1-Deoxy-d-xylulose 5-phosphate reductoisomerase: an overview". *Bioorg. Chem.* **2004**, *32*, 483-493.

(14) Hoeffler, J. F.; Tritsch, D.; Grosdemange-Billiard, C.; Rohmer, M. "Isoprenoid biosynthesis via the methylerythritol phosphate pathway. Mechanistic investigations of the 1-deoxy-D-xylulose 5-phosphate reductoisomerase". *Eur. J. Biochem.* **2002**, *269*, 4446-4457.

(15) Proteau, P. J.; Woo, Y. H.; Williamson, R. T.; C, P. "Stereochemistry of the reduction step mediated by recombinant 1-deoxy-D-xylulose 5-phosphate isomeroreductase". *Org .Lett.* **1999**, *1*, 921-923.

(16) Radykewicz, T.; Rohdich, F.; Wungsintaweekul, J.; Herz, S.; Kis, K. et al. "Biosynthesis of terpenoids: 1-deoxy-D-xylulose-5-phosphate reductoisomerase from *Escherichia coli* is a class B dehydrogenase". *FEBS Lett.* **2000**, *465*, 157-160.

(17) Arigoni, D.; Sagner, S.; Latzel, C.; Eisenreich, W.; Bacher, A. et al. "Terpenoid biosynthesis from 1-deoxy-D-xylulose in higher plants by intramolecular skeletal rearrangement". *Proc. Natl. Acad. Sci. U S A* **1997**, *94*, 10600-10605.

(18) Wong, A.; Munos, J. W.; Devasthali, V.; Johnson, K. A.; Liu , H. W. "Study of 1-deoxy-D-xylulose-5-phosphate reductoisomerase: synthesis and evaluation of fluorinated substrate analogues". *Org. Lett.* **2004**, *6*, 3625-3628.

(19) Meyer, O.; Grosdemange-Billiard, C.; Tritsch, D.; Rohmer, M. "Isoprenoid biosynthesis via the MEP pathway. Synthesis of (3,4)-3,4-dihydroxy-5-oxohexylphosphonic acid, an isosteric analogue of 1-deoxy-D-xylulose 5-phosphate, the substrate of the 1-deoxy-D-xylulose 5-phosphate reducto-isomerase". *Org. Biomol. Chem.* **2003**, *1*, 4367-4372.

(20) Phaosiri, C.; Proteau, P. J. "Substrate analogs for the investigation of deoxyxylulose 5-phosphate reductoisomerase inhibition: synthesis and evaluation". *Bioorg. Med. Chem. Lett* **2004**, *14*, 5309-5312.

(21) Reuter, K.; Sanderbrand, S.; Jomaa, H.; Wiesner, J.; Steinbrecher, I. et al. "Crystal structure of 1-deoxy-D-xylulose-5-phosphate reductoisomerase, a crucial enzyme in the non-mevalonate pathway of isoprenoid biosynthesis". *J. Biol. Chem.* **2002**, *277*, 5378-5384.

(22) Yajima, S.; Nonaka, T.; Kuzuyama, T.; Seto, H.; Ohsawa, K. "Crystal structure of 1-deoxy-D-xylulose 5-phosphate reductoisomerase complexed with cofactors: implications of a flexible loop movement upon substrate binding". *J. Biochem.* **2002**, *131*, 313-317.

(23) Steinbacher, S.; Kaiser, J.; Eisenreich, W.; Huber, R.; Bacher, A. et al. "Structural basis of fosmidomycin action revealed by the complex with 2-*C*-methyl-D-erythritol 4-phosphate synthase (IspC). Implications for the catalytic mechanism and anti-malaria drug development". *J. Biol. Chem.* **2003**, *278*, 18401-18407.

(24) Taylor, S. D. V., L. D.; Begley, T. P.; Schorken, U.; Grolle, S.; Sprenger, G. A.; Bringer-Meyer, S.; Sahm, H. J. "Chemical and enzymatic synthesis of 1-deoxy-D-xylulose-5-phosphate". *J. Org. Chem.* **1998**, *63*, 2375-2377.

(25) Schurmann, M. S., M.; Sprenger, G. A. "Fructose 6-phosphate aldolase and 1-deoxy-D-xylulose 5-phosphate synthase from Escherichia coli as tolls in enzymatic synthesis of 1-deoxysugars". *J. of Mol. Catys. B: Enzym.* **2002**, *19-20*, 247.252.

(26) Mac Sweeney, A.; Lange, R.; Fernandes, R. P. M.; Schulz, H.; Dale, G. E. et al. "The Crystal Structure of *E. coli* 1-Deoxy-d-xylulose-5-phosphate Reductoisomerase in a Ternary Complex with the Antimalarial Compound Fosmidomycin and NADPH Reveals a Tight-binding Closed Enzyme Conformation". *J. Mol. Biol.* **2005**, *345*, 115-127.

(27) Sambrook, J. R., D. *Molecular cloning A laboratory manual 3 ed*; Cold Spring Harbor Laboratory Press, 2001.

(28) Laemmli, U. K. "Cleavage of structural proteins during the assembly of the head of bacteriophage T4". *Nature* **1970**, *227*, 680-685.

(29) Bradford, M. M. "A rapid and sensitive method for the quantitation of microgram quantities of protein utilizing the principle of protein-dye binding". *Anal. Biochem.* **1976**, *72, 248-54*.

(30) Sprenger, G. A.; Schörken, U.; Wiegert, T.; Grolle, S.; de Graaf, A. A. et al. "Identification of a thiamin-dependent synthase in *Escherichia coli* required for the formation of the 1-deoxy-D-xylulose 5-phosphate precursor to isoprenoids, thiamine, and pyridoxal". *Proc. Natl. Acad. Sci. U S A* **1997**, *94*, 12857-12862.

(31) Martin, J. B.; Doty, D. "Determination of inorganic phosphate". *Anal. Chem.* **1949**, *21*, 965-967.

(32) Teige, M.; Melzer, M.; Süss, K. H. "Purification, properties and in situ localization of the amphibolic enzymes D-ribulose 5-phosphate 3-epimerase and transketolase from spinach chloroplasts". *Eur. J. Biochem.* **1998**, *252*, 237-244.

(33) Zimmermann, F. T. S., A.; Schorken, U.; Sprenger, G. A.; Fessner, WD. "Efficient multi-enzymatic synthesis of D-xylulose 5-phosphate". *Tetrahedron: Asymmetry* **1999**, *10*, 1643-1646.

CHAPTER THREE

Mutagenesis studies on 1-deoxy-D-xylulose 5-phosphate reductoisomerase

1. Introduction

Since 2002 five crystal structures of the *E. coli* DXR and one of the *Z. mobilis* DXR have been reported. The apoenzyme (PDB # 1K5H),[1] a binary complex with NADPH (PDB # 1JVS),[2] a complex with fosmidomycin, a DXR inhibitor, and Mn^{2+} (PDB # 1ONP),[3] a complex with fosmidomycin or DXP and NADPH (PDB # 1QOH and 1QOL)[4], and a complex with two different bisphosphonate inhibitors and manganese (PDB # 1T1S and 1T1R)[5] have been resolved. The *Z. mobilis* DXR structure was solved as an apoenzyme (PDB # 1ROK) and in complex with NADPH (PDB # 1QOL).[6] All of the structures show the same overall architecture and comparison of the *E. coli* and *Z. mobilis*[6] structures shows that the active site architecture of the two enzymes in these two different species is highly conserved. DXR is an elongated homodimer with a cleft-like structure in each monomer that is covered by a flexible loop. This flexible loop is proposed to act as a "lid" that closes the active site upon cofactor and substrate binding. This closure has the role of shielding the active site from solvent. The loop includes residues 186 through 216 (*E. coli* numbering) and is disordered to varying degrees in all of the structures except in the one that has fosmidomycin and NADPH bound. This last reported structure is proposed to represent an induced fit. Each monomer of DXR is subdivided into three domains: a N-terminal domain that binds NADPH and contains the motif that is characteristic of the NADPH-dependent oxidoreductases, a central (or catalytic) domain that contains the binding site for substrates, metal ions and catalytic residues, and the C-terminal region that appears to have a structural role in supporting the catalytic domain.[1, 2, 3]

Based on these X-ray structures, important active site residues have been identified (Figure 3.1). A cluster of carboxylic acids, Asp^{150}, Glu^{152} and Glu^{231} bind the

metal ion in the DXR structure that has fosmidomycin and Mn^{2+} bound.[3] In DXR catalysis, it is likely that the divalent metal ion plays a dual role. It can assist ionization of the hydroxyl group, at C3 of DXP, and also stabilize the intermediate of the reaction.[7] The functions of these acidic residues can be similar to the acidic residues of acetohydroxy acid isomeroreductase (AHIR). This enzyme is involved in the biosynthesis of the branched amino acids valine, leucine and isoleucine in plants and microorganisms and catalyzes a two-step reaction, an isomerization followed by a NADPH-dependent reduction, as does DXR. This enzyme has two different sites for cation binding and one of the cations plays a role in the isomerization and the other is responsible for the reduction step.[8,9] AHIR and DXR do not show significant sequence similarity but they are related in their function and use the same cofactor NADPH.

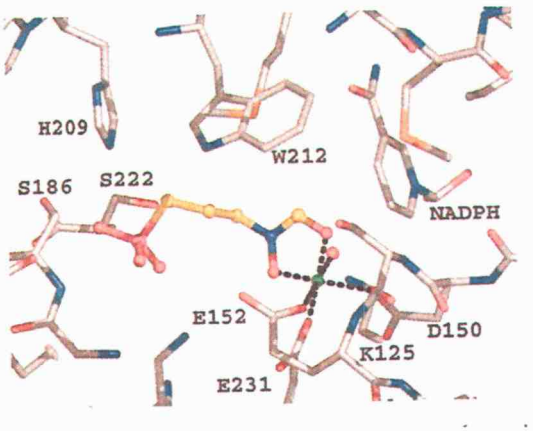

Figure 3.1. Proposed fosmidomycin binding.[4]

The residues His209, Trp212 and Met 214, present in the flexible loop, are proposed to be important for DXP binding. Hydrogen bonds of Ser186, His 209, Asn227 and Lys228 with the phosphate group are observed when DXP is bound to the DXR crystals.[4] The essential role of the phosphate group of DXP in DXP binding is supported by the fact that 1-deoxyxylulose is not a substrate for DXR.[10]

Mutagenesis studies of the *E. coli* DXR, done prior to the X-ray structures being available, show the effects of mutations of a few of the residues at the DXR active site. The E231K mutation produced an enzyme with less than 0.24% of the wild-type k_{cat}, although it had a wild-type K_m, which suggests a role of this residue in catalysis.[10] The role of three highly conserved histidines was also studied by site-

directed mutagenesis. H209Q and H257Q showed 7.6- and 20-fold increases in the K_m for DXP and a drastic reduction in the specificity constant, k_{cat}/K_m, when compared with the wild-type enzyme. His^{257} was later proposed to make stabilizing interactions with NADPH while His^{209} makes a hydrogen-bond with the phosphate group of DXP.[3,4] Kinetic characterization of the mutant H153Q showed a small increase in the K_m but a 10-fold increase in k_{cat}, which suggests that the His^{153} is involved in catalysis.[10]

Detailed knowledge of the interactions between the enzyme residues at the active site and substrate can help in the understanding of the mechanism of reaction and is also fundamental for the design of specific inhibitors. Mutation of active-site residues is frequently used to provide evidence for the importance of individual enzyme residues in substrate binding and catalysis. The goal of this project was to obtain mutants of the *Synechocystis sp.* DXR and analyze the effects of the mutations on the kinetic parameters, in comparison with the wild-type DXR. This information should help us to better understand the structure-activity relationships of this important enzyme.

2. *Results*

2.1. Selection of amino acids for site-directed mutagenesis

Our first mutagenesis studies were initiated prior to the publication of the crystal structures of DXR. To search for residues that might be important for substrate binding and catalysis, the amino acid sequences for DXR from several organisms were compared. A multiple sequence alignment of DXR was used to choose the amino acids to be mutated (Figure 3.2). The alignment revealed several highly conserved residues, including the histidine residues shown to be involved in catalysis and substrate binding for the *E. coli* DXR.[10]

```
P. falciparum       MKKYIYIYFFFITITINDLVINNTSKCVSIERRKNNAYINYGIGYNGPDNKITKSRRCKR
M. tuberculosis     ----------MATGGRVVIRRRGDNEVVAHNDEVTNSTDGRADGR----
E. coli             ----------MKQ----------
Synechocystis       ----------MVKR----------
H. pylori           ----------
Chlamydia           ----------MKH----------

P. falciparum       IKLCKKDLIDIGAIKKPINVAIFGSTGSIGTNALNIIRECNKIENVFNVKALYVNKSVNE
M. tuberculosis     ----------LRVVVLGSTGSIGTQALQVIADN--PDRFEVVGLAAGGAHLDT
E. coli             ----------LTILGSTGSIGCSTLDVVRHN--PEHFRVVA-LVAGKNVTR
Synechocystis       ----------ISILGSTGSIGTQTLDIVTHH--PDAFQVVG-LAAGGNVAL
H. pylori           ----------MVVLGSTGSIGKNALKIAKKFG-----IEIEALSCGKNIAL
Chlamydia           ----------LALIGSTGSIGRQVLQVVRSI--PDTFIIETLAAYGRNQEA
                                . * ***.*   * .

P. falciparum       LYEQAREFLPEYLCIHDKSVYEELKELVKNIKDYKPIILCGDEGMKEICSSNSIDKIVIG
M. tuberculosis     LLRQRAQTGVTNIAVADEHAAQRVGDIP----------YHGSDAATRLVEQTEADVVLNA
E. coli             MVEQCLEFSPRYAVMDDEASAKLLKTMLQQ-QGSRTEVLSGQQAACDMAALEDVDQVMAA
Synechocystis       LAQQVAEFRPEIVAIRQAEKLEDLKAAVAELTDYQPMYVVGEEGVVEVARYGDAESVVTG
H. pylori           INEQIQVFKPKKVAILDPSDLNDLEPLG-------AEVFVGLEGIDAMIEECTSNLVLNA
Chlamydia           LISQIREFNPRVVAVREETTYKELRKLFP-----HIEILLGEEGLVSVATEPSVTMTIVA
                                                     *                .

P. falciparum       IDSFQGLYSTMYAIMNNKIVALANKESIVSAGFFLKKLLNIHKNAKIIPVDSEHSAIFQC
M. tuberculosis     LVGALGLRPTLAALKTGARLALANKESLVAGGSLVLRAARPG---QIVPVDSEHSALAQC
E. coli             IVGAAGLLPTLAAIRAGKTILLANKESLVTCGRLFMDAVKQSK-AQLLPVDSEHNAIFQS
Synechocystis       IVGCAGLLPTMAAIAAGKDIALANKETLIAGAPVVLPLVEKMG-VKLLPADSEHSAIFQC
H. pylori           IVGVAGLKASFKSLQRNKKLALANKESLVSAGHLLDIS-------QITPIDSEHFGLWAL
Chlamydia           SSGIDALPAVIAAIRQKKTIALANKESLVAAGELVTTLARENG-VQILPIDSEHNALFQC
                              .     .  .***...                . * ****  .

P. falciparum       LDNNKVLKTKCLQDNFSKINNINKIFLCSSGGPFQNLTMDELKNVTSENALKHPKWKMGK
M. tuberculosis     LRGGTPD------------EVAKLVLTASGGPFRGWSAADLEHVTPEQAGAHPTWSMGP
E. coli             LPQPIQHNLGYADL---EQNGVVSILLTGSGGPFRETPLRDLATMTPDQACRHPNWSMGR
Synechocystis       LQGVPEG------------GLRRIILTASGGAFRDLPVERLPFVTVQDALKHPNWSMGQ
H. pylori           LQNKTLK-------------PKSLIISASGGAFRDTPLEFIPIQNAQNALKHPNWSMGS
Chlamydia           LEGRDSS------------TIKKLLLTASGGPLRNKSKEELQKVSLQEVLRHPVWNMGP
                    .                        . . ***  .                ** * **

P. falciparum       KITIDSATMMNKGLEVIETHFLFDVDYNDIEVIVHKECIIHSCVEFIDKSVISQMYYPDM
M. tuberculosis     MNTLNSASLVNKGLEVIETHLLFGIPYDRIDVVVHPQSIIHSMVTFIDGSTIAQASPPDM
E. coli             KISVDSATMMNKGLEYIEARWLFNASASQMEVLIHPQSVIHSMVRYQDGSVLAQLGEPDM
Synechocystis       KITIDSATLMNKGLEVIEAHYLFGLDYDHIDIVIHPQSIIHSLIEVQDTSVLAQLGWPDM
H. pylori           KITIDSASMVNKLFEILETYWLFGASLK-IDALIERSSIVHALVEFEDNSIIAHLASADM
Chlamydia           KITVDSSTLVNKGLEIIEAFWLFGLEAVEIEAVIHPQSLVHGMVEFCDGTILSVMNPPSM
                      .. *... **  * .*.  *       .  ..  . .*  .              *

P. falciparum       QIPILYSLTWPDRIKT-NLKPLDLAQVSTLTFHKPSLEHFPCIKLAYQAGIKGNFYPTVL
M. tuberculosis     KLPISLALGWPRRVSG-AAAACDFHTASSWEFEPLDTDVFPAVELARQAGVAGGCMTAVY
E. coli             RTPIAHTMAWPNRVNS-GVKPLDFCKLSALTFAAPDYDRYPCLKLAMEAFEQGQAATTAL
Synechocystis       RLPLLYALSWPERIYT-DWEPLDLVKAGSLSFREPDHDKYPCMQLAYGAGRAGGAMPAVL
H. pylori           QLPISYAIDPKLASLSASIKPLDLYALSAIKFEPISMERY-TLWCYKDLLLENPKLGVVL
Chlamydia           LFPIQHVLTFPERSPA-IGPGFDFLSNRTLEFFPIDEDRFPSVHLAKRVLLEKGSMGCFF
                      *.   .                    *       .  .

P. falciparum       NASNEIANNLFLNNKIKYFDISSIISQVLESFNSQKVSENSEDLMKQILQIHSWAKDKAT
M. tuberculosis     NAANEEAAAAFLAGRIGFPAIVGIIADVLHAADQWAVEPAT---VDDVLDAQRWARERAQ
E. coli             NAANEITVAAFLAQQIRFTDIAALNLSVLEK--MDMREPQC---VDDVLSVDANAREVAR
Synechocystis       NAANEQAVALFLQEKISFLDIPRLIEKTCDLYVGQNTASPD---LETILAADQWARRTVL
H. pylori           NASNEVAMEKFLNKEIAFGGLIQTISQALESYDKMPFKLSS---LEEVLELDKEVRERFK
Chlamydia           NGANEALVHRFLAGEISWHQIVPKLQALVDQ--HRVQSCLS---LEEILSVDAEARARAQ
                      . *     **   *   .

P. falciparum       DIYNKHNSS----------
M. tuberculosis     RAVSGMASVAIASTAKPGAAGRHASTLERS
E. coli             KEVMRLAS-----------
Synechocystis       ENSACVATRP---------
H. pylori           NVAGV--------------
Chlamydia           E------------------
```

Figure 3.2. Alignment of multiple amino acid sequences of DXR. Identical residues (*) and conservative changes in the amino acid residue (.) are noted.

In the later part of this study, in addition to the multiple sequence alignment of DXR, the selection of candidate amino acids for site-directed mutagenesis was also based on the X-ray structural information of the *E. coli* DXR. Amino acid residues of

the *Synechocystis* DXR in the following position were selected: D152, S153, E154, H155, M206, E223. These residues are equivalent to the residues D150, S151, E152, H153, M214 and E231 of the *E. coli* DXR. The single mutants D151A, D152N, S153A, S153N, S153T, E145D, E154Q, H155A, M206A, M206V, E223H and E223Q were prepared by site-directed mutagenesis.

2.2. Expression of the DXR mutants

After sequence verification, the mutant proteins were heterologously overexpressed in *E. coli* Top 10 cells. Initial small scale experiments were conducted to determine the conditions for overexpression. The mutants were expressed as soluble proteins and there was no significant difference in the expression level among the wild-type DXR and the mutants, except for the mutant E154Q that showed less expression. A typical SDS-PAGE gel obtained after overexpression is shown in the Figure 3.3.

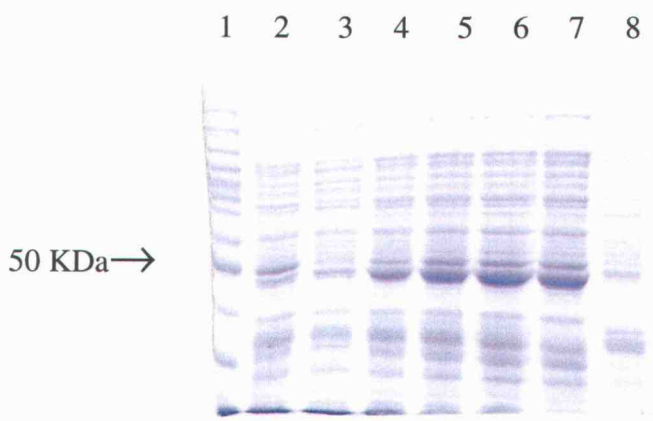

Figure 3.3. SDS-PAGE gel for overexpression of the D152Q mutant. The gel was stained with Coomassie Blue. Lane 1) molecular markers, lane 2) control culture not induced, grown for 5 h, lane 3) expression immediately before induction, lane 4, 5 and 6) whole cells from culture 3, 4 and 5 h after induction, lane 7) supernatant from cells after 5 h growth, lane 8) pellet from cells after 5 h growth.

The SDS-PAGE data showed that all the mutants have the same molecular mass (47 KDa) as the wild-type enzyme. In order to purify an adequate quantity of

protein for the enzyme assays, a one liter culture of each mutant was used. The recombinant proteins have a 6xHis tag at the N-terminus, which allowed purification of the mutants by metal ion affinity chromatography. A single step purification was sufficient to obtain highly purified protein for the kinetic assays (Figure 3.4)

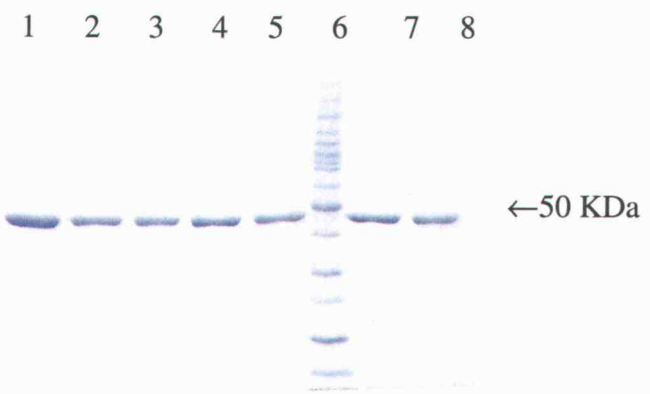

Figure 3.4. SDS-PAGE for part of the D152Q purification. The gel was stained with Coomassie Blue. Lanes 1-5 and 7-8 fractions eluted with 100 mM imidazole in the affinity chromatography purification. Lane 6) molecular markers.

2.3. DXR activity of the mutants

All amino acid substitutions, except for H155A, significantly decreased the enzymatic activity. A comparison of the V_{max} values is presented in the Table 3.1. The E154Q and E223H mutants were not further characterized due to a very low activity. The activity of mutants E154Q and E223H presented in the Table 3.1 was determined with 10 mM of DXP.

Table 3.1. V_{max} of the wild-type and mutant DXR proteins.

DXR	V_{max} (μmol $min^{-1}mg^{-1}$)	Relative V_{max} (%)
Wild-type	22	100
D152N	0.52	4.1
D152A	No activity[a]	-
S153A	0.025	0.11
S153N	0.17	0.76
S153T	1.04	4.8
E154D	0.06	0.28
E154Q	0.0018[a]	0.008
H155A	7.0	32
M206A	2.0	9
M206V	No activity[a]	-
E223H	0.0015[a]	0.007
E223Q	No activity[a]	-

[a]- activity determined in assays conducted using 10 mM DXP

Although the mutants D152A, E223Q and M206V were expressed and purified as soluble proteins, they showed no detectable activity (activity lower than 6 x 10^{-4} μmol min^{-1} mg^{-1}) under various assay conditions including much higher concentrations of substrate and enzyme and longer incubations time. Figure 3.5 shows graphically the sharp decrease of the DXR activity in the mutant proteins. Mutants D152N, S153A, S153N, S153T, E154D, H155A and M206A were fully characterized with regard to the kinetic parameters.

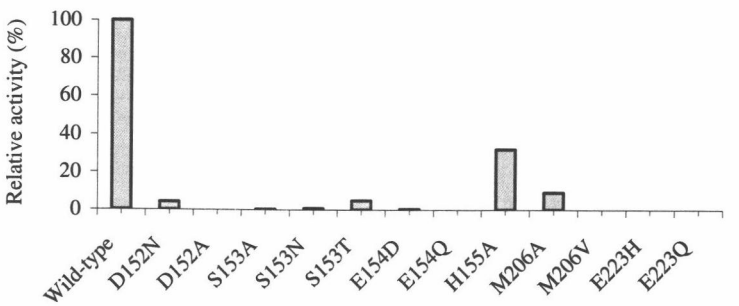

Figure 3.5. Graphic representation of the comparison between the activity of the wild-type and mutants DXRs.

2.4. Determination of kinetic constants

Steady-state kinetic measurements were performed to compare the catalytic properties of the various mutants with those of the wild-type DXR. The kinetic constants were obtained by non-linear regression plots of the saturation curves. Substrate saturation curves for DXP and NADPH were hyperbolic and consistent with the Michaelis-Menten kinetics. The kinetic properties of the mutants and wild-type DXR are shown in the Table 3.2.

D152 mutants

In the crystal structure of DXR that has Mn^{2+} bound, the residue D152 is coordinated to the Mn^{2+} ion. This residue is highly conserved in all reported DXR sequences. To understand the effect of D152 on catalysis, two types of substitution were made. The D152N mutant is an isosteric replacement with the loss of charge and the D152A mutant represents loss of charge, metal ion coordination ability, and steric bulk. The two mutants were expressed as soluble proteins, but when tested for activity the D152A mutant did not give any detectable activity under various assays conditions.

Table 3.2. Steady-state kinetic parameters for wild-type and mutant DXRs.

DXR	K_m (μM)		V_{max} (μmol $min^{-1}mg^{-1}$)	k_{cat} (sec^{-1})	$k_{cat}/K_{m(DXP)}$ (sec^{-1} μM^{-1})
	DXP	NADPH			
Wild-type	210 ± 30	3.5 ± 0.3	22	17	0.1
D152N	1500 ± 200	8 ± 2	0.52	0.41	2.7×10^{-4}
S153A	1700 ± 300	8.8 ± 1.7	0.025	0.019	1.1×10^{-5}
S153N	240± 40	5.5 ± 0.8	0.17	0.13	5.1×10^{-4}
S153T	1800 ± 300	17 ± 3	1.04	0.81	4.5×10^{-4}
E154D	250 ± 20	5.1 ± 0.8	0.06	0.047	1.9×10^{-4}
H155A	94 ± 7	2.5 ± 0.3	7.0	4.67	0.054
M206A	5300 ± 900	18 ± 5	2.0	1.55	2.9×10^{-4}

The loss of enzymatic activity likely is due to the fact that the side chain of alanine, a methyl group, can no longer act as a ligand for the metal ion. The mutant D152N showed an activity level equivalent to 2.4% of that of the wild-type enzyme (Table 3.1). Although the K_m value for DXP was 7-fold higher than that of the wild-type, the decrease in the specificity constant was 370-fold (Table 2.2). The K_m increase for the NADPH was 3.1-fold compared with the wild-type DXR. Because the carboxamide of asparagine is weaker in metal binding than the aspartate carboxylate, the K_ms for DXP at two concentrations of Mn^{2+} (1 mM and 15 mM), were determined. No major difference was observed in the kinetic parameters. The plots used for determination of the kinetic parameters determined with 1 mM of Mn^{2+} are shown in the Figure 3.6.

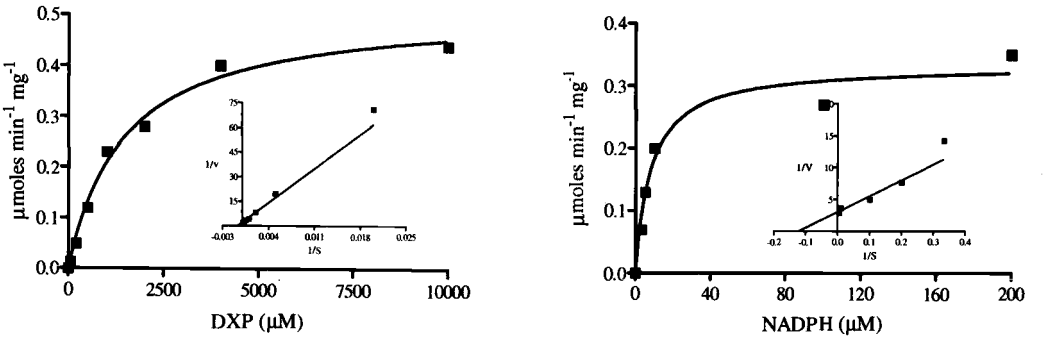

Figure 3.6. Hyperbolic curves and Lineweaver-Burk plots for determination of the kinetics parameters for DXP and NADPH for the mutant D152N.

E154 mutants

The glutamate side chain (E154) also coordinates the Mn^{2+} ion in the *E. coli* crystal structure and it is conserved in all DXR sequences available. Two mutants were constructed, E154D and E154Q. Because the Asp side chain residue is one carbon shorter than the Glu side chain and it can also be a good metal binding ligand, the change may have a major effect on the substrate binding. The E154D mutant showed only minor increases in the K_m for both DXP and NADPH (Table 3.2). Interestingly the k_{cat} of the mutant was 0.28% of the wild-type k_{cat}, which suggests that this amino acid has an important role in catalysis. The mutant E154Q showed very low enzymatic activity when the assays were performed with 10 mM of DXP for 30 min. The specific activity was 0.008% of the wild-type V_{max}. Due to this low specific activity and, therefore, the requirement for a large amount of enzyme for K_m determinations, this mutant was not further characterized. The plots used for determination of the kinetics parameters are shown in the Figure 3.7.

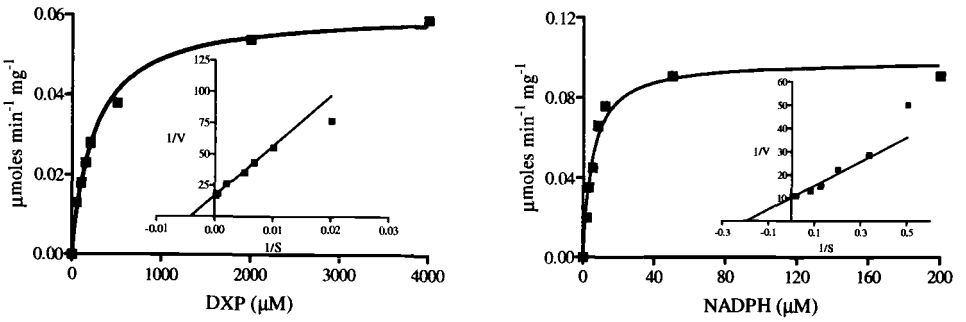

Figure 3.7. Hyperbolic curves and Lineweaver-Burk plots for determination of the kinetics parameters for DXP and NADPH for the mutant E154D.

S153 mutants

The Ser153 hydroxyl hydrogen appears to be a hydrogen bond donor to the DXP ketone carbonyl in one of the DXR crystal structure.[4] This residue is also identical in all DXR sequences available. The importance of this interaction was probed by replacing the Ser codon with the codon for Ala, Thr and Asn and three different single mutants were prepared. Elimination of the hydroxyl group by mutation to Ala had an effect on K_m for DXP (10-fold increase) and V_{max} (880-fold decrease), which led to a pronounced decrease (9000-fold) in the catalytic efficiency, k_{cat}/K_m, confirming the importance of the hydroxyl group in a H-bond. Mutant S153T showed an approximately 9-fold increase in the K_m for DXP, but its catalytic efficiency (k_{cat}/K_m) was reduced by 200-fold. When Ser was replaced by Asn no significant change in the K_m for DXP or NADPH but a 200-fold decrease in the catalytic efficiency was observed. The decrease in the catalytic efficiency of the S153 mutants suggest that this residue is important for the DXR catalysis. The K_m values for NADPH for the mutants S153T, S153N and S153A are 4.9, 1.6 and 2.5-fold higher than the value for the wild type. The plots for determination of the kinetic parameters are shown in the Figures 3.8, 3.9 and 3.10.

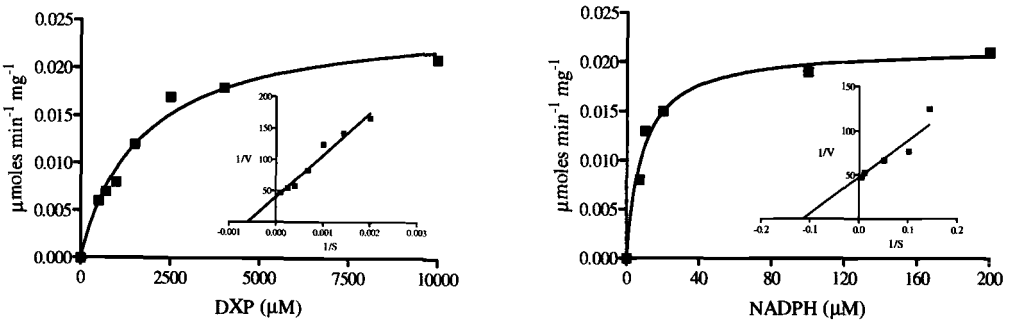

Figure 3.8. Hyperbolic curves and Lineweaver-Burk plots for determination of the kinetic parameters for DXP and NADPH for the mutants S153A.

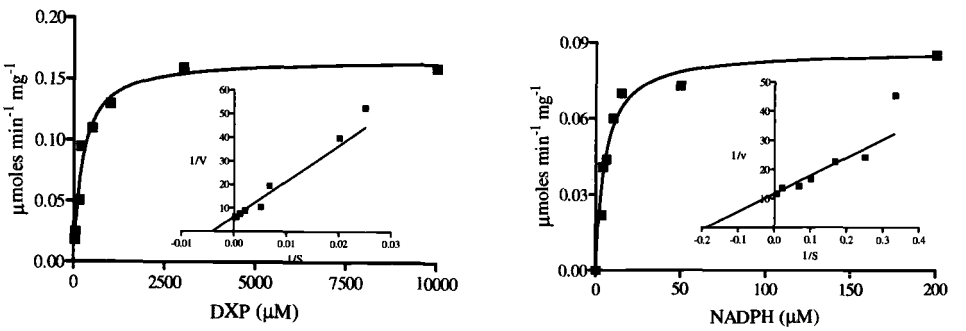

Figure 3.9. Hyperbolic curves and Lineweaver-Burk plots for determination of the kinetic parameters for DXP and NADPH for the mutants S153N.

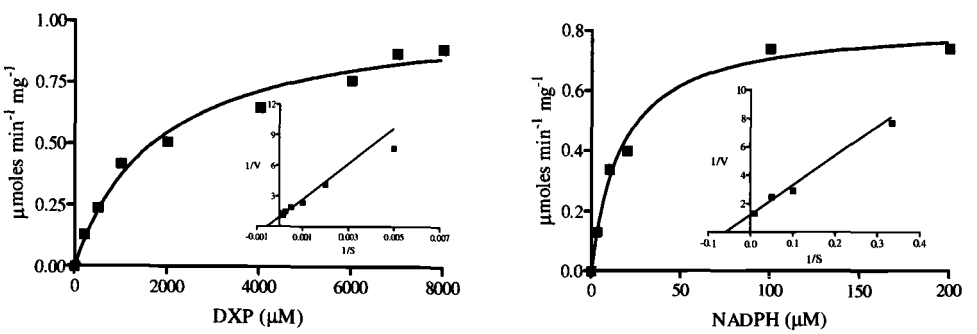

Figure 3.10. Non-linear and linear plots for determination of the kinetic parameters for DXP and NADPH for the mutants S153T.

H155A

The residue H155 was chosen based on the multiple sequence alignment of DXR. It is highly conserved in the DXR from several organisms. However our results

showed that the catalytic activity of the mutant H155A was decreased 3.6-fold, while the $K_{m(DXP)}$ actually was lower than the wild-type DXR, suggesting that this residue may not be critical for substrate binding or catalysis. In previous work with the *E. coli* DXR, this histidine had been shown to be involved in catalysis based in the kinetic characterization of a mutant H153Q (*E. coli* numbering). This *E. coli* mutant showed a 3.5–fold increase in the K_m and a 10-fold decrease in the k_{cat}.[10] The plots for determination of the kinetic parameters are shown in the Figure 3.11.

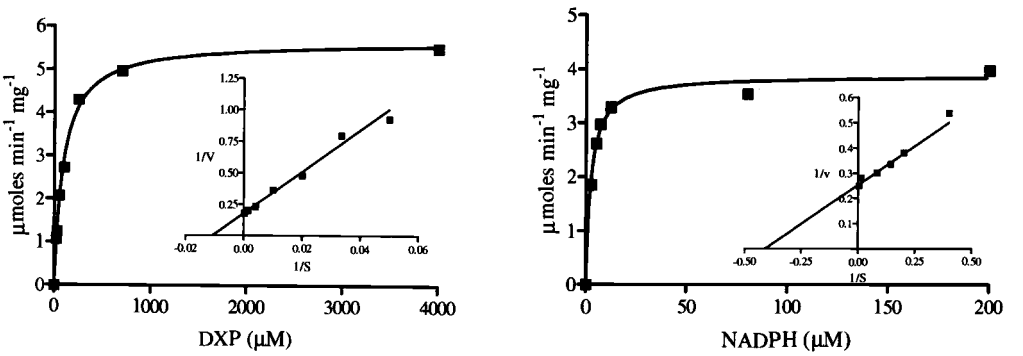

3.11. Hyperbolic curves and Lineweaver-Burk plots for determination of the kinetic parameters for DXP and NADPH for the mutants H155A.

M206 mutant

The residue M206 is in the flexible loop and may play a role in DXP binding. The effect of the mutation at position 206 on the substrate binding is clearly seen in the value of K_m for the substrate DXP. The mutation M206A resulted in a 32-fold increase in K_m for DXP, and a slight increase in K_m for NADPH. The k_{cat} decrease, 11-fold, was lower than the K_m increase, supporting the role of Met^{206} in substrate binding (Table 3.2). The mutant M206V had no detectable activity although it was expressed as a soluble protein at a similar level to the wild-type enzyme, as judged by SDS-PAGE. The plots for determination of the kinetic parameters are shown in the Figure 3.12.

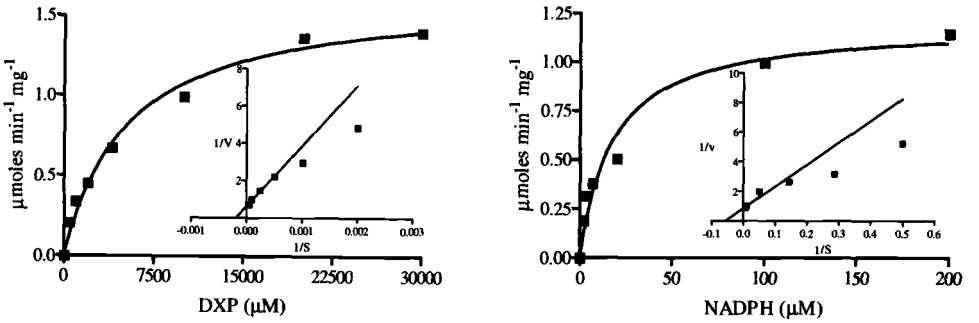

3.12. Hyperbolic curves and Lineweaver-Burk plots for determination of the kinetic parameters for DXP and NADPH for the mutant M206A.

E223 mutants

In the crystal structure of DXR that has Mn^{2+} bound, the residue E223 is coordinated to the Mn^{2+} ion. This residue is highly conserved in all reported DXR sequences. The expressed mutant E223H exhibited only very low enzyme activity (Table 3.2). The specific activity decreased 15,000-fold compared with the wild-type DXR. Further kinetic analysis was not conducted with this mutant due to the low specific activity. The E223Q mutant did not give any detectable activity under various assays conditions. The inactivation of DXR by the mutation E223Q probably occurred due to lower affinity of the glutamine chain for the metal ion.

3. Discussion

The recently solved crystal structures of the *E. coli* DXR established a foundation for the design of mutants based on the structure of this enzyme. Examination of the X-ray crystallographic structures of *E. coli* DXR complexed with fosmidomycin and Mn^{2+} (PDB # 1ONP) and fosmidomycin and NADPH (PDB # 1Q0H and 1Q0L) reveals several residues that might be involved in the substrate binding as well as residues that act as ligands for the metal ion.

Divalent metal ions are essential for the DXR activity. DXR activity is observed in the presence of Mn^{2+}, Mg^{2+} and Co^{2+} but when Ni^{2+}, Fe^{2+}, Cu^{2+} are used in the reaction no DXR activity is observed.[11,12] Although the DXR mechanism is not certainly known, the divalent metal ion is proposed to play a dual role in the DXR

catalysis; it can assist the deprotonation of the hydroxyl group, at C3 of DXP, and the stabilization of the intermediate of the reaction.[7] Based on the X-ray crystallographic structure of DXR complexed with fosmidomycin and Mn^{2+} the residues D150, E152 and E231 (*E. coli* numbering) are ligands to Mn^{2+}. Because the metal ions are essential for the DXR activity, we were interested in examining the effects of mutations in the residues E231, D152 and E154 on the DXR activity.

Experimentally, the mutant E223Q was found to be inactive under various assay conditions, while the mutant E223H remained active, but with only 0.008% of the wild-type DXR specific activity. The role of Glu^{231} has been studied for the *E. coli* DXR.[10] An E231K mutant was isolated in a screen for *dxr*-deficient mutants that absolutely required 2-*C*-methylerythritol, a free alcohol of MEP, for growth and survival, illustrating the importance of this residue for DXR activity. Kinetic characterization of the *E. coli* E231K mutant showed less than 0.24% of the wild-type k_{cat}, but wild-type K_ms for DXP and NADPH suggesting a role of Glu^{231} in catalysis. It is interesting to note that this drastic change in the *E. coli* enzyme had less effect on the enzymatic activity than the less drastic changes in the *Synechocystis* mutants E223Q and E223H. Although the mutants E223Q and E223H were not fully characterized, a significant decrease in the specific activity for the mutant E223H suggests that this residue is also important for the catalysis of *Synechocystis* DXR.

As expected for the proposed function of the Asp^{152} in metal binding the isosteric substitution of aspartate by asparagine resulted in less severe effects than the more severe change of aspartate to alanine. Although the asparagine side chain may also weekly coordinate the metal ion, the k_{cat} of this mutant was 17-fold lower than for the wild-type. The replacement of D152 by Ala, a residue with a side chain that cannot coordinate the metal ion, caused the enzyme to be totally inactive based on the detection limit of the DXR assay (Table 3.2).

The conservative mutation E154D showed almost the same K_m for DXP and NADPH, but it gave an unexpectedly large decrease in the catalytic efficiency (500-fold). The replacement of Glu154 by Gln afforded some activity, but it was only 0.008% of the wild-type level. A wild-type K_m, but a significant decrease in k_{cat} for the mutant E154D suggests that a minor conformational change in the active site of DXR

profoundly affects catalysis. The low activity of the mutant E154Q also suggests that a carboxylate seems to be the ideal metal ion ligand at this precise location.

An important structural characteristic of the DXR enzyme is the flexible loop. Differences in the conformation of this loop in different crystal structures are known. However, in the ternary complex of DXR with fosmidomycin (or DXP) and NADPH the loop becomes more ordered which is attributed to increased order due to substrate binding. Most of the residues forming this loop are highly conserved in the multiple sequence alignment of DXR sequences available in the Swiss-Prot databank. Residues in this loop are proposed to be involved in proper substrate binding and orientation. The methionine residue M206 is absolutely conserved in all DXR sequences. The His 209, also present in this loop, has been shown through site-directed mutagenesis to be involved in substrate binding.[10] In addition Met214, Trp212 and His257 form a barrier between the active site and bulk water.[4] Our results with the M206A mutant show that it is important for substrate binding. Interestingly the mutant M206V showed no detectable activity. It is possible that proper packing of the residues in this loop is necessary for DXR activity. The Val side chain probably packs differently from the methionine, which may cause a very drastic change in the loop conformation. Because Ala is a smaller than Val it may not have caused a drastic disruption in the loop arrangement.

Based on the X-ray structure (PDB # 1Q0H and 1Q0L), S153 forms a hydrogen bond with the hydroxyl group of fosmidomycin or the DXP ketone. Thus we supposed that this residue plays an important role in substrate binding. Although the highest increase in the $K_{m(DXP)}$ for the three mutants prepared (S153A, S153T and S153N) was 11-fold, the V_{max} decrease was between 21-fold for the mutant S153T and 880-fold for the mutant S153A compared with the wild-type DXR. The catalytic efficiencies (k_{cat}/K_m) were reduced substantially by 200- to 9000-fold. The mutations S153A, S153T and S153N compromised the catalytic activity of DXR with a decrease of k_{cat} as high as 900-fold for the S153A mutant (Table 3.2). On the other hand, S153N showed no difference in the K_m for DXP and NADPH. According to the crystal structure analysis, the hydroxyl group of the serine 153 residue is pointing to the DXP substrate. Although the loss of a group that can make a hydrogen-bond (mutant

S153A) did not show a large increase in the K_m it resulted in a 9000-fold decrease in the k_{cat}/K_m suggesting the importance of this hydrogen-bond for the optimal function of DXR. The amino acid residues changed in this study are shown in the Figure 3.13.

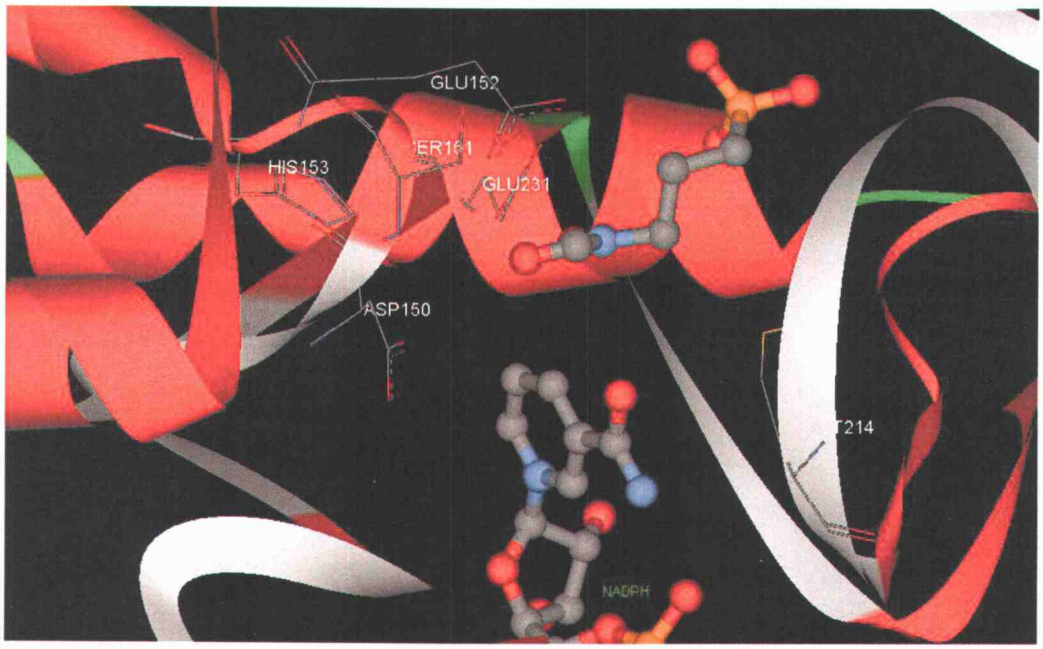

Figure 3.13. Amino acids mutated in this work. *E. coli* DXR crystal in a ternary complex with fosmidomycin and NADPH [4].

It is likely that the decrease in the specificity constants of the mutants are due to the amino acid change introduced by the mutation, not structural changes in the enzyme. Supporting evidence for that is the fact that the K_ms for NADPH are similar to the wild-type DXR (Table 3.2). Other evidence that supports no structural change is a preliminary circular dichroism (CD) experiment that showed the same pattern of folding for the M204V mutant, which has no detectable activity, and the wild-type DXR.

It was found that substitution, conservative or not, in the residues shown to be in the DXR active site in the available *E. coli* crystal structures, reduced the DXR catalytic activity. The residues studied are at the active site and in the loop and were shown to be important for maintaining a proper conformation of the active site. The results confirm that these are key amino acids responsible for the DXR catalytic efficiency.

4. Experimental procedures

4.1. General methods, overexpression, purification and assay for DXR are described in Chapter Two. DXR multiple sequence alignments were from the Swiss-Prot databank (www.expasy.org).

4.2. Site-directed mutagenesis

Site-directed mutagenesis was undertaken using the QuikChange® mutagenesis kit from Stratagene as described in Chapter Two. Primers were synthesized by MWG Biotech (Table 3.3). The mutated codon is in italics and the introduced restriction site in each primer is underlined. The presence of each mutation and the absence of unwanted mutations were confirmed by automated dye terminator sequencing which was performed by Oregon State University Central Service Laboratory. Mutants were constructed in the pBAD-HIS*dxr* plasmid previously constructed as in Yin and Proteau.[12]

4.3. Enzyme assays

The enzyme activity was assayed by monitoring the decrease in absorbance at 340 nm.[11] Routine assays to check mutant activity after expression were performed in a 1 mL mixture containing 50 mM Tris-HCl pH 7.8, 1 mM $MnCl_2$, 0.3 mM DXP and 0.2 mM NADPH. The reaction was initiated by adding the enzyme to the total assay mixture. The oxidation of NADPH was monitored at 37 °C in a Hitachi U-2000 Spectrophotometer typically for four minutes. One unit of DXP reductoisomerase activity was defined as the amount of enzyme that caused the oxidation of 1 μmol NADPH per minute.

Table 3.3. Primers used for site-directed mutagenesis of DXR.

Mutant	Primer	Sequence
D152A	sense	5' GGGGTGAAGTTATTGCCGGCGGCTAGCGAACATTCAGCC 3'
	antisense	5'GGCTGAATGTTCGCTAGCCGCCGGCAATAACTTCACCCC 3'
D152N	sense	5'- GGGGTGAAGTTATTGCCAGCGAATTCAGAACATTCAGCC 3'
	antisense	5'- GGCTGAATGTTCTGAATTCGCTGGCAATAACTTCACCCC 3'
S153A	sense	5' GGGGTGAAGTTATTGCCAGCGGATGCGGAACATTCAGCC 3'
	antisense	5' GGCTGAATGTTCCGCATCCGCTGGCAATAACTTCACCCC 3'
S153 N	sense	5' GGGGTGAAGTTATTGCCAGCGGATAACGAACATTCAGCC 3'
	antisense	5' GGCTGAATGTTCGTTATCCGCTGGCAATAACTTCACCCC 3'
S153 T	sense	5' GGGGTGAAGTTATTGCCAGCGGATACCGAACATTCAGCC 3'
	antisense	5' GGCTGAATGTTCGGTATCCGCTGGCAATAACTTCACCCC 3'
E154D	sense	5' CGGATTCAGATCATTCAGCCATTTTTCAATGTCTGCAGGGGGTT C 3'
	antisense	5' GAACCCCCTGCAGACATTGAAAAATGGCTGAATGATCTGAATCCG 3'
E154Q	sense	5' CGGATTCACAGCATTCAGCCATTTTTCAATGTCTGCAGGGGGTT C 3'
	antisense	5' G AACCCCCTGCAGACATTGAAAAATGGCTGAATGCTGTGAATCCG 3'
H155A	sense	5' GGATTCAGAAGCTTCAGCCATTTTTCAATGTCTGCAGGGGGTTCC 3'
	antisense	5' GGAACCCCCTGCAGACATTGAAAAATGGCTGAAGCTTCTGAATCC 3'
M206A	sense	5' CAGGATGCCCTTAAGCATCCCAACTGGTCTGCGGGACAAAAAATC 3'
	antisense	5' GATTTTTTGTCCCGCTGACCAGTTGGGATGCTTAAGGGCATCCTG 3'
E223H	sense	5' CGCCACATTGATGAACAAGGGTTTGCACGTCATTGAAGCCC 3'
	antisense	5' GGGCTTCAATCACGTCCAAACCCTTGTTCATCAATGTGGCG 3'
E223D	sense	5' CGCCACATTGATGAACAAGGGTTTGGACGTCATTGAAGCCC 3'
	antisense	5' GGGCTTCAATGACGTCCAAACCCTTGTTCATCAATGTGGCG 3'

The introduced restriction sites are as follows: *Nhe*I (D152A), *Pst*I (E154D, E154Q, H155A), *Aat*II (E223D), *BspT*I (M206A and M206V) and *BbrP*I (E223H). The restriction site for *Nae*I was eliminated in the mutants S153A, S153N, S153T and D150N

4.4. Kinetic studies

Using the standard spectrophotometric DXR standard assay, the kinetic parameters for the DXR mutants were determined using varying DXP and NADPH concentrations. Kinetic parameters were calculated using the initial velocities obtained from 5-7 varying substrate concentrations in triplicate, except for the mutants D152N, S153A and S153T. For these mutants determination of the kinetic parameters for NADPH were conducted in duplicate due to the high concentrations of DXP necessary to saturate the mutant enzyme. The concentration ranges for DXP and NADPH were 0.030-10 mM and 2-200 μM. To determine the kinetic parameters for each substrate, the fixed substrate was kept at least 10 times its K_m value while the concentration of the other substrate was varied. The enzyme amount was adjusted to give a velocity for each substrate where the percentage of conversion of substrate at each concentration was less than 5% per minute. Kinetic parameters were calculated by fitting the initial velocity versus substrate concentration to the Michaelis equation, $v = (V_{max}.[S])/(K_m + [S])$, using GraphPad Prism software.

5. References

(1) Reuter, K.; Sanderbrand, S.; Jomaa, H.; Wiesner, J.; Steinbrecher, I. et al. "Crystal structure of 1-deoxy-D-xylulose-5-phosphate reductoisomerase, a crucial enzyme in the non-mevalonate pathway of isoprenoid biosynthesis". *J. Biol. Chem.* **2002**, *277*, 5378-5384.

(2) Yajima, S.; Nonaka, T.; Kuzuyama, T.; Seto, H.; Ohsawa, K. "Crystal structure of 1-deoxy-D-xylulose 5-phosphate reductoisomerase complexed with cofactors: implications of a flexible loop movement upon substrate binding". *J. Biochem.* **2002**, *131*, 313-317.

(3) Steinbacher, S.; Kaiser, J.; Eisenreich, W.; Huber, R.; Bacher, A. et al. "Structural basis of fosmidomycin action revealed by the complex with 2-*C*-methyl-D-erythritol 4-phosphate synthase (IspC). Implications for the catalytic mechanism and anti-malaria drug development". *J. Biol. Chem.* **2003**, *278*, 18401-18407.

(4) Mac Sweeney, A.; Lange, R.; Fernandes, R. P. M.; Schulz, H.; Dale, G. E. et al. "The Crystal Structure of *E. coli* 1-Deoxy-d-xylulose-5-phosphate Reductoisomerase in a Ternary Complex with the Antimalarial Compound Fosmidomycin and NADPH Reveals a Tight-binding Closed Enzyme Conformation". *J. Mol. Biol.* **2005**, *345*, 115-127.

(5) Yajima, S.; Hara, K.; Sanders, J. M.; Yin, F.; Ohsawa, K. et al. "Crystallographic structures of two bisphosphonate:1-deoxyxylulose-5-phosphate reductoisomerase complexes". *J. Am. Chem. Soc.* **2004**, *126*, 10824-10825.

(6) Ricagno, S.; Grolle, S.; Bringer-Meyer, S.; Sahm, H.; Lindqvist, Y. et al. "Crystal structure of 1-deoxy-d-xylulose-5-phosphate reductoisomerase from *Zymomonas mobilis* at 1.9-A resolution". *Biochim. Biophys. Acta* **2004**, *1698*, 37-44.

(7) Argyrou, A.; Blanchard, J. S. "Kinetic and chemical mechanism of *Mycobacterium tuberculosis* 1-deoxy-D-xylulose-5-phosphate isomeroreductase". *Biochemistry* **2004**, *43*, 4375-4384.

(8) Dumas, R.; Butikofer, M. C.; Job, D.; Douce, R. "Evidence for two catalytically different magnesium-binding sites in acetohydroxy acid isomeroreductase by site-directed mutagenesis". *Biochemistry* **1995**, *34*, 6026-6036.

(9) Biou, V.; Dumas, R.; Cohen-Addad, C.; Douce, R.; Job, D. et al. "The crystal structure of plant acetohydroxy acid isomeroreductase complexed with NADPH, two magnesium ions and a herbicidal transition state analog determined at 1.65 A resolution". *EMBO J.* **1997**, *16*, 3405-3415.

(10) Kuzuyama, T.; Takahashi, S.; Takagi, M.; Seto, H. "Characterization of 1-deoxy-D-xylulose 5-phosphate reductoisomerase, an enzyme involved in isopentenyl diphosphate biosynthesis, and identification of its catalytic amino acid residues". *J. Biol. Chem.* **2000**, *275*, 19928-19932.

(11) Takahashi, S.; Kuzuyama, T.; Watanabe, H.; Seto, H. "A 1-deoxy-D-xylulose 5-phosphate reductoisomerase catalyzing the formation of 2-*C*-methyl-D-erythritol 4-phosphate in an alternative nonmevalonate pathway for terpenoid biosynthesis". *Proc. Natl. Acad. Sci. U S A* **1998**, *95*, 9879-9884.

(12) Yin, X.; Proteau, P. J. "Characterization of native and histidine-tagged deoxyxylulose 5-phosphate reductoisomerase from the cyanobacterium *Synechocystis sp. PCC6803*". *Biochim. Biophys. Acta* **2003**, *1652*, 75-81.

CHAPTER FOUR

Inhibition Studies

1. Introduction

Malaria is one of the leading causes of morbidity and mortality in the tropics, with 300-500 million estimated clinical cases and 1.5-2.7 million deaths per year. Chloroquine and other related compounds were used with high efficacy for decades to treat malaria, but in the late 1950's chloroquine resistance began to spread.[1] After the introduction of these drugs it was believed that malaria would be eradicated, but this did not happen due to the rise of *Plasmodium* species resistant to these compounds. The search for new drugs for the treatment of multidrug-resistance *Plasmodium falciparum* malaria is still a priority in malaria research. The new drug has to meet the needs once filled by chloroquine, such as efficacy, affordability, easy administration and low toxicity.[1] A novel target that is parasite specific is also desired.

Although only a few isoprenoids have been described in malaria parasites, they have been demonstrated to be essentially involved in the parasite metabolism.[2] The MVA pathway is absent in *P. falciparum,* while the MEP pathway is associated with the apicoplast.[3] The apicoplast is an unusual, self-replicating organelle essential for the *Plasmodium* survival. The apicoplast arose through a process of secondary endosymbiosis, in which the parasite ancestor engulfed a eukaryotic alga, and retained the algal plastid,[4] which evolved to be the apicoplast. The algal plastid itself is the product of a prior endosymbiosis with a cyanobacterium.[5] Once the presence of the MEP pathway to isoprenoids in the *P. falciparum* parasite was confirmed it was recognized as a promising target for the development of new antimalarial drugs.[6]

Enzymes involved in isoprenoid biosynthesis are known as important drug targets. Inhibitors of some of these enzymes are widely used as drugs. The statins, such as simvastatin (Zocor®) and lovastatin (Mevacor®), which inhibit 3-hydroxy-3-methylglutaryl coenzyme A reductase (HMG-CoA reductase) are the most successful example.[7] These inhibitors are used as cholesterol-lowering drugs. Bisphosphonates

inhibit farnesyl diphosphate synthase and are used for bone reabsorption[8] in the treatment of osteoporosis (e.g. Actonel® and Fosamax®). Bisphosphonates also have antiparasitic[9] and anticancer activity (e.g. Aredia®).[10] The azoles such as sulconazole nitrate and ketoconazole, which inhibit ergosterol biosynthesis, are widely used as antifungal agents.[11]

The inhibition of the MEP pathway, more specifically the enzyme 1-deoxy-D-xylulose 5-phosphate reductoisomerase (DXR), in the *Plasmodium* parasites was first reported by Jomaa and coworkers.[12] They demonstrated that fosmidomycin (**1**) and its analog FR900098 (**2**) (Figure 4.1) are able to inhibit growth of *P. falciparum* culture in submicromolar concentrations and also are able to cure mice infected with the malaria parasite *Plasmodium vinckei.*

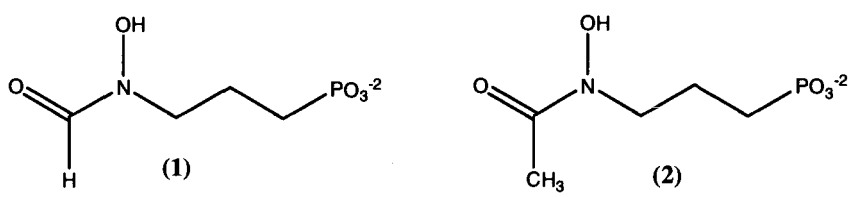

Figure 4.1. Fosmidomycin (**1**) and FR900098 (**2**) structures.

These experiments conclusively established the MEP pathway as a novel target for antimalarial chemotherapy. Clinical trials have shown fosmidomycin can be used with a high rate of success for the malaria treatment.[13,14] However, when fosmidomycin is used alone a high level of recrudescence or return of malaria, has been observed. Studies have shown that the recrudescence can be eliminated with the combined use of fosmidomycin and clindamycin.[15,16]

Besides fosmidomycin some biphosphonates compounds were found to inhibit the growth of *P. falciparum.* They were proposed to stop growth by inhibition of DXR and perhaps could be alternatives to fosmidomycin in the development of new antimalarial drugs. To find out if these compounds were inhibiting DXR, screening with the *E. coli* DXR assay was conducted. Two compounds showed IC_{50} values varying between 4 and 7 μM. These values were much higher than the fosmidomycin IC_{50} (~0.035 μM), but similar to the values found for 30 compounds that came out

from a program that screened 32000 compounds for DXR inhibition.[17] The compounds named [(1-isoquinolonylamino) methylene]-1,1-bisphosphonate (**3**) and [(5-chloro-2-pyrydinyl)amino] methylene]-1,1-bisphosphonate (**4**) (Figure 4.2), were soaked into DXR crystals and shown to bind to DXR in a fashion similar to DXP binding.[18]

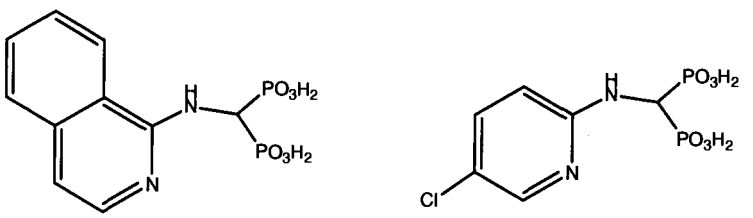

(3) (4)

Figure 4.2. Bisphosphonate inhibitors of DXR.

Fosmidomycin is a natural product produced by *Streptomyces lavendulae* and has strong antibacterial activity against bacteria that harbor the MEP pathway.[19] When fosmidomycin was first described, its target was unknown, but it achieved good safety and efficacy in a phase I clinical trial.[20,21] The development of fosmidomycin as an antibiotic was not continued because of the high frequency of resistance that was due to the fact that fosmidomycin is transported into bacterial cells by a sugar phosphate transport system that can be readily lost.[22] Pioneering studies of fosmidomycin suggested that its mode of action was inhibition of isoprenoid biosynthesis, possibly a prenyltransferase, due to the inhibition of carotenoid and menaquinone biosynthesis in *Micrococcus luteus*.[23] Years later the MEP pathway, more specifically the DXR enzyme, was found to be the true target of fosmidomycin.[19]

Fosmidomycin was first suggested to be binding in the DXR active site in the same mode as the intermediate of the DXR reaction, 2-C-methylerythrose 4-phosphate (**5**).[19] This conclusion was based on the structural similarity of the two compounds (Figure 4.3). However, analysis of a crystal structure of DXR with fosmidomycin bound concluded that it binds in a different way than the aldehyde intermediate.[24] A model where DXP can be excellently superimposed onto fosmidomycin was proposed, indicating that fosmidomycin was binding in a fashion similar to the DXP substrate.

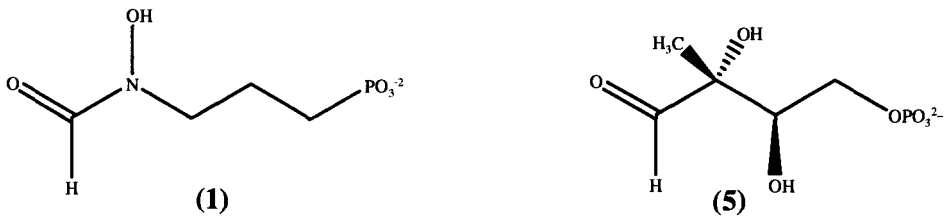

Figure 4.3. Fosmidomycin (**1**) and 2-C-methylerythrose-4-phosphate (**5**) structures.

Enzymatic assays using fosmidomycin as an inhibitor showed that DXR is strongly inhibited by this compound with an IC_{50} value of 24 nM, while in vivo assays using 3.13 μg/ml of fosmidomycin showed complete inhibition of *E. coli* growth.[19] Initial kinetic studies using fosmidomycin and the *E. coli* DXR showed a K_i of 38 nM and a mixed inhibition pattern.[19] Different results were found using the *Z. mobilis* DXR. The enzyme from this organism showed a K_i of 600 nM and a competitive inhibition pattern.[25] Later, detailed inhibition studies of the *E. coli* DXR showed that this inhibitor has slow, tight-binding properties that could explain the mixed inhibition pattern found earlier.[26] According to this mechanism of inhibition, two different inhibition constants can be obtained. K_i describes the formation of the EI complex while K_i*, represents conversion to the tightly bound complex and can be considered the overall inhibition constant.[27]

The efficacy of fosmidomycin against the DXR of plants was studied in chromoplasts of *Capsicum*[28]. Fosmidomycin at 100 μM completely inhibited the conversion of [1,2-^{14}C] DXP into β-carotene. The IC_{50} value was found to be 2.5 μM, which is much higher than in bacteria. This higher value might be explained by a poor uptake of fosmidomycin inside the chromoplasts cells or could be due to a higher K_i. Addition of MEP or IPP in the system restored the β-carotene production.[28] From these results it was possible to conclude that fosmidomycin specifically inhibits DXR in both plants and microorganisms.

Due to the promising use of fosmidomycin for treating malaria and as a lead compound for the development of new drugs, several studies with this compound have been reported. In an early study several carboxylic acid and hydroxyurea analogs of

fosmidomycin (Figure 4.4) were synthesized but, their biological activity was not evaluated.[29,30]

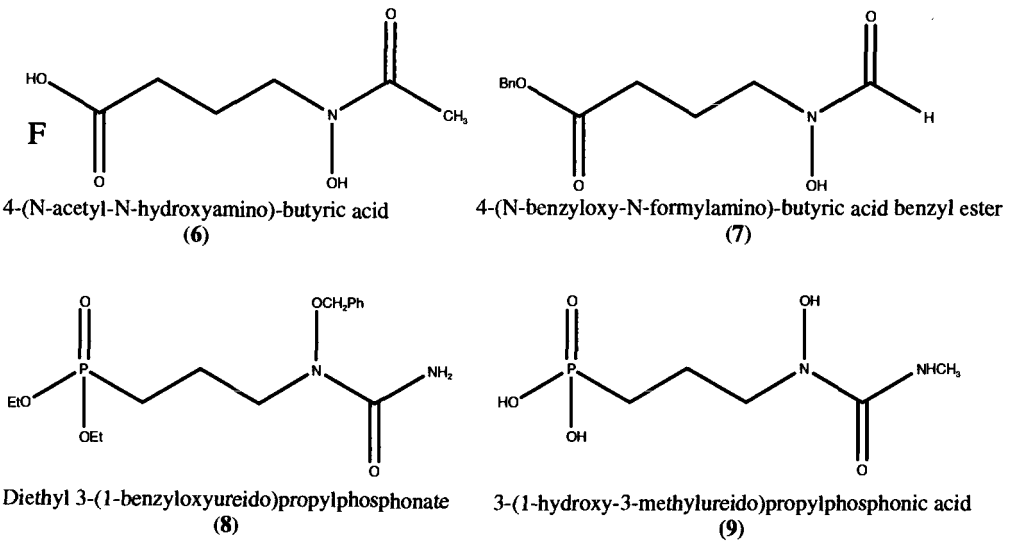

Figure 4.4. Examples of the carboxylic acid (**6,7**) and hydroxyurea (**8,9**) analogs of fosmidomycin.

More recent efforts have reported two new hydroxamate inhibitors related to fosmidomycin (Figure 4.5). They are slow, tight-binding inhibitors and nearly as efficient as fosmidomycin in enzyme assays using *E. coli* DXR, showing K_i and K_i* values of 169 and 68 nM for 4-(hydroxyamino)4-oxobutylphosphonic acid (**10**) and 54 and 3 nM for 4-[hydroxyl(methyl) amino]4-oxobutyl phosphonic acid (**11**).[31]

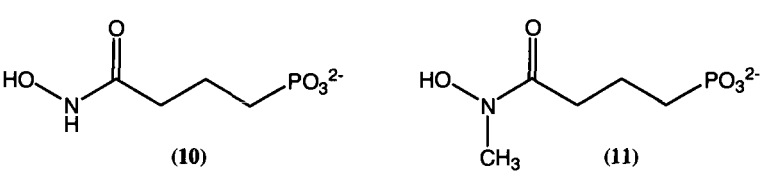

Figure 4.5. Fosmidomycin analogs.

However, as to antimicrobial activity, these inhibitors are less efficient against *E. coli* than fosmidomycin, but 4-[hydroxyl(methyl)amino]4-oxobutyl phosphonic acid was active against an *E. coli* strain resistant to fosmidomycin.

In our laboratory several fosmidomycin analogs were synthesized and evaluated for the ability to inhibit the *Synechocystis* DXR (Figure 4.6).[32] These inhibitors were prepared before the crystal structure of the DXR was available and were designed to give better insight into the structural requirement of the inhibitor for optimal interactions with the active site residues. Some of the inhibitors showed greater affinity to DXR than fosmidomycin.

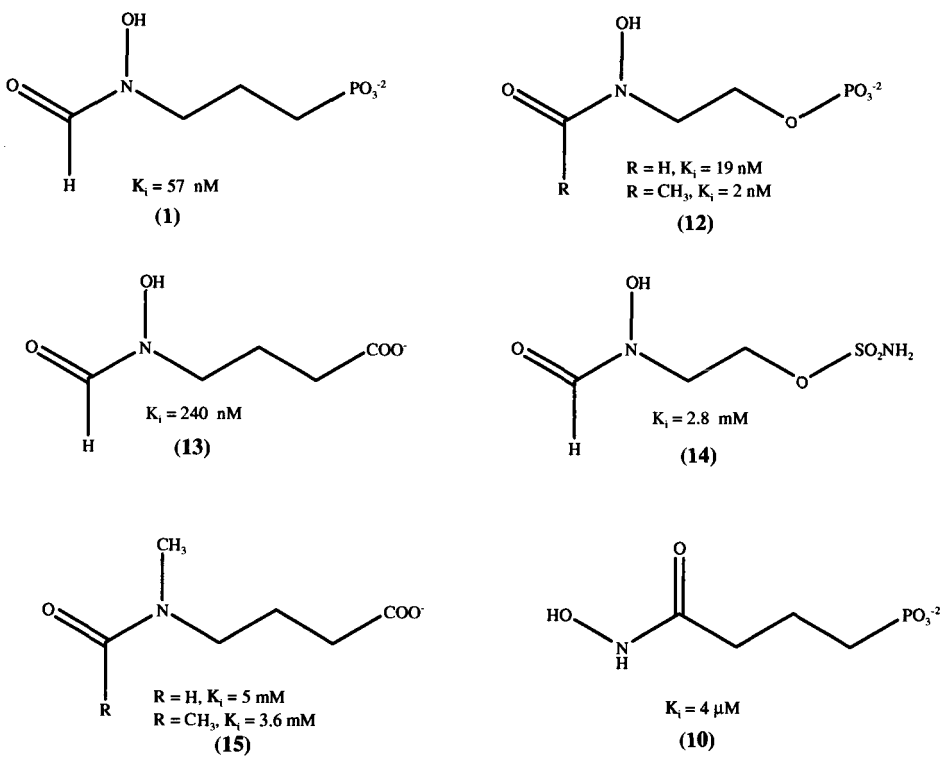

Figure 4.6. Structure of fosmidomycin (**1**) and the phosphate (**12**), carboxylate (**13**), sulfamoyl (**14**), N-methyl-N-formyl and N-methyl-N-acetyl (**15**) and reversed hydroxamate (**10**) analogs.

In the kinetic studies using the *Synechocystis sp.* PCC6803 DXR and both fosmidomycin and its hydroxamate analog as inhibitors, it was noticed that sometimes the rate of the reaction was higher in the first minute than in the last minutes. These inhibitors also showed a mixed type of inhibition (competitive and noncompetitive) that was consistent with reports that fosmidomycin and some of its analogs are slow, tight-binding inhibitors.[32] In the second part of this Chapter the re-evaluation of the

inhibition constants of fosmidomycin and the hydroxamate analog will be presented. Experiments suitable for the analysis of slow, tight-binding inhibitors were conducted.

The initial mode of fosmidomycin binding to DXR was revealed by the soaking of fosmidomycin and Mn^{2+} in DXR crystals.[24] However, this structure lacked NADPH, which is known to bind to DXR prior to DXP,[26] so the true mode of fosmidomycin binding was not known. A DXR crystal structure representing the tight binding mode of fosmidomycin binding was recently obtained.[33] Interestingly in this structure it was observed that fosmidomycin and NADPH were bound in the absence of the metal ion, although Mg^{2+} was present at 10 mM in the crystallization buffer. Motivated by a crystal structure we carried out inhibition studies of fosmidomycin with the *E. coli* DXR. Our experiments were designed to answer two questions: 1) Is the metal ion necessary for DXR inhibition by fosmidomycin? and 2) Is the inhibition of DXR dependent on a specific metal ion? In the first part of this Chapter, inhibition studies of fosmidomycin using the three metal ions, Co^{2+}, Mg^{2+} and Mn^{2+}, that support DXR activity, will be presented. Determination of the K_ms for Co^{2+}, Mg^{2+} and Mn^{2+} was also carried out. These latter experiments will provide an explanation for the absence of the metal ion in the DXR crystal structure.

2. Results and Discussion

2.1. Fosmidomycin inhibition studies using the E. coli DXR.

Before performing the fosmidomycin inhibition studies using the *E. coli* DXR, the K_ms for DXP in the presence of Mg^{2+} and Mn^{2+} were evaluated. All of the experiments to determine the Michaelis constants presented in this Chapter utilized at least seven concentrations of the variable substrate and were run in triplicate. The kinetic parameters were calculated using non-linear regression analysis. The K_m (DXP) using Mn^{2+} as the divalent ion was determined to be 190 μM ± 20 μM and Mg^{2+} 230 μM ± 30 μM. These values are similar to the ones reported by other laboratories using His-tag *E. coli* DXR.[34,35] They are somewhat higher K_ms than what others found with Mg^{2+} to native *E. coli* DXR.[26]

Additional studies determined the K_ms for the metal ions Co^{2+}, Mg^{2+} and Mn^{2+}. Although the K_ms for these metal ions had already been determined for the *Synechocystis sp.*[36] and *M. tuberculosis*[37] DXRs, there were no reports of these parameters for the *E. coli* DXR. These experiments were important due to the requirement for saturation during the experiments for determination of the K_i values. (Figure 4.7)

The K_ms determined at pH 7.6 for the ions Co^{2+} and Mn^{2+} are 2 μM and 17 μM, respectively, and showed no major differences for the K_ms found for these ions for the DXR from *Synechocystis*[36] and *Mycobacterium tuberculosis*[37] (Table 1). The K_m value observed for Mg^{2+} was 210 μM. Although this value is higher than those determined for Mn^{2+} and Co^{2+}, it is lower than the values found for the *Synechocystis* (11-fold) and *Mycobacterium tuberculosis* (6-fold) DXRs. Mg^{2+} has been proposed to be the physiologically relevant metal ion activator for DXR.[26] The intracellular concentration of free Mg^{2+} in *E. coli* is around 1-2 mM[38], so a K_m of 210 μM for Mg^{2+} is reasonable for this ion to be used as the in vivo co-factor in the DXR. The intracellular concentrations of Mn^{2+} (~0.01 μM)[39] and Co^{2+} (<0.001 μM)[40] are much lower than the K_m values for these ions, which strengthens the early suggestions that Mg^{2+} is likely the physiologically relevant metal ion.

Table 4.1 - Michaelis constants for divalent cations.

Cation	Organism	K_m (μM)
Co^{2+}	*E. coli*	2.0 ± 0.7
	M. tuberculosis[37]	1.2 ± 0.1
	Synechocystis[36]	10 ± 3
Mg^{2+}	*E. coli*	210 ± 20
	M. tuberculosis	1200 ± 100
	Synechocystis	2400 ± 200
Mn^{2+}	*E. coli*	17 ± 2
	M. tuberculosis	21 ± 2
	Synechocystis	15 ± 1

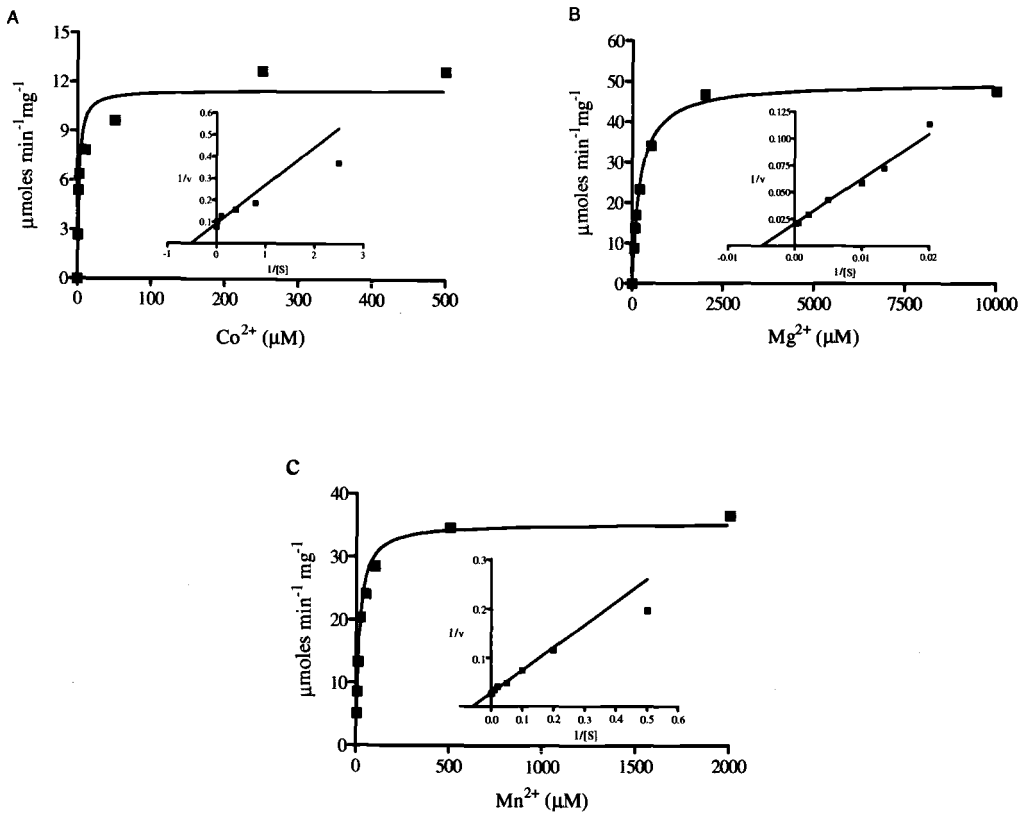

Figure 4.7. Hyperbolic curves and Lineweaver-Burk (inset) plots for determination of the kinetic constants for the metal ions Co^{2+}(A), Mg^{2+} (B) and Mn^{2+} (C).

Fosmidomycin inhibition studies were conducted using at least four concentrations of DXP and five concentrations of the inhibitor. The metal ion concentrations used were 1 mM for Co^{2+} and Mn^{2+} and 2 mM for Mg^{2+}. Based on the K_m values, those concentrations are enough to saturate the enzyme. The concentration of NADPH, 150 µM, used was also enough to saturate the enzyme.

Analysis of the progress curves of the fosmidomycin inhibition, independent of the metal ion used and inhibitor or substrate concentrations, revealed a lack of linearity, although linearity could be observed for the reaction in the absence of inhibitor (Figure 4.8). The non-linearity of the progress curves is indicative of slow-tight inhibition, which is in agreement with previous studies of fosmidomycin and the *E. coli* DXR.[26]

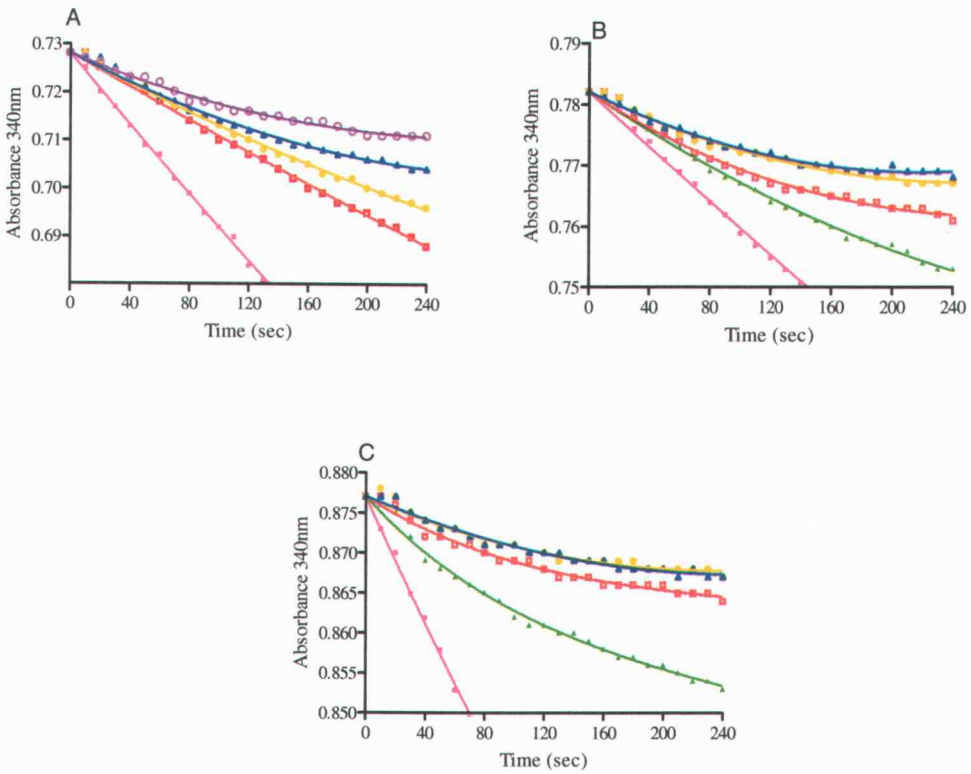

Figure 4.8. Progress curves for fosmidomycin inhibition using 200 µM DXP. A) Assays using Co^{2+} as divalent ion, B) Mg^{2+} and C) Mn^{2+}. 0 (■), 25(▲), 50(□), 100 (●), 200 (▲), 400 (○) nM of fosmidomycin. The curves were fitted to the equation: Absorbance = $v_s t + (v_o - v_s)(1-e^{-kt})/k$

The mechanism of inhibition of DXR by fosmidomycin has been described to be as in Scheme 1.[26]

$$E + I \underset{k_4}{\overset{k_3}{\rightleftharpoons}} EI \underset{k_6}{\overset{k_5}{\rightleftharpoons}} EI^*$$

Scheme 1 : Mechanism for slow, tight-binding inhibitors.

In this mechanism the inhibitor binds rapidly forming the EI complex, which isomerizes to a tightly bound, slow dissociating EI* complex. The isomerization is a consequence of conformational changes induced in DXR due to the binding of fosmidomycin.

According to the mechanism described in the Scheme 1, two different inhibition constants can be obtained. K_i (k_4/k_3) describes the formation of the EI complex while K_i^* ($K_i[k_6/(k_5+k_6)]$), represents the tightly bound complex and can be considered the overall inhibition constant.[27] For a typical slow, tight-binding inhibitor, K_i^* is smaller than K_i. Analysis of the progress curves can give two different velocities, an initial velocity (v_0) and the final velocity (v_s). The initial velocity is used to calculate K_i while the final velocity is used for the K_i^* calculation.

The progress curves obtained for these inhibitors show two distinct phases: a first portion that does not deviate much from linearity (v_0) and a second portion, which arises after an inflection point, where the curve becomes flatter (v_s). We calculated v_0 and v_s by direct examination of the progress curves for formation of $NADP^+$. The curves revealed that in the first 50-60 sec the initial rate (v_0) of reaction did not deviate from linearity. Therefore the conversion of EI to EI* is minimal. This velocity was used to calculate K_i. The parameter K_i^* was calculated by the second portion of the progress curve (v_s). The v_0 and v_s values were also calculated directly from the fitted progress curves using the equation: Absorbance = $v_s t + (v_o-v_s)(1-e^{-kt})/k$. The values obtained using the equation agreed with the ones obtained by examination of the curves.

The non-linear saturation curves and Lineweaver-Burk plots for inhibition of DXR by fosmidomycin, constructed with v_0 and v_s separately, in the presence of the three metal ions tested, are shown in Figures 4.9, 4.10 and 4.11.

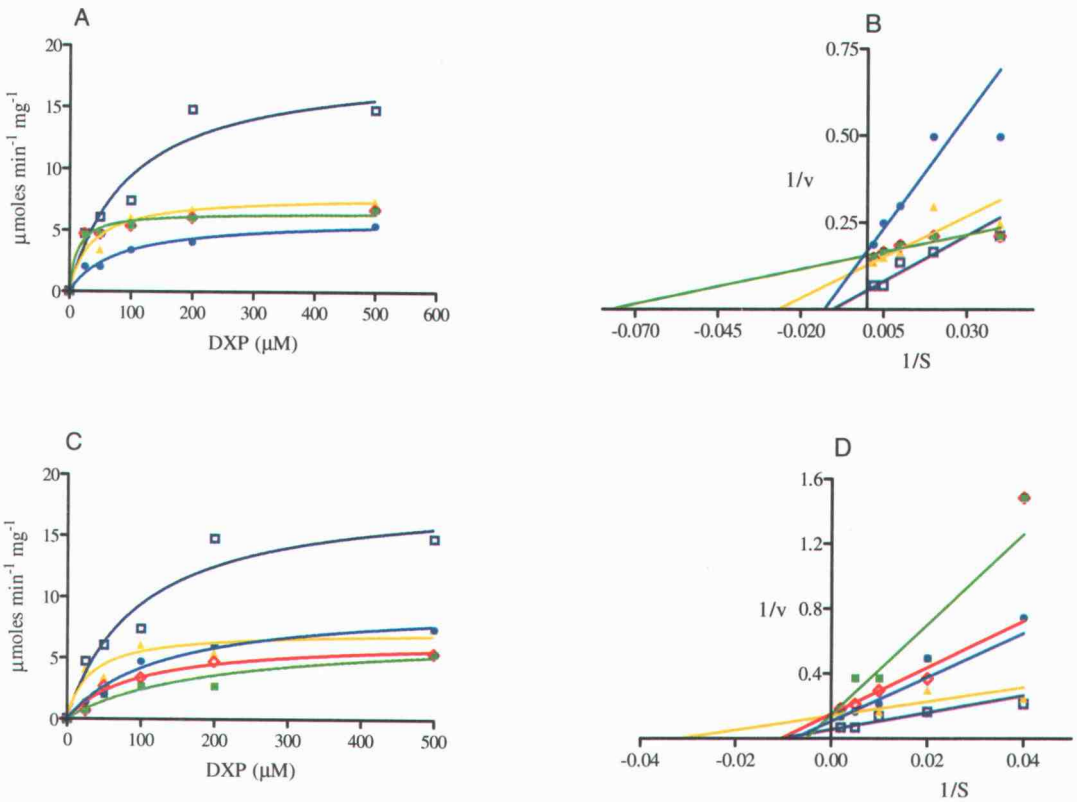

4.9. Fosmidomycin inhibition using Co^{2+}. 0 (□) , 50(▲) , 100 (◊), (■) 200 nM and (●) 400 nM of fosmidomycin. Ahyperbolic curves for v_0, B) Lineweaver-Burk plot for v_0, C) Hyperbolic curves for v_s and D) Lineweaver-Burk plot for v_s.

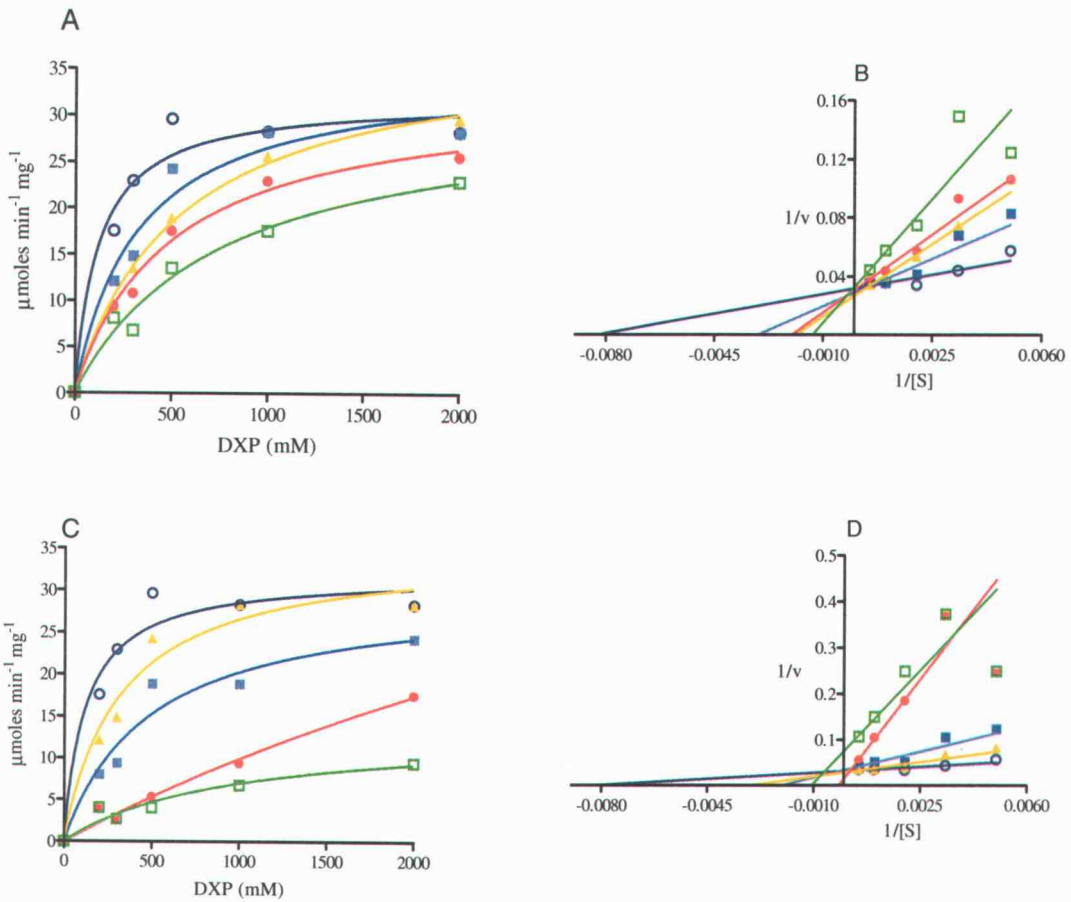

4.10. Fosmidomycin inhibition using Mg^{2+}. 0 (○), 25(■), 50(▲), 100 (●), 200(□) nM of fosmidomycin. A) Hyperbolic curves for v_0, B) Lineweaver-Burk plot for v_0, C) Hyperbolic curves for v_s and D) Lineweaver-Burk plot for v_s.

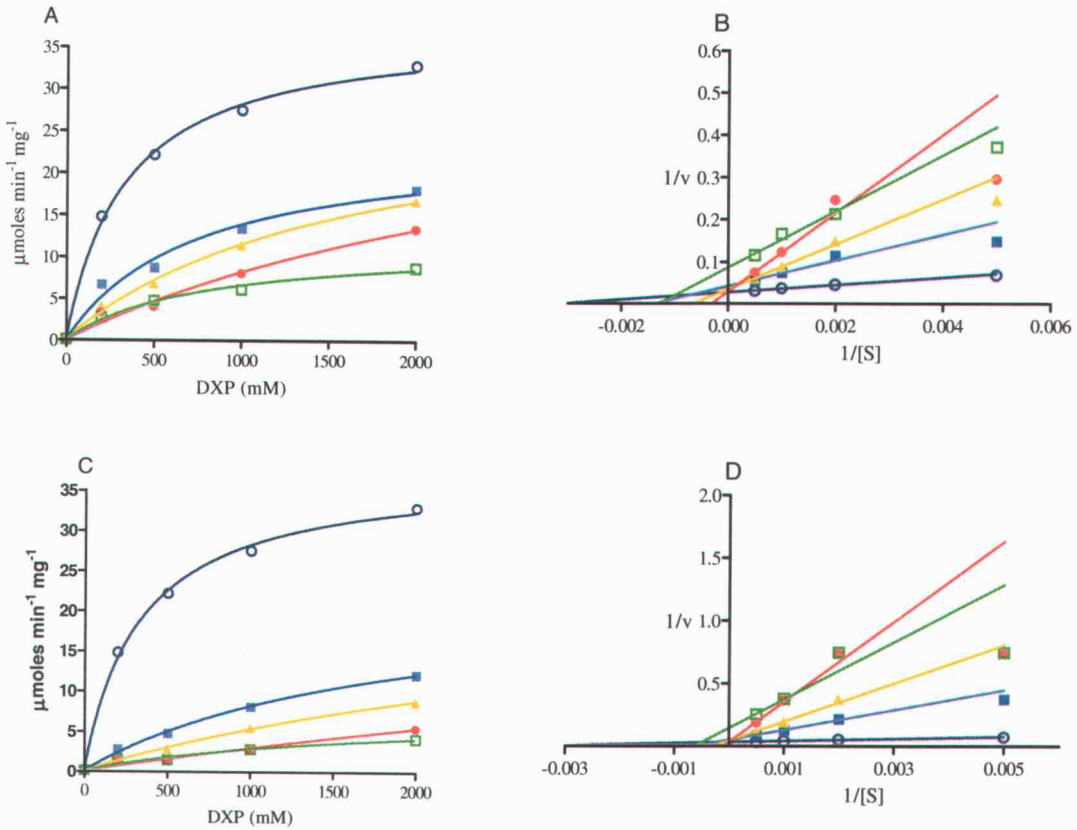

4.11. Fosmidomycin inhibition using Mn^{2+}. 0 (○), 25(■), 50(▲), 100(●), 200 (□) nM of fosmidomycin. A) Hyperbolic curves for v_0, B) Lineweaver-Burk plot for v_0, C) Hyperbolic curves for v_s and D) Lineweaver-Burk plot for v_s.

The Enzyme Kinetics program from Trinity software was used to calculate K_i and K_i* based on a non-linear regression method (Table 4.2). The inhibition constants determined using the three different metal ions did not show remarkable differences. A slightly higher K_i was observed when Co^{2+} was used as the divalent cation necessary for the DXR activity. However after equilibrium the K_i* value was slightly lower from the K_i* values for the other two ions. Our results suggest that the inhibition of DXR by fosmidomycin is not dependent on a specific metal ion.

Table 4.2. Inhibition constants for DXR with fosmidomycin as an inhibitor.

Divalent cation	K_i (nM)	K_i^* (nM)
Co^{2+}	250	30
Mg^{2+}	109	52
Mn^{2+}	90	56

The K_i values for fosmidomycin agreed well with those previously reported. Using the native *E. coli* DXR a K_i of 215 nM and a K_i^* of 21 nM[26] were obtained. For the His-tagged *E. coli* DXR the values for K_i and K_i^* were 40 nM and 10 nM[31], respectively.

As an alternative to the progress curve analysis to obtain the inhibition constants, preincubation experiments were conducted. In this experiment, the reaction was initiated with a fixed amount of substrate after a 10 min preincubation of enzyme with the inhibitor. The preincubation period allowed an equilibrium to be established, after which most of the enzyme is in the form EI*. The observed activity upon substrate addition corresponds to the final steady-state velocity in the presence of inhibitor. Highly linear correlations were obtained between 1/V and [I] (Figure 4.12). The K_i*s were calculated from the X-intercept of the Dixon plot (1/V versus [I]).[41] From this experiment the K_i*s values were determined to be 6 nM for Co^{2+} and Mg^{2+} and 8 nM for Mn^{2+}. Because these values are lower than the ones estimated by the progress curves, it indicates that some of the EI complex was still present in the third and fourth minutes of the reaction.

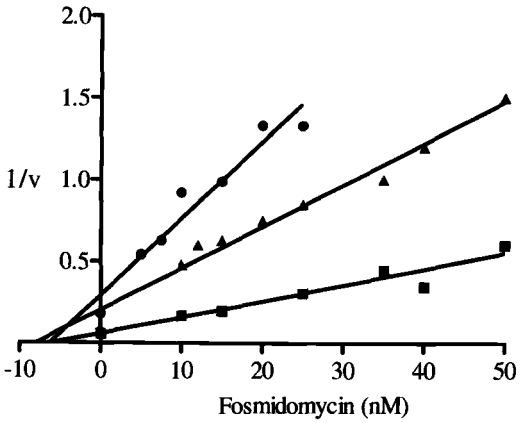

Figure 4.12. Dixon Plot for the preincubation experiment. Inhibition assays using Co^{2+} (●), Mg^{2+} (■) and Mn^{2+} (▲) as divalent ion.

Our inhibition experiments, however, did not explain the absence of Mg^{2+} in the DXR crystal structure. It had been reported for the *M. tuberculosis* DXR that the K_m value for the Mn^{2+} ion increased 243-fold when the pH decreased from 8.75 to 6.0.[37] These results are explained by the protonation of the residues that bind the metal ion at the lower pH. The *E. coli* DXR crystals were formed from a crystallization solution at pH 5.0. At pH 5.0 some of the the acidic amino acids Asp^{150}, Glu^{152}, and Glu^{234}, present at the DXR active site and proposed to bind the metal ion, are present in the neutral carboxylic acid form instead of the carboxylate ion that is present at pH 7.6. Carboxylic acid functional groups still can bind metal ions, but the affinity is less than for the negatively charged carboxylates.[37] To test this hypothesis, an attempt was made to determine the K_ms at pH 5.0, but the enzymatic activity was negligible in either acetate or citrate buffer at this pH. The DXR activity was then tested in MES buffer at pH 5.5 and 6.0. Although some activity was seen at pH 5.5, the activity was still very low. At pH 6.0 the activity was sufficient to proceed further. The Michaelis constants for Mg^{2+} and Mn^{2+} ions were determined at pH 6.0. The results are summarized in the Table 4.3 and Figure 4.13.

Table 4.3. Michaelis constants for divalent cations using *E. coli* DXR

Cations	K_m (μM)	
	pH 7.8	pH 6.0
Mn^{2+}	17 ± 2	520 ± 60
Mg^{2+}	210 ± 20	17000 ± 2000
Co^{2+}	2.0 ± 0.7	nd

nd – not determined

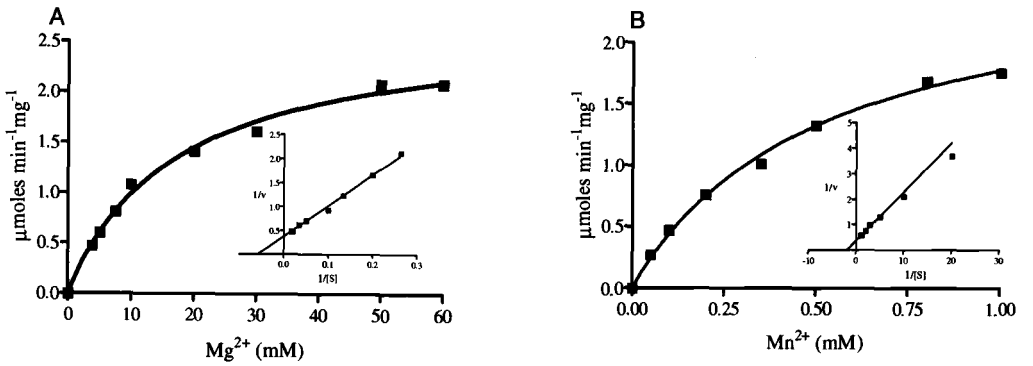

Figure 4.13. Hyperbolic curves and Lineweaver-Burk (inset) plots for determination of the kinetic constants for the metal ions Mg^{2+} (A) and Mn^{2+} (B) using the *E. coli* DXR. DXR assays conducted at pH 6.0.

An increase in the K_m values was observed when the assays were carried out at pH 6.0 (Table 4.3). The K_m for Mg^{2+} increased 31-fold and for Mn^{2+} 81-fold. A similar pH effect was observed using the *M. tuberculosis* DXR, where the K_m for Mn^{2+} increased sharply (243-fold) from 7 μM at pH 8.75 to 1.7 mM at pH 6.0.[37] The higher K_m value for Mg^{2+} at pH 6.0 (17 mM) may explain its absence in the crystal structure. It is likely that the K_m at pH 5.0 is even higher than 17 mM. Based on these results, the concentration of 10 mM that was used during the crystallization experiment was likely insufficient to saturate DXR with Mg^{2+}.

2.2. Inhibition studies using the Synechocystis DXR.

Analyses of fosmidomycin (**1**), the reverse hydroxamate analog (**10**) and FR900098 (**2**) inhibition of *Synechocystis* DXR were conducted in the same manner as for the inhibition experiments using the *E. coli* DXR. Inhibition of DXR by the three compounds tested does not take place immediately (Figure 4.14). As observed for the inhibition of the *E. coli* DXR by fosmidomycin, the decrease in the absorbance was not linear and decreased with the time from an initial v_0 to a final velocity v_s. This behavior indicate that these inhibitors are slow, tight-binding inhibitors for the *Synechocystis sp.* DXR, as fosmidomycin has been demonstrated for the *E. coli* DXR. The general non-linearity of the inhibition curves for the inhibitor (**10**) for the *Synechocystis sp.* DXR has been observed in previous studies in our laboratory.[32]

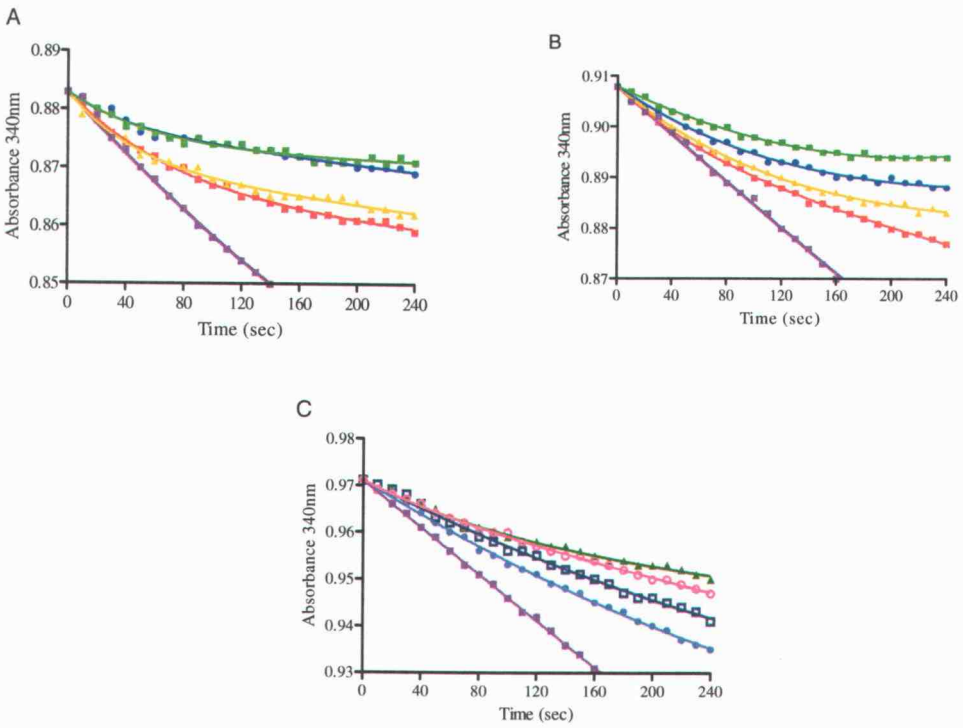

Figure 4.14. Progress curves for fosmidomycin inhibition using 200 μM DXP. A) fosmidomycin B) the reverse hydroxamate analog C) FR900098. 0 (■), 25(■), 50(▲), 100 (●), 200 (■), 400 (□) nM 1000 nM (○) and 2000 (▲) of inhibitor. The curves were fitted to the equation: $A = v_s t + (v_o - v_s)(1-e^{-kt})/k + At_0$

The v_0 and v_s estimated from the progress curves were used to construct the plots used to calculate the inhibition constants by nonlinear regression (Figures 4.15, 4.16 and 4.17).

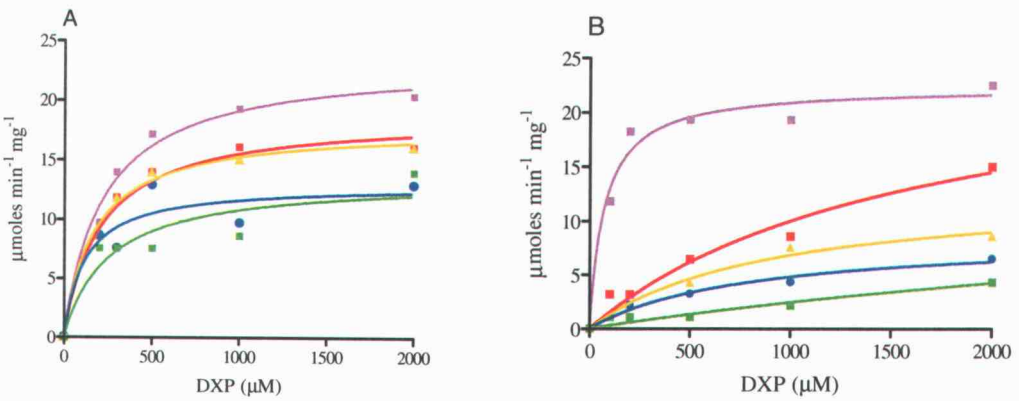

Figure 4.15. Hyperbolic curves for the inhibition of the *Synechocystis* DXR by fosmidomycin (1). A) Plot constructed using v_0 and B) using v_s. 0 (■), 25(■), 50(▲), 100 (●), 200 nM of inhibitor.

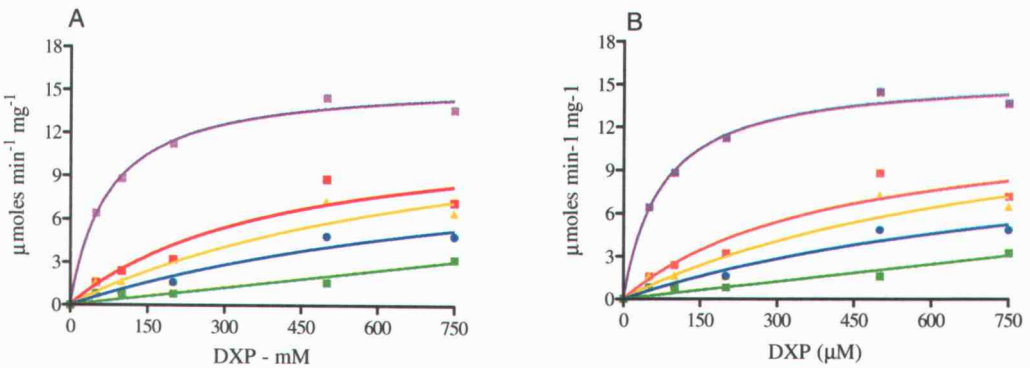

Figure 4.16. Hyperbolic curves for the inhibition of the *Synechocystis* DXR by FR900098 (2). A) Plot constructed using v_0 and B) using v_s. 0 (■), 25(■), 50(▲), 100 (●), 200 nM (■) of inhibitor.

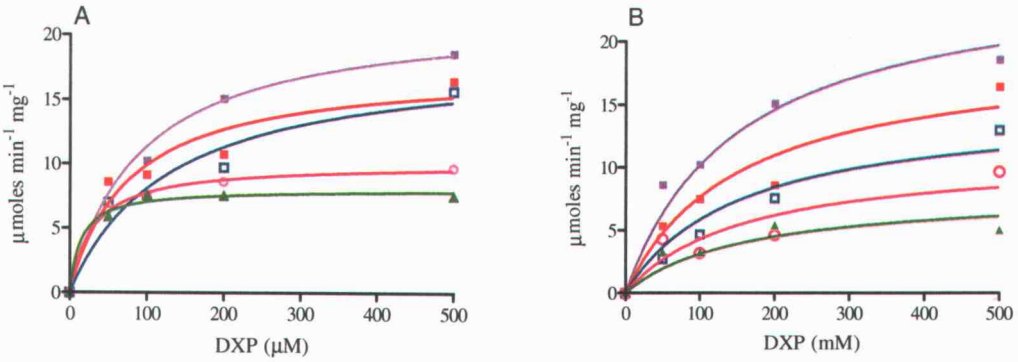

Figure 4.17. Hyperbolic curves for the inhibition of the *Synechocystis* DXR by the hydroxamate analog of fosmidomycin (3). A) Plot constructed using v_0 and B) using v_s. 0 (■), 100(■), 400 (□), 1000 nM (○) and 2000 nM (▲) of inhibitor.

The inhibition constants calculated are shown in the Table 4.4. The K_i values for fosmidomycin are higher than the ones reported for the *E. coli* DXR. Comparing our results with the His-tagged *E. coli* DXR the K_i for the *Synechocystis* DXR was 22-fold higher. However the value for the K_i* was only 2.5-fold higher. It is possible that the isomerization of the *Synechocystis* DXR to form the tightly bound complex EI*, occurs slower than for the *E. coli* DXR. After formation of the EI* complex both enzymes presented similar K_i* values. These results show that enzymes from different organisms can have a slightly different affinity for the inhibitors, as well for the substrates and cofactors. Although the K_m for the DXP for the DXR from His-tagged *E. coli*, 97-99 µM,[34,35] and *Synechocystis*, 190 µM, are similar, a higher difference in the affinity of these DXRs for the metal ions was observed. For example the K_m for Mg^{2+} for the *E. coli* DXR is 210 µM while for the *Synechocystis* DXR it is 2400 µM.

Table 4.4. Inhibition constants for *Synechocystis* DXR

Inhibitor	K_i (nM)	K_i* (nM)
Fosmidomycin	900	4
FR900098	500	0.9
Hydroxamate analog	5000	2400

The acetyl analog of fosmidomycin, FR900098, also is a natural product with antibacterial activity.[42] This compound has been shown to be twice as effective as fosmidomycin for inhibiting the *P. falciparum* DXR based on in vitro studies and in vivo, using the malaria *P. vinckei* mouse model[12] However, no K_i values for this inhibitor have been reported. The inhibition constants for FR900098 with the *Synechocystis* DXR were determined as for fosmidomycin. The K_i was 1.8 fold lower than the K_i for fosmidomycin, while the K_i* was 4.4-fold lower.

Binding of the reverse hydroxamate **(10)** was weaker than fosmidomycin **(1)** and FR900098 **(2)** with K_i and K_i* in the micromolar range. The K_i for this analog was 5.5-fold and 10-fold higher than the K_i determined for fosmidomycin and FR90098 for the *Synechoscystis* DXR, respectively. More pronounced differences were observed between the K_i* for the reverse hydroxamate (2.4 μM) and fosmidomycin (4 nM) and FR900098 (0.9 nM). Although the K_i determined in this work is much higher (30-fold) than the K_i for the same inhibitor with the *E. coli* DXR,[31] it is in agreement with the K_i previously determined (4 μM) for this compound as a mixed inhibitor of the *Synechocystis* DXR.[32] Despite the differences in the hydroxamate and fosmidomycin K_is for the *E. coli*[31] and *Synechocystis* DXRs, the increase in the K_i for the reverse hydroxamate compared to fosmidomycin in the Kuntz work using the *E. coli* DXR was 4.2-fold, which is in agreement with the increase determined to the *Synechocystis* DXR in this work (5.5-fold).

In the alternative method, a second estimate of K_i* was obtained from reactions initiated by addition of substrate after preincubation of the inhibitors and DXR (Figure 4.18). The K_i*s determined using a plot of I versus 1/v are 4 nM for fosmidomycin, 2 nM for FR90098 and 350 nM for the hydroxamate.

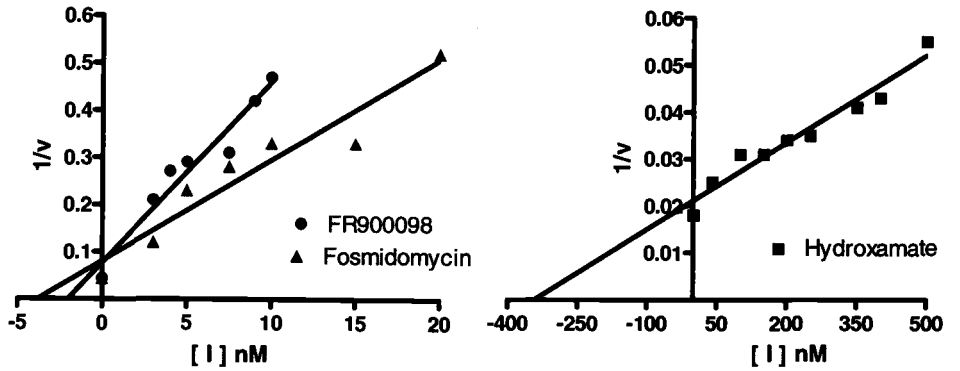

Figure 4.18. Dixon Plot for the preincubation experiment.

The K_i* values obtained for fosmidomycin and FR900098 in the preincubation study are in good agreement with the ones obtained from the progress curves. As observed in our experiments of inhibition of the *E. coli* DXR by fosmidomycin, the K_i* value obtained in the preincubation experiment for the hydroxamate analog of fosmidomycin showed a 7-fold lowering of the inhibition, when compared to the K_i* value obtained from the progress curves.

In summary the potent inhibition of DXR by fosmidomycin and its analogs was confirmed for the *Synechocystis* DXR. Fosmidomycin and FR 900098 have inhibition constants in the low nM range. In addition the patterns of progress curves for fosmidomycin, FR900098 and the hydroxamate analog were prototypical for the slow, tight-binding inhibitors,[27] in which progressive time-dependent inhibition arises from the slow establishment of a binding equilibrium between the enzyme and inhibitor.

4. Experimental section

4.1. E. coli DXR

Purified *E. coli* DXR was provided by Dr. Aengus Mc Sweeney, Morphochem AG – Switzerland. The enzyme has a N-terminal tag of 14 additional residues including six consecutive histidine residues.

4.2. Expression and purification of the Synechocystis sp. PCC6803 DXR

Synechocystis DXR was expressed in *E. coli* Top 10 cells as described in the Chapter 1. Purification involved a single metal affinity chromatography step, using the Talon® spin columns and followed the manufacter's protocol. DXR was eluted using imidazole concentrations from 40-150 mM. Fractions containing DXR were verified by SDS-PAGE.[43] The enzyme solution was dialyzed against 50 mM Tris/HCl, 300 mM NaCl, pH 7.8 buffer, overnight. Protein concentrations were measured using the Protein Assay Kit (Bio-Rad), based on the Bradford method.[44]

4.3. Assay for DXP reductoisomerase

The enzyme activity was assayed by monitoring the decrease in absorbance at 340 nm.[45] The oxidation of NADPH was monitored at 37 °C in a Hitachi U-2000 Spectrophotometer. One unit of DXP reductoisomerase activity was defined as the amount of enzyme required for the oxidation of 1 μmol NADPH per minute. The concentration of DXR used in the *E. coli* inhibition studies was 5 nM and in the *Synechocystis* studies 3 nM.

4.4. Determination of the Michaelis constants for the metal ions

Using the DXR standard assay conditions, the kinetic parameters for three metal ions, Co^{2+}, Mg^{2+} and Mn^{2+}, were determined at pH 7.6 (100 mM Tris-HCl buffer) and pH 6.0 (100 mM MES buffer). The concentration of the substrate DXP was 2 mM and NADPH 0.2 mM. Kinetic parameters were determined using at least seven varying concentration of these ions, in triplicate. The concentration ranges for Mn^{2+}, Mg^{2+} and Co^{2+} were 2-2000 μM, 50-60000 μM and 0.4-500 μM. Kinetic parameters were calculated using GraphPad Prism software by fitting the initial velocity versus substrate concentration to the Michaelis equation,

$$v = (V_{max}[S])/(K_m + [S]). \quad \text{(Eq.1)}$$

4.5. Enzyme inhibition studies

Inhibition studies were carried out using at least four concentrations of DXP and five concentrations of the inhibitor in triplicate. The varying concentrations of DXP and inhibitors were added in 50 mM Tris/HCl buffer pH 7.6-7.8, 1 mM $MnCl_2$, BSA 1 mg/mL and 0.15 mM NADPH in a final volume of 1 mL. For the inhibition of *E. coli* DXR by fosmidomycin using different metal ions, the concentrations used were 1 mM for Co^{2+} and Mn^{2+} and 2 mM for Mg^{2+}. Based on the K_m values, those concentrations are enough to saturate the enzyme. The concentration of NADPH used was also enough to saturate the enzyme.

Progress curves for slow, tight-binding inhibition analysis were obtained by initiating the reaction by adding the enzyme to the reaction mixture. The decrease in the absorbance at 340 nm was monitored for 4 min. The progress curves were fitted to equation 2,

$$A = v_s t + (v_o - v_s)(1 - e^{-kt})/k \quad \text{(Eq.2)}$$

where A is the absorbance at any time t, v_0 and v_s are the initial and final steady-state rates, respectively, and k is the apparent first-order rate constant for the establishment of the final steady-state equilibrium. The curves were fitted by the nonlinear least squares, using GraphPad Prism software. The inhibition constants were estimated

from v_0 and v_s by nonlinear regression using the Enzyme Kinetics program from Trinity Software.

5. References

(1) Wellems, T. E. "*Plasmodium* chloroquine resistance and the search for a replacement antimalarial drug". *Science* **2002**, *298*, 124-126.

(2) Wiesner, J.; Borrmann, S.; Jomaa, H. "Fosmidomycin for the treatment of malaria". *Parasitol. Res.* **2003**, *90*, S71-76.

(3) Gardner, M. J.; Hall, N.; Fung, E.; White, O.; Berriman, M. et al. "Genome sequence of the human malaria parasite *Plasmodium falciparum*". *Nature* **2002**, *419*, 498-511.

(4) Köhler, S.; Delwiche, C. F.; Denny, P. W.; Tilney, L. G.; Webster, P. et al. "A plastid of probable green algal origin in Apicomplexan parasites". *Science* **1997**, *275*, 1485-1489.

(5) Palmer, J. D.; Delwiche, C. F. "Second-hand chloroplasts and the case of the disappearing nucleus". *Proc. Natl. Acad. Sci. U S A* **1996**, *93*, 7432-7435.

(6) Wiesner, J.; Hintz, M.; Altincicek, B.; Sanderbrand, S.; Weidemeyer, C. et al. "*Plasmodium falciparum*: detection of the deoxyxylulose 5-phosphate reductoisomerase activity". *Exp. Parasitol.* **2000**, *96*, 182-186.

(7) Slater, E. E.; MacDonald, J. S. "Mechanism of action and biological profile of HMG CoA reductase inhibitors. A new therapeutic alternative". *Drugs* **1988**, *36*, 72-82.

(8) Szabo, C. M.; Matsumura, Y.; Fukura, S.; Martin, M. B.; Sanders, J. M. et al. "Inhibition of geranylgeranyl diphosphate synthase by bisphosphonates and diphosphates: a potential route to new bone antiresorption and antiparasitic agents". *J. Med. Chem.* **2002**, *45*, 2185-2196.

(9) Martin, M. B.; Sanders, J. M.; Kendrick, H.; de Luca-Fradley, K.; Lewis, J. C. et al. "Activity of bisphosphonates against *Trypanosoma brucei rhodesiense*". *J. Med. Chem.* **2002**, *45*, 2904-2914.

(10) Wilhelm, M.; Kunzmann, V.; Eckstein, S.; Reimer, P.; Weissinger, F. et al. "Gammadelta T cells for immune therapy of patients with lymphoid malignancies". *Blood* **2003**, *102*, 200-206.

(11) Maertens, J. A. "History of the development of azole derivatives". *Clin. Microbiol. Infect.*. **2004**, *10*, 1-10.

(12) Jomaa, H.; Wiesner, J.; Sanderbrand, S.; Altincicek, B.; Weidemeyer, C. et al. "Inhibitors of the nonmevalonate pathway of isoprenoid biosynthesis as antimalarial drugs". *Science* **1999**, *285*, 1573-1576.

(13) Missinou, M. A.; Borrmann, S.; Schindler, A.; Issifou, S.; Adegnika, A. A. et al. "Fosmidomycin for malaria". *Lancet* **2002**, *360*, 1941-1942.

(14) Lell, B.; Ruangweerayut, R.; Wiesner, J.; Missinou, M. A.; Schindler, A. et al. "Fosmidomycin, a novel chemotherapeutic agent for malaria". *Antimicrob. Agents Chemother.* **2003**, *47*, 735-738.

(15) Wiesner, J.; Henschker, D.; Hutchinson, D. B.; Beck, E.; Jomaa, H. "In vitro and in vivo synergy of fosmidomycin, a novel antimalarial drug, with clindamycin". *Antimicrob. Agents Chemother.* **2002**, *46*, 2889-2894.

(16) Borrmann, S.; Issifou, S.; Esser, G.; Adegnika, A. A.; Ramharter, M. et al. "Fosmidomycin-clindamycin for the treatment of *Plasmodium falciparum* malaria". *J. Infect. Dis.* **2004**, *190*, 1534-1540.

(17) Gottlin, E. B.; Benson, R. E.; Conary, S.; Antonio, B.; Duke, K. et al. "High-throughput screen for inhibitors of 1-deoxy-d-xylulose 5-phosphate reductoisomerase by surrogate ligand competition". *J. Biomol. Screen* **2003**, *8*, 332-339.

(18) Yajima, S.; Hara, K.; Sanders, J. M.; Yin, F.; Ohsawa, K. et al. "Crystallographic structures of two bisphosphonate:1-deoxyxylulose-5-phosphate reductoisomerase complexes". *J. Am. Chem. Soc.* **2004**, *126*, 10824-10825.

(19) Kuzuyama, T.; Seto, H.; Takahashi, S.; Shimizu, T. "Fosmidomycin, a specific inhibitor of 1-deoxy-D-xylulose 5-phosphate reductoisomerase in the nonmevalonate pathway for terpenoid biosynthesis." *Tetrahedron Lett.* **1998**, *39*, 7913-7916.

(20) Kuemmerle, H. P.; Murakawa, T.; Soneoka, K.; Konishi, T. "Fosmidomycin: a new phosphonic acid antibiotic. Part I: Phase I tolerance studies". *Int. J. Clin. Pharmacol. Ther. Toxicol.* **1985**, *23*, 515-520.

(21) Kuemmerle, H. P.; Murakawa, T.; Sakamoto, H.; Sato, N.; Konishi, T. et al. "Fosmidomycin, a new phosphonic acid antibiotic. Part II: 1. Human pharmacokinetics. 2. Preliminary early phase IIa clinical studies". *Int. J. Clin. Pharmacol. Ther. Toxicol.* **1985**, *23*, 521-528.

(22) Sakamoto, Y.; Furukawa, S.; Ogihara, H.; Yamasaki, M. "Fosmidomycin resistance in adenylate cyclase deficient (cya) mutants of *Escherichia coli*". *Biosci. Biotechnol. Biochem.* **2003**, *67*, 2030-2033.

(23) Shigi, Y. "Inhibition of bacterial isoprenoid synthesis by fosmidomycin, a phosphonic acid-containing antibiotic". *J. Antimicrob. Chemother.* **1989**, *24*, 131-145.

(24) Steinbacher, S.; Kaiser, J.; Eisenreich, W.; Huber, R.; Bacher, A. et al. "Structural basis of fosmidomycin action revealed by the complex with 2-C-methyl-D-erythritol 4-phosphate synthase (IspC). Implications for the catalytic mechanism and anti-malaria drug development". *J. Biol. Chem.* **2003**, *278*, 18401-18407.

(25) Grolle, S.; Bringer-Meyer, S.; Sahm, H. "Isolation of the dxr gene of *Zymomonas mobilis* and characterization of the 1-deoxy-D-xylulose 5-phosphate reductoisomerase". *FEMS Microbiol. Lett.* **2000**, *191*, 131-137.

(26) Koppisch, A. T.; Fox, D. T.; Blagg, B. S.; Poulter, C. D. "*E. coli* MEP synthase: steady-state kinetic analysis and substrate binding". *Biochemistry* **2002**, *41*, 236-243.

(27) Morrison, J. F. W., C. T. "The behavior and significance of slow-binding enzyme inhibitors". *Adv. Enzymol. Relat. Areas Mol. Biol.* **1988**, *61*, 201-301.

(28) Fellermeier, M.; Bacher, A.; Zenk, M. H.; Maier, U.; Kis, K. et al. "Cell-free conversion of 1-deoxy-D-xylulose 5-phosphate and 2-C-methyl-D-erythritol 4-phosphate into beta-carotene in higher plants and its inhibition by fosmidomycin." *Tetrahedron Lett.* **1999**, *40*, 2743-2746.

(29) Kurz, T. G., D.; Wackendorff "Carboxilic acid analogues of fosmidomycin". *Z. Naturforsch.* **2003**, *58b*, 457-461.

(30) Kurz, T. G., D.; Wackendorff "Hydroxyurea analogues of fosmidomycin". *Z. Naturforsch.* **2003**, *58b*, 106-110.

(31) Kuntz, L. T., D.; Grosdemange-Billiard, C.; Hemmerlin, A.; Willem, A.; Bach, T. J.; Rohmer, M. "Isoprenoid biosynthesis as target for antibacterial and antiparasitic drugs: phosphonohydroxamic acids as inhibitors of deoxyxylulose phosphate reducto-isomerase". *Biochem. J.* **2005**, *386*, 127-135.

(32) Woo, Y.-H. Studies of Non-Mevalonate isoprenoid Biosynthesis: The 1-Deoxy-D-xylulose-5-phosphate isomeroreductase (DXR) mediated reaction. In *Pharmacy*; Oregon state University: Corvallis, 2002; pp 140.

(33) Mac Sweeney, A.; Lange, R.; Fernandes, R. P. M.; Schulz, H.; Dale, G. E. et al. "The Crystal Structure of *E.coli* 1-Deoxy-d-xylulose-5-phosphate Reductoisomerase in a Ternary Complex with the Antimalarial Compound Fosmidomycin and NADPH Reveals a Tight-binding Closed Enzyme Conformation". *J. Mol. Biol.* **2005**, *345*, 115-127.

(34) Kuzuyama, T.; Takahashi, S.; Takagi, M.; Seto, H. "Characterization of 1-deoxy-D-xylulose 5-phosphate reductoisomerase, an enzyme involved in isopentenyl diphosphate biosynthesis, and identification of its catalytic amino acid residues". *J. Biol. Chem.* **2000**, *275*, 19928-19932.

(35) Hoeffler, J. F.; Tritsch, D.; Grosdemange-Billiard, C.; Rohmer, M. "Isoprenoid biosynthesis via the methylerythritol phosphate pathway. Mechanistic investigations of the 1-deoxy-D-xylulose 5-phosphate reductoisomerase". *Eur. J. Biochem.* **2002**, *269*, 4446-4457.

(36) Yin, X.; Proteau, P. J. "Characterization of native and histidine-tagged deoxyxylulose 5-phosphate reductoisomerase from the cyanobacterium *Synechocystis sp.* PCC6803". *Biochim. Biophys. Acta* **2003**, *1652*, 75-81.

(37) Argyrou, A.; Blanchard, J. S. "Kinetic and chemical mechanism of *Mycobacterium tuberculosis* 1-deoxy-D-xylulose-5-phosphate isomeroreductase". *Biochemistry* **2004**, *43*, 4375-4384.

(38) Alatossava, T.; Jütte, H.; Kuhn, A.; Kellenberger, E. "Manipulation of intracellular magnesium content in polymyxin B nonapeptide-sensitized *Escherichia coli* by ionophore A23187". *J. Bacteriol.* **1985**, *162*, 413-419.

(39) Frausto da Silva, J. J. R. W., R. J. P. *The Biological Chemistry of the Elements. The inorganic Chemistry of Life*; Claredon Press: Oxford, U. K., 1991; 379.

(40) D'Souza V, M.; Holz, R. C. "The methionyl aminopeptidase from *Escherichia coli* can function as an iron(II) enzyme". *Biochemistry* **1999**, *38*, 11079-11085.

(41) Segel, I. H. *Enzyme Kinetics*; Wiley-Interscience, 1975; 957.

(42) Okuhara, M.; Kuroda, Y.; Goto, T.; Okamoto, M.; Terano, H. et al. "Studies on new phosphonic acid antibiotics. III. Isolation and characterization of FR-31564, FR-32863 and FR-33289". *J. Antibiotic.* **1980**, *33*, 24-28.

(43) Laemmli, U. K. "Cleavage of structural proteins during the assembly of the head of bacteriophage T4". *Nature* **1970**, *227*, 680-685.

(44) Bradford, M. M. "A rapid and sensitive method for the quantitation of microgram quantities of protein utilizing the principle of protein-dye binding". *Anal. Biochem.* **1976**, *72*, *248-54*.

(45) Takahashi, S.; Kuzuyama, T.; Watanabe, H.; Seto, H. "A 1-deoxy-D-xylulose 5-phosphate reductoisomerase catalyzing the formation of 2-*C*-methyl-D-erythritol 4-phosphate in an alternative nonmevalonate pathway for terpenoid biosynthesis". *Proc. Natl. Acad. Sci. U S A* **1998**, *95*, 9879-9884.

CHAPTER FIVE

Conclusions

The enzyme 1-deoxy-D-xylulose 5-phosphate reductoisomerase (DXR) was the focus of this dissertation. It is the second enzyme in the methyl erythritol phosphate (MEP) pathway to isoprenoids. Because the MEP pathway is present in several pathogenic microorganisms and plants, but is not present in humans, this enzyme has been considered an ideal target for new drugs. The first compound described to inhibit the MEP pathway was fosmidomycin. This compound was shown to strongly inhibit the DXR enzyme and thus validated the MEP pathway as a target for development of new drugs.

In this dissertation two aspects of the DXR enzyme were investigated. In Chapter Two and Three site directed mutagenesis was used to study the roles of amino acids important for substrate binding and catalysis. The recently solved crystal structures of the *E. coli* DXR established a foundation for the design of mutants of the *Synechocystis sp.* PCC6803 DXR. In Chapter Four inhibition studies of DXR by fosmidomycin and two of its analogs were conducted.

DXR mutants of the highly conserved Trp^{204} were designed to accept a new substrate, explaining the role of a key conserved amino acid residue for substrate binding and specificity. The role of Trp^{204} was studied using an analog of the DXR substrate. The compound 1,2-dideoxy-D-threo-3-hexulose 6-phosphate (1-methyl-DXP or Me-DXP) is not an alternate substrate for DXR, but is a weak competitive inhibitor. Modeling of the intermediate of the DXR reaction, 2-*C*-methylerythrose 4-phosphate, in the DXR active site indicated that Trp^{204} indole ring might interact strongly with the methyl group of the intermediate. Four mutants with a progressive decrease in size of the side chain were prepared. Further studies with one of them, W204F showed that this mutant can accept Me-DXP as a substrate, concluding that the Trp^{204} is the amino acid that prevents the wild-type DXR from using Me-DXP as a substrate.

Examination of the X-ray crystallographic structures of *E. coli* DXR complexed with fosmidomycin and Mn^{2+}, and fosmidomycin and NADPH revealed several residues that are apparently involved in the substrate binding as well residues that act as ligands for the metal ion. The effects of changes in these residues were studied in Chapter Three through site-directed mutagenesis. Mutants in residues that bind the metal ion and the DXP substrate were obtained. After the kinetic characterization of these mutants and comparison with the wild-type enzyme, we found that substitution, conservative or not, of the residues caused an accentuated decreased in the DXR catalytic activity. These results confirmed that these are key amino acids responsible for the DXR catalytic efficiency.

DXR inhibition studies were conducted with the *E. coli* and *Synechocystis* DXR. In the first part of Chapter Four inhibition of the *E. coli* DXR by fosmidomycin in the presence of three metal ions, Co^{2+}, Mg^{2+} and Mn^{2+} showed that the inhibition does not depend on a specific metal ion. It was also shown that an increase in the K_m for Mg^{2+} when the pH decreased from pH 7.6 and 6.0 is responsible for the absence of Mg^{2+} in a DXR crystal structure. Evaluation of the patterns of progress curves for the inhibition of the *Synechocystis* DXR by fosmidomycin, FR 900098 and the reversed hydroxamate analog showed that they are prototypical for slow, tight-binding inhibitors. Those compounds were shown to be potent inhibitors of the *Synechoscystis* DXR with fosmidomycin and FR 900098 having inhibition constants in the low nM range. The K_is determined for fosmidomycin and its reverse hydroxamate inhibitor using the *Synechocystis* DXR are higher than the K_is found for the *E. coli* DXR, which suggests a difference in the affinity of DXRs from different organisms.

In conclusion, a better understanding of the DXR active site was obtained with the mutagenesis studies. These studies showed that even a very conservative change in an amino acid residue at the active site decreased the catalytic activity of DXR suggesting that a very structured conformation of the active site is necessary for high efficiency of DXR. The inhibition and metal ion studies showed that the affinity of the *Synechocystis* DXR for inhibitors and metal ions is different from the *E. coli* DXR affinity. In spite of the differences in affinity, fosmidomycin and the reverse

hydroxamate analog were shown to be slow, tight-binding inhibitors for the *Synechocystis* DXR as they are for the *E. coli* DXR.

Bibliography

Adam, K. P.; Thiel, R.; J, Z. "Incorporation of 1-[1-(13)C]Deoxy-D-xylulose in chamomile sesquiterpenes". *Arch. Biochem. Biophy.s* **1999**, *369*, 127-132.

Alatossava, T.; Jütte, H.; Kuhn, A.; Kellenberger, E. "Manipulation of intracellular magnesium content in polymyxin B nonapeptide-sensitized *Escherichia coli* by ionophore A23187". *J. Bacteriol.* **1985**, *162*, 413-419.

Alberts, A. W.; Chen, J.; Kuron, G.; Hunt, V.; Huff, J. et al. "Mevinolin: a highly potent competitive inhibitor of hydroxymethylglutaryl-coenzyme A reductase and a cholesterol-lowering agent". *Proc. Natl. Acad. Sci. U S A* **1980**, *77*, 3957-3961.

Altincicek, B.; Hintz, M.; Sanderbrand, S.; Wiesner, J.; Beck, E. et al. "Tools for discovery of inhibitors of the 1-deoxy-D-xylulose 5-phosphate (DXP) synthase and DXP reductoisomerase: an approach with enzymes from the pathogenic bacterium *Pseudomonas aeruginosa*". *FEMS Microbiol. Lett.* **2000**, *190*, 329-333.

Altincicek, B.; Kollas, A. K.; Sanderbrand, S.; Wiesner, J.; Hintz, M. et al. "GcpE is involved in the 2-C-methyl-D-erythritol 4-phosphate pathway of isoprenoid biosynthesis in *Escherichia coli*". *J. Bacteriol.* **2001**, *183*, 2411-2416.

Argyrou, A.; Blanchard, J. S. "Kinetic and chemical mechanism of *Mycobacterium tuberculosis* 1-deoxy-D-xylulose-5-phosphate isomeroreductase". *Biochemistry* **2004**, *43*, 4375-4384.

Arigoni, D.; Sagner, S.; Latzel, C.; Eisenreich, W.; Bacher, A. et al. "Terpenoid biosynthesis from 1-deoxy-D-xylulose in higher plants by intramolecular skeletal rearrangement". *Proc. Natl. Acad. Sci. U S A* **1997**, *94*, 10600-10605.

Bach, T. J. "Some new aspects of isoprenoid biosynthesis in plants - a review". *Lipids* **1995**, *30*, 191-202.

Bach, T. J. L., H.K "Inhibition by mevinolin of plant growth, sterol formation and pigment accumulation". *Physiol. Plant* **1983**, *59*, 50-60.

Bach, T. J.; Lichtenthaler, H. K. "Mechanisms of inhibition by mevinolin (MK 803) of microsome-bound radish and of partially purified yeast HMG-CoA reductase (EC.1.1.1.34)". *Z. Naturforsch. [C]* **1983**, *38*, 212-219.

Bach, T. J.; Lichtenthaler, H. K. "Mevinolin: a highly specific inhibitor of microsomal 3-hydroxy-3-methylglutaryl-coenzyme A reductase of radish plants". *Z. Naturforsch. [C]* **1982**, *37*, 46-50.

Biou, V.; Dumas, R.; Cohen-Addad, C.; Douce, R.; Job, D. et al. "The crystal structure of plant acetohydroxy acid isomeroreductase complexed with NADPH, two magnesium ions and a herbicidal transition state analog determined at 1.65 A resolution". *EMBO J.* **1997**, *16*, 3405-3415.

Bloch, K. "Sterol molecule: structure, biosynthesis, and function". *Steroids* **1992**, *57*, 378-383.

Borrmann, S.; Adegnika, A. A.; Matsiegui, P. B.; Issifou, S.; Schindler, A. et al. "Fosmidomycin-clindamycin for *Plasmodium falciparum* Infections in African children". *J. Infect. Dis.* **2004**, *189*, 901-908.

Borrmann, S.; Issifou, S.; Esser, G.; Adegnika, A. A.; Ramharter, M. et al. "Fosmidomycin-clindamycin for the treatment of *Plasmodium falciparum* malaria". *J. Infect. Dis.* **2004**, *190*, 1534-1540.

Boucher, Y.; Doolittle, W. F. "The role of lateral gene transfer in the evolution of isoprenoid biosynthesis pathways". *Mol. Microbiol.* **2000**, *37*, 703-716.

Bradford, M. M. "A rapid and sensitive method for the quantitation of microgram quantities of protein utilizing the principle of protein-dye binding". *Anal. Biochem.* **1976**, *72,248-254.*

Broers, S. T. J.; Eidgenossische Technische Hochschule: Zurich, 1994.

Campos, N.; Rodríguez-Concepción, M.; Seemann, M.; Rohmer, M.; Boronat, A. "Identification of gcpE as a novel gene of the 2-C-methyl-D-erythritol 4-phosphate pathway for isoprenoid biosynthesis in *Escherichia coli*". *FEBS Lett.* **2001**, *488*, 170-173.

Cane, D. E.; Chow, C.; Lillo, A.; Kang, I. "Molecular cloning, expression and characterization of the first three genes in the mevalonate-independent isoprenoid pathway in *Streptomyces coelicolor*". *Bioorg. Med. Chem.* **2001**, *9*, 1467-1477.

Chappell, J. "Biochemistry and molecular biology of the isoprenoid biosynthetic pathway in plants". *Annu. Rev. Plant Physiol. Plant Mol. Biol.* **1995**, *46*, 521-527.

Croteau, R. K., T.M.; Lewis, N.G. Natural Products (Secondary Metabolites). *Biochemistry & Molecular Biology of Plants*; American Society of Plant Physiologists, 2000; pp 1250-1268.

Cunningham, F. X., Jr.; Lafond, T. P.; Gantt, E. "Evidence of a role for LytB in the nonmevalonate pathway of isoprenoid biosynthesis". *J. Bacteriol.* **2000**, *182*, 5841-5848.

Dewick, P. M. "The biosynthesis of C5-C25 terpenoid compounds". *Nat. Prod. Rep.* **1997**, *14*, 111-144.

Dewick, P. M. "The biosynthesis of C5-C25 terpenoid compounds". *Nat.Prod. Rep.* **1999**, *19*, 97-130.

Disch, A.; Schwender, J.; Müller, C.; Lichtenthaler, H. K.; M., R. "Distribution of the mevalonate and glyceraldehyde phosphate/pyruvate pathways for isoprenoid biosynthesis in unicellular algae and the cyanobacterium *Synechocystis* PCC 6714". *Biochem. J.* **1998**, *333*, 381-388.

Drewke, C.; Leistner, E. "Biosynthesis of vitamin B6 and structurally related derivatives". *Vitam. Horm.* **2001**, *61*, 121-155.

D'Souza V, M.; Holz, R. C. "The methionyl aminopeptidase from *Escherichia coli* can function as an iron(II) enzyme". *Biochemistry* **1999**, *38*, 11079-11085.

Dumas, R.; Butikofer, M. C.; Job, D.; Douce, R. "Evidence for two catalytically different magnesium-binding sites in acetohydroxy acid isomeroreductase by site-directed mutagenesis". *Biochemistry* **1995**, *34*, 6026-6036.

Duvold, T. B., J. M.; Pale-Grodemange, C.; Rhomer, M. "Biosynthesis of 2-C-methyl-D-erythritol, a putative C-5 intermediate in the mevalonate independent pathway for isoprenoid biosynthesis". *Tetrahedron Lett.* **1997**, *38*, 4769-4772.

Duvold, T. C., P.; Bravo, J. M.; Rhomer, M. "Incorporation of 2-C-methyl-D-erythritol, a putative C-5 intermediate precursor in the mevalonate-independent pathway, into ubiquinone and menaquinone of *Escherichia coli*". *Tetrahedron Lett.* **1997**, *38*, 6181-6184.

Eisenreich, W.; Schwarz, M.; Cartayrade, A.; Arigoni, D.; Zenk, M. H. et al. "The deoxyxylulose phosphate pathway of terpenoid biosynthesis in plants and microorganisms". *Chem. Biol.* **1998**, *5*, R221-233.

Eubanks, L. M.; Poulter, C. D. "Rhodobacter capsulatus 1-deoxy-D-xylulose 5-phosphate synthase: steady-state kinetics and substrate binding". *Biochemistry* **2003**, *42*, 1140-1149.

Fellermeier, M.; Bacher, A.; Zenk, M. H.; Maier, U.; Kis, K. et al. "Cell-free conversion of 1-deoxy-D-xylulose 5-phosphate and 2-*C*-methyl-D-erythritol 4-phosphate into beta-carotene in higher plants and its inhibition by fosmidomycin." *Tetrahedron Lett.* **1999**, *40*, 2743-2746.

Fellermeier, M.; Raschke, M.; Sagner, S.; Wungsintaweekul, J.; Schuhr, C. A. et al. "Studies on the nonmevalonate pathway of terpene biosynthesis. The role of 2*C*-methyl-D-erythritol 2,4-cyclodiphosphate in plants". *Eur. J. Biochem.* **2001**, *268*, 6302-6310.

Frausto da Silva, J. J. R. W., R. J. P. *The Biological Chemistry of the Elements. The inorganic Chemistry of Life*; Claredon Press: Oxford, U. K., 1991; 379.

Gardner, M. J.; Hall, N.; Fung, E.; White, O.; Berriman, M. et al. "Genome sequence of the human malaria parasite *Plasmodium falciparum*". *Nature* **2002**, *419*, 498-511.

Goldstein, J. L.; Brown, M. S. "Regulation of the mevalonate pathway". *Nature* **1990**, *343*, 425-430.

Gottlin, E. B.; Benson, R. E.; Conary, S.; Antonio, B.; Duke, K. et al. "High-throughput screen for inhibitors of 1-deoxy-d-xylulose 5-phosphate reductoisomerase by surrogate ligand competition". *J. Biomol. Screen* **2003**, *8*, 332-339.

Grolle, S.; Bringer-Meyer, S.; Sahm, H. "Isolation of the dxr gene of *Zymomonas mobilis* and characterization of the 1-deoxy-D-xylulose 5-phosphate reductoisomerase". *FEMS Microbiol. Lett.* **2000**, *191*, 131-137.

Hahn, F. M.; Eubanks, L. M.; Testa, C. A.; Blagg, B. S.; Baker, J. A. et al. "1-Deoxy-D-xylulose 5-phosphate synthase, the gene product of open reading frame (ORF) 2816 and ORF 2895 in *Rhodobacter capsulatus*". *J. Bacteriol.* **2001**, *183*, 1-11.

Hecht, S.; Eisenreich, W.; Adam, P.; Amslinger, S.; Kis, K. et al. "Studies on the nonmevalonate pathway to terpenes: the role of the GcpE (IspG) protein". *Proc. Natl. Acad. Sci. U S A* **2001**, *98*, 14837-14842.

Hemmerlin, A.; Hoeffler, J. F.; Meyer, O.; Tritsch, D.; Kagan, I. A. et al. "Cross-talk between the cytosolic mevalonate and the plastidial methylerythritol phosphate pathways in tobacco bright yellow-2 cells". *J. Biol. Chem.* **2003**, *278*, 26666-26676.

Herz, S.; Wungsintaweekul, J.; Schuhr, C. A.; Hecht, S.; Luttgen, H. et al. "Biosynthesis of terpenoids: YgbB protein converts 4-diphosphocytidyl-2*C*-methyl-D-erythritol 2-phosphate to 2*C*-methyl-D-erythritol 2,4-cyclodiphosphate". *Proc. Natl. Acad. Sci. U S A* **2000**, *97*, 2486-2490.

Hill, R. E.; Himmeldirk, K.; Kennedy, I. A.; Pauloski, R. M.; Sayer, B. G. et al. "The biogenetic anatomy of vitamin B6. A 13C NMR investigation of the biosynthesis of pyridoxol in *Escherichia coli*". *J. Biol. Chem.* **1996**, *271*, 30426-30435.

Hintz, M.; Reichenberg, A.; Altincicek, B.; Bahr, U.; Gschwind, R. M. et al. "Identification of (E)-4-hydroxy-3-methyl-but-2-enyl pyrophosphate as a major activator for human gammadelta T cells in Escherichia coli". *FEBS Lett.* **2001**, *509*, 317-322.

Hoeffler, J. F.; Tritsch, D.; Grosdemange-Billiard, C.; Rohmer, M. "Isoprenoid biosynthesis via the methylerythritol phosphate pathway. Mechanistic investigations of the 1-deoxy-D-xylulose 5-phosphate reductoisomerase". *Eur. J. Biochem.* **2002**, *269*, 4446-4457.

Jomaa, H.; Wiesner, J.; Sanderbrand, S.; Altincicek, B.; Weidemeyer, C. et al. "Inhibitors of the nonmevalonate pathway of isoprenoid biosynthesis as antimalarial drugs". *Science* **1999**, *285*, 1573-1576.

Kawasaki, T.; Kuzuyama, T.; Furihata, K.; Itoh, N.; Seto, H. et al. "A relationship between the mevalonate pathway and isoprenoid production in actinomycetes". *J. Antibiotic.* **2003**, *56*, 957-966.

Kim, D.; Filtz, M. R.; Proteau, P. J. "The methylerythritol phosphate pathway contributes to carotenoid but not phytol biosynthesis in *Euglena gracilis*". *J Nat Prod* **2004**, *67*, 1067-1069.

Klayman, D. L. "Qinghaosu (artemisinin): an antimalarial drug from China". *Science* **1985**, *228*, 1049-1055.

Kleinig, H. "The role of plastids in isoprenoid biosynthesis". *Annu. Rev. Plant Physiol. Plant Mol. Biol.* **1989**, *40*, 39-59.

Köhler, S.; Delwiche, C. F.; Denny, P. W.; Tilney, L. G.; Webster, P. et al. "A plastid of probable green algal origin in Apicomplexan parasites". *Science* **1997**, *275*, 1485-1489.

Kojo, H.; Shigi, Y.; Nishida, M. "FR-31564, a new phosphonic acid antibiotic: bacterial resistance and membrane permeability". *J. Antibiotic.* **1980**, *33*, 44-48.

Koppisch, A. T.; Fox, D. T.; Blagg, B. S.; Poulter, C. D. "*E. coli* MEP synthase: steady-state kinetic analysis and substrate binding". *Biochemistry* **2002**, *41*, 236-243.

Kuemmerle, H. P.; Murakawa, T.; Sakamoto, H.; Sato, N.; Konishi, T. et al. "Fosmidomycin, a new phosphonic acid antibiotic. Part II: 1. Human pharmacokinetics. 2. Preliminary early phase IIa clinical studies". *Int. J. Clin. Pharmacol. Ther. Toxicol.* **1985**, *23*, 521-528.

Kuemmerle, H. P.; Murakawa, T.; Soneoka, K.; Konishi, T. "Fosmidomycin: a new phosphonic acid antibiotic. Part I: Phase I tolerance studies". *Int. J. Clin. Pharmacol. Ther. Toxicol.* **1985**, *23*, 515-520.

Kuntz, L. T., D.; Grosdemange-Billiard, C.; Hemmerlin, A.; Willem, A.; Bach, T. J.; Rohmer, M. "Isoprenoid biosynthesis as target for antibacterial and antiparasitic drugs: phosphonohydroxamic acids as inhibitors of deoxyxylulose phosphate reducto-isomerase". *Biochem. J.* **2005**, *386*, 127-135.

Kuroda, Y.; Okuhara, M.; Goto, T.; Okamoto, M.; Terano, H. et al. "Studies on new phosphonic acid antibiotics. IV. Structure determination of FR-33289, FR-31564 and FR-32863". *J. Antibiotic.* **1980**, *33*, 29-35.

Kurz, T. G., D.; Wackendorff "Carboxilic acid analogues of fosmidomycin". *Z. Naturforsch.* **2003**, *58b*, 457-461.

Kurz, T. G., D.; Wackendorff "Hydroxyurea analogues of fosmidomycin". *Z. Naturforsch.* **2003**, *58b*, 106-110.

Kuzuyama, T. "Mevalonate and nonmevalonate pathways for the biosynthesis of isoprene units". *Biosci. Biotechnol. Biochem.* **2002**, *66*, 1619-1627.

Kuzuyama, T.; Seto, H. "Diversity of the biosynthesis of the isoprene units". *Nat. Prod. Rep.* **2003**, *20*, 171-183.

Kuzuyama, T.; Seto, H.; Takahashi, S.; Shimizu, T. "Fosmidomycin, a specific inhibitor of 1-deoxy-D-xylulose 5-phosphate reductoisomerase in the nonmevalonate pathway for terpenoid biosynthesis." *Tetrahedron Lett.* **1998**, *39*, 7913-7916.

Kuzuyama, T.; Seto, H.; Takahashi, S.; Shimizu, T. "Fosmidomycin, a specific inhibitor of 1-deoxy-D-xylulose 5-phosphate reductoisomerase in the nonmevalonate pathway for terpenoid biosynthesis." *Tetrahedron Lett.* **1998**, *39*, 7913-7916.

Kuzuyama, T.; Takahashi, S.; Seto, H. "Construction and characterization of *Escherichia coli* disruptants defective in the yaeM gene". *Biosci. Biotechnol. Biochem.* **1999**, *63*, 776-778.

Kuzuyama, T.; Takahashi, S.; Takagi, M.; Seto, H. "Characterization of 1-deoxy-D-xylulose 5-phosphate reductoisomerase, an enzyme involved in isopentenyl diphosphate biosynthesis, and identification of its catalytic amino acid residues". *J. Biol. Chem.* **2000**, *275*, 19928-19932.

Laber, B.; Maurer, W.; Scharf, S.; Stepusin, K.; Schmidt, F. S. "Vitamin B6 biosynthesis: formation of pyridoxine 5'-phosphate from 4-(phosphohydroxy)-L-threonine and 1-deoxy-D-xylulose-5-phosphate by PdxA and PdxJ protein". *FEBS Lett.* **1999**, *449*, 45-48.

Laemmli, U. K. "Cleavage of structural proteins during the assembly of the head of bacteriophage T4". *Nature* **1970**, *227*, 680-685

Lange, B. M.; Croteau, R. "Isoprenoid biosynthesis via a mevalonate-independent pathway in plants: cloning and heterologous expression of 1-deoxy-D-xylulose-5-phosphate reductoisomerase from peppermint". *Arch. Biochem. Biophys.* **1999**, *365*, 170-174.

Lange, B. M.; Rujan, T.; Martin, W.; Croteau, R. "Isoprenoid biosynthesis: the evolution of two ancient and distinct pathways across genomes". *Proc. Natl. Acad. Sci. U S A* **2000**, *97*, 13172-13177.

Lange, B. M.; Wildung, M. R.; McCaskill, D.; Croteau, R. "A family of transketolases that directs isoprenoid biosynthesis via a mevalonate-independent pathway". *Proc. Natl. Acad. Sci. U S A* **1998**, *95*, 2100-2104.

Laule, O.; Fürholz, A.; Chang, H. S.; Zhu, T.; Wang, X. et al. "Crosstalk between cytosolic and plastidial pathways of isoprenoid biosynthesis in Arabidopsis thaliana". *Proc. Natl. Acad. Sci. U S A* **2003**, *100*, 6866-6871.

Lell, B.; Ruangweerayut, R.; Wiesner, J.; Missinou, M. A.; Schindler, A. et al. "Fosmidomycin, a novel chemotherapeutic agent for malaria". *Antimicrob. Agents Chemother.* **2003**, *47*, 735-738.

Lichtenthaler, H. K. "Non-mevalonate isoprenoid biosynthesis: enzymes, genes and inhibitors". *Biochem. Soc. Trans.* **2000**, *28*, 785-789.

Lichtenthaler, H. K.; Schwender, J.; Disch, A.; Rohmer, M. "Biosynthesis of isoprenoids in higher plant chloroplasts proceeds via a mevalonate-independent pathway". *FEBS Lett.* **1997**, *400*, 271-274.

Lichtenthaler, H. K.; Zeidler, J.; Schwender, J.; Müller, C. "The non-mevalonate isoprenoid biosynthesis of plants as a test system for new herbicides and drugs against pathogenic bacteria and the malaria parasite". *Z Naturforsch. [C]* **2000**, *55*, 305-313.

Lois, L. M.; Campos, N.; Putra, S. R.; Danielsen, K.; Rohmer, M. et al. "Cloning and characterization of a gene from Escherichia coli encoding a transketolase-like enzyme that catalyzes the synthesis of D-1-deoxyxylulose 5-phosphate, a common precursor for isoprenoid, thiamine, and pyridoxal biosynthesis". *Proc. Natl. Acad. Sci. U S A* **1998**, *95*, 2105-2110.

Lutke-Brinkhaus, F. K., H. "Formation of isopentenyl diphosphate via mevalonate does not occur within etioplasts and etiochloroplasts of mustard (*Sinapis alba* L.) seedlings". *Planta* **1987**, *171*, 406-411.

Lüttgen, H.; Rohdich, F.; Herz, S.; Wungsintaweekul, J.; Hecht, S. et al. "Biosynthesis of terpenoids: YchB protein of Escherichia coli phosphorylates the 2-hydroxy group of 4-diphosphocytidyl-2*C*-methyl-D-erythritol". *Proc. Natl. Acad. Sci. U S A* **2000**, *97*, 1062-1067.

Mac Sweeney, A.; Lange, R.; Fernandes, R. P. M.; Schulz, H.; Dale, G. E. et al. "The Crystal Structure of *E. coli* 1-Deoxy-d-xylulose-5-phosphate Reductoisomerase in a Ternary Complex with the Antimalarial Compound Fosmidomycin and NADPH Reveals a Tight-binding Closed Enzyme Conformation". *J. Mol. Biol.* **2005**, *345*, 115-127.

Maertens, J. A. "History of the development of azole derivatives". *Clin. Microbiol. Infect.* **2004**, *10*, 1-10.

Martin, J. B.; Doty, D. "Determination of inorganic phopshate". *Anal. Chem.* **1949**, *21*, 965-967.

Martin, M. B.; Sanders, J. M.; Kendrick, H.; de Luca-Fradley, K.; Lewis, J. C. et al. "Activity of bisphosphonates against *Trypanosoma brucei rhodesiense*". *J. Med. Chem.* **2002**, *45*, 2904-2914.

McGarvey, D. J.; Croteau, R. "Terpenoid metabolism". *Plant Cell* **1995**, *7*, 1015-1026.

Meyer, O.; Grosdemange-Billiard, C.; Tritsch, D.; Rohmer, M. "Isoprenoid biosynthesis via the MEP pathway. Synthesis of (3,4)-3,4-dihydroxy-5-oxohexylphosphonic acid, an isosteric analogue of 1-deoxy-D-xylulose 5-phosphate, the substrate of the 1-deoxy-D-xylulose 5-phosphate reducto-isomerase". *Org Biomol. Chem.* **2003**, *1*, 4367-4372.

Miallau, L.; Alphey, M. S.; Kemp, L. E.; Leonard, G. A.; McSweeney, S. M. et al. "Biosynthesis of isoprenoids: crystal structure of 4-diphosphocytidyl-2*C*-methyl-D-erythritol kinase". *Proc. Natl. Acad. Sci. U S A* **2003**, *100*, 9173-9178.

Miller, B.; Heuser, T.; Zimmer, W. "Functional involvement of a deoxy-D-xylulose 5-phosphate reductoisomerase gene harboring locus of Synechococcus leopoliensis in isoprenoid biosynthesis". *FEBS Lett.* **2000**, *481*, 221-226.

Miller, B.; Oschinski, C.; Zimmer, W. "First isolation of an isoprene synthase gene from poplar and successful expression of the gene in *Escherichia* coli". *Planta* **2001**, *213*, 483-487.

Mine, Y.; Kamimura, T.; Nonoyama, S.; Nishida, M.; Goto, S. et al. "In vitro and in vivo antibacterial activities of FR-31564, a new phosphonic acid antibiotic". *J. Antibiotic.* **1980**, *33*, 36-43.

Missinou, M. A.; Borrmann, S.; Schindler, A.; Issifou, S.; Adegnika, A. A. et al. "Fosmidomycin for malaria". *Lancet* **2002**, *360*, 1941-1942.

Morrison, J. F. W., C. T. "The behavior and significance of slow-binding enzyme inhibitors". *Adv. Enzymol. Relat. Areas Mol. Biol.* **1988**, *61*, 201-301.

Mueller, C.; Schwender, J.; Zeidler, J.; K., L. H. "Properties and inhibition of the first two enzymes of the non-mevalonate pathway of isoprenoid biosynthesis". *Biochem. Soc. Trans.* **2000**, *28*, 792-793.

Nagata, N.; Suzuki, M.; Yoshida, S.; Muranaka, T. "Mevalonic acid partially restores chloroplast and etioplast development in *Arabidopsis* lacking the non-mevalonate pathway". *Planta* **2002**, *216*, 345-350.

Neu, H. C.; Kamimura, T. "In vitro and in vivo antibacterial activity of FR-31564, a phosphonic acid antimicrobial agent". *Antimicrob Agents Chemother* **1981**, *19*, 1013-1023.

Okuhara, M.; Kuroda, Y.; Goto, T.; Okamoto, M.; Terano, H. et al. "Studies on new phosphonic acid antibiotics. III. Isolation and characterization of FR-31564, FR-32863 and FR-33289". *J. Antibiotic.* **1980**, *33*, 24-28.

Palmer, J. D.; Delwiche, C. F. "Second-hand chloroplasts and the case of the disappearing nucleus". *Proc. Natl. Acad. Sci. U S A* **1996**, *93*, 7432-7435.

Phaosiri, C.; Proteau, P. J. "Substrate analogs for the investigation of deoxyxylulose 5-phosphate reductoisomerase inhibition: synthesis and evaluation". *Bioorg. Med. Chem. Lett* **2004**, *14*, 5309-5312.

Proteau, P. J. "1-Deoxy-d-xylulose 5-phosphate reductoisomerase: an overview". *Bioorg. Chem.* **2004**, *32*, 483-493.

Proteau, P. J.; Woo, Y. H.; Williamson, R. T.; C, P. "Stereochemistry of the reduction step mediated by recombinant 1-deoxy-D-xylulose 5-phosphate isomeroreductase". *Org. Lett.* **1999**, *1*, 921-923.

Putra, S. R.; Disch, A.; Bravo, J. M.; M., R. "Distribution of mevalonate and glyceraldehyde 3-phosphate/pyruvate routes for isoprenoid biosynthesis in some gram-negative bacteria and mycobacteria". *FEMS Microbiol. Lett.* **1998**, *164*, 169-175.

Radykewicz, T.; Rohdich, F.; Wungsintaweekul, J.; Herz, S.; Kis, K. et al. "Biosynthesis of terpenoids: 1-deoxy-D-xylulose-5-phosphate reductoisomerase from *Escherichia coli* is a class B dehydrogenase". *FEBS Lett.* **2000**, *465*, 157-160.

Ramos-Valdivia, A. C.; van der Heijden, R.; Verpoorte, R. "Isopentenyl diphosphate isomerase: a core enzyme in isoprenoid biosynthesis. A review of its biochemistry and function". *Nat. Prod. Rep.* **1997**, *14*, 591-603.

Reuter, K.; Sanderbrand, S.; Jomaa, H.; Wiesner, J.; Steinbrecher, I. et al. "Crystal structure of 1-deoxy-D-xylulose-5-phosphate reductoisomerase, a crucial enzyme in the non-mevalonate pathway of isoprenoid biosynthesis". *J. Biol. Chem.* **2002**, *277*, 5378-5384.

Ricagno, S.; Grolle, S.; Bringer-Meyer, S.; Sahm, H.; Lindqvist, Y. et al. "Crystal structure of 1-deoxy-d-xylulose-5-phosphate reductoisomerase from *Zymomonas mobilis* at 1.9-A resolution". *Biochim Biophys Acta* **2004**, *1698*, 37-44.

Richard, S. B.; Bowman, M. E.; Kwiatkowski, W.; Kang, I.; Chow, C. et al. "Structure of 4-diphosphocytidyl-2-C- methylerythritol synthetase involved in mevalonate-independent isoprenoid biosynthesis". *Nat Struct Biol* **2001**, *8*, 641-648.

Rodríguez-Concepción, M.; Ahumada, I.; Diez-Juez, E.; Sauret-Güeto, S.; Lois, L. M. et al. "1-Deoxy-D-xylulose 5-phosphate reductoisomerase and plastid isoprenoid biosynthesis during tomato fruit ripening". *Plant J.* **2001**, *27*, 213-222.

Rodríguez-Concepción, M.; Boronat, A. "Elucidation of the methylerythritol phosphate pathway for isoprenoid biosynthesis in bacteria and plastids. A metabolic milestone achieved through genomics". *Plant Physiol.* **2002**, *130*, 1079-1089.

Rohdich, F.; Bacher, A.; Eisenreich, W. "Perspectives in anti-infective drug design. The late steps in the biosynthesis of the universal terpenoid precursors, isopentenyl diphosphate and dimethylallyl diphosphate". *Bioorg. Chem.* **2004**, *32*, 292-308.

Rohdich, F.; Hecht, S.; Gärtner, K.; Adam, P.; Krieger, C. et al. "Studies on the nonmevalonate terpene biosynthetic pathway: metabolic role of IspH (LytB) protein". *Proc. Natl. Acad. Sci. U S A* **2002**, *99*, 1158-1163.

Rohdich, F.; Kis, K.; Bacher, A.; Eisenreich, W. "The non-mevalonate pathway of isoprenoids: genes, enzymes and intermediates". *Curr. Opin. Chem. Biol.* **2001**, *5*, 535-540.

Rohdich, F.; Wungsintaweekul, J.; Eisenreich, W.; Richter, G.; Schuhr, C. A. et al. "Biosynthesis of terpenoids: 4-diphosphocytidyl-2C-methyl-D-erythritol synthase of *Arabidopsis thaliana*". *Proc. Natl. Acad. Sci. U S A* **2000**, *97*, 6451-6456.

Rohdich, F.; Wungsintaweekul, J.; Fellermeier, M.; Sagner, S.; Herz, S. et al. "Cytidine 5'-triphosphate-dependent biosynthesis of isoprenoids: YgbP protein of Escherichia coli catalyzes the formation of 4-diphosphocytidyl-2-C-methylerythritol". *Proc. Natl. Acad. Sci. U S A* **1999**, *96*, 11758-11763.

Rohdich, F.; Wungsintaweekul, J.; Luttgen, H.; Fischer, M.; Eisenreich, W. et al. "Biosynthesis of terpenoids: 4-diphosphocytidyl-2-C-methyl-D-erythritol kinase from tomato". *Proc. Natl. Acad. Sci. U S A* **2000**, *97*, 8251-8256.

Rohdich, F.; Zepeck, F.; Adam, P.; Hecht, S.; Kaiser, J. et al. "The deoxyxylulose phosphate pathway of isoprenoid biosynthesis: studies on the mechanisms of the reactions catalyzed by IspG and IspH protein". *Proc. Natl. Acad. Sci. U S A* **2003**, *100*, 1586-1591.

Rohmer, M. "The discovery of a mevalonate-independent pathway for isoprenoid biosynthesis in bacteria, algae and higher plants". *Nat. Pro. Rep.* **1999**, *16*, 565-574.

Rohmer, M. S., M.; Horbach, S.; Bringer-Meyer, S.; Sahm, H. "Glyceraldehyde 3-phosphate and pyruvate as precursors of isoprenic units in an alternative non-mevalonate pathway for terpenoid biosynthesis". *J. Am.Chem. Soc.* **1996**, *118*, 2564-2566.

Rohmer, M.; Grosdemange-Billiard, C.; Seemann, M.; Tritsch, D. "Isoprenoid biosynthesis as a novel target for antibacterial and antiparasitic drugs". *Curr Opin Investig Drugs* **2004**, *5*, 154-162.

Rohmer, M.; Knani, M.; Simonin, P.; Sutter, B.; Sahm, H. "Isoprenoid biosynthesis in bacteria: a novel pathway for the early steps leading to isopentenyl diphosphate". *Biochem. J.* **1993**, *295*, 517-524.

Sacchettini, J. C.; Poulter, C. D. "Creating isoprenoid diversity". *Science* **1997**, *277*, 1788-1789.

Sakamoto, Y.; Furukawa, S.; Ogihara, H.; Yamasaki, M. "Fosmidomycin resistance in adenylate cyclase deficient (cya) mutants of *Escherichia coli*". *Biosci. Biotechnol. Biochem.* **2003**, *67*, 2030-2033.

Sambrook, J. R., D. *Molecular cloning A laboratory manual 3 ed*; Cold Spring Harbor Laboratory Press, 2001.

Sauret-Güeto, S.; Ramos-Valdivia, A.; Ibáñez, E.; Boronat, A.; Rodríguez-Concepción, M. "Identification of lethal mutations in *Escherichia coli* genes encoding enzymes of the methylerythritol phosphate pathway". *Biochem. Biophys. Res. Commun.* **2003**, *307*, 408-415.

Schurmann, M. S., M.; Sprenger, G. A. "Fructose 6-phosphate aldolase and 1-deoxy-D-xylulose 5-phosphate synthase from Escherichia coli as tolls in enzymatic synthesis of 1-deoxysugars". *Journal of molecular catalysis B: Enzymatic* **2002**, *19-20*, 247.252.

Schwarz, M. A., D. Ginkgolide biosynthesis. *Comprehensive Natural Products Chemistry: Isoprenoids including carotenoids and steroids*; Elsevier: Amsterdan, 1999; pp 367-401.

Schwender, J.; Seemann, M.; Lichtenthaler, H. K.; Rohmer, M. "Biosynthesis of isoprenoids (carotenoids, sterols, prenyl side-chains of chlorophylls and plastoquinone) via a novel pyruvate/glyceraldehyde 3-phosphate non-mevalonate pathway in the green alga *Scenedesmus obliquus*". *Biochem. J.* **1996**, *316*, 73-80.

Schwender, J.; Zeidler, J.; Gröner, R.; Müller, C.; Focke, M. et al. "Incorporation of 1-deoxy-D-xylulose into isoprene and phytol by higher plants and algae". *FEBS Lett.* **1997**, *414*, 129-134.

Seemann, M.; Bui, B. T.; Wolff, M.; Tritsch, D.; Campos, N. et al. "Isoprenoid biosynthesis through the methylerythritol phosphate pathway: the (E)-4-hydroxy-3-methylbut-2-enyl diphosphate synthase (GcpE) is a [4Fe-4S] protein". *Angew. Chem. In.t Ed. Engl.l* **2002**, *41*, 4337-4339.

Segel, I. H. *Enzyme Kinetics*; Wiley-Interscience, 1975; 957.

Shigi, Y. "Inhibition of bacterial isoprenoid synthesis by fosmidomycin, a phosphonic acid-containing antibiotic". *J. Antimicrob. Chemother.* **1989**, *24*, 131-145.

Silver, G. M.; Fall, R. "Characterization of aspen isoprene synthase, an enzyme responsible for leaf isoprene emission to the atmosphere." *J. Biol. Chem.* **1995**, *270*, 13010-13016.

Silver, G. M.; Fall, R. "Enzymatic synthesis of isoprene from dimethylallyl diphosphate in Aspen leaf extracts." *Plant Physiol.* **1991**, *97*, 1588-1591.

Slater, E. E.; MacDonald, J. S. "Mechanism of action and biological profile of HMG CoA reductase inhibitors. A new therapeutic alternative". *Drugs* **1988**, *36*, 72-82.

Smit, A.; Mushegian, A. "Biosynthesis of isoprenoids via mevalonate in Archaea: the lost pathway". *Genome Res.* **2000**, *10(*1468-1484.

Sprenger, G. A.; Schörken, U.; Wiegert, T.; Grolle, S.; de Graaf, A. A. et al. "Identification of a thiamine-dependent synthase in *Escherichia coli* required for the formation of the 1-deoxy-D-xylulose 5-phosphate precursor to isoprenoids, thiamine, and pyridoxal". *Proc. Natl. Acad. Sci. U S A* **1997**, *94*, 12857-12862.

Steinbacher, S.; Kaiser, J.; Eisenreich, W.; Huber, R.; Bacher, A. et al. "Structural basis of fosmidomycin action revealed by the complex with 2-*C*-methyl-D-erythritol 4-phosphate synthase (IspC). Implications for the catalytic mechanism and anti-malaria drug development". *J. Biol. Chem.* **2003**, *278*, 18401-18407.

Szabo, C. M.; Matsumura, Y.; Fukura, S.; Martin, M. B.; Sanders, J. M. et al. "Inhibition of geranylgeranyl diphosphate synthase by bisphosphonates and diphosphates: a potential route to new bone antiresorption and antiparasitic agents". *J Med Chem* **2002**, *45*, 2185-2196.

Takahashi, S.; Kuzuyama, T.; Watanabe, H.; Seto, H. "A 1-deoxy-D-xylulose 5-phosphate reductoisomerase catalyzing the formation of 2-*C*-methyl-D-erythritol 4-phosphate in an alternative nonmevalonate pathway for terpenoid biosynthesis". *Proc. Natl. Acad. Sci. U S A* **1998**, *95*, 9879-9884.

Taylor, S. D. V., L. D.; Begley, T. P.; Schorken, U.; Grolle, S.; Sprenger, G. A.; Bringer-Meyer, S.; Sahm, H. J. "Chemical and enzymatic synthesis of 1-deoxy-D-xylulose-5-phosphate". *J. Org. Chem.* **1998**, *63*, 2375-2377.

Teige, M.; Melzer, M.; Süss, K. H. "Purification, properties and in situ localization of the amphibolic enzymes D-ribulose 5-phosphate 3-epimerase and transketolase from spinach chloroplasts". *Eur. J. Biochem.* **1998**, *252*, 237-244.

Testa, C. A.; Brown, M. J. "The methylerythritol phosphate pathway and its significance as a novel drug target". *Curr. Pharm. Biotechnol.* **2003**, *4*, 248-259.

Vyas, D. M.; Kadow, J. F. "Paclitaxel: a unique tubulin interacting anticancer agent". *Prog. Med. Chem.* **1995**, *32*.

Wellems, T. E. "*Plasmodium* chloroquine resistance and the search for a replacement antimalarial drug". *Science* **2002**, *298*, 124-126.

White, R. J.; Margolis, P. S.; Trias, J.; Yuan, Z. "Targeting metalloenzymes: a strategy that works". *Curr Opin Pharmacol* **2003**, *3*, 502-507.
Wiesner, J.; Borrmann, S.; Jomaa, H. "Fosmidomycin for the treatment of malaria". *Parasitol. Res.* **2003**, *90*, S71-76.

Wiesner, J.; Henschker, D.; Hutchinson, D. B.; Beck, E.; Jomaa, H. "In vitro and in vivo synergy of fosmidomycin, a novel antimalarial drug, with clindamycin". *Antimicrob. Agents Chemother.* **2002**, *46*, 2889-2894.

Wiesner, J.; Hintz, M.; Altincicek, B.; Sanderbrand, S.; Weidemeyer, C. et al. "Plasmodium falciparum: detection of the deoxyxylulose 5-phosphate reductoisomerase activity". *Exp. Parasitol.* **2000**, *96*, 182-186.

Wilhelm, M.; Kunzmann, V.; Eckstein, S.; Reimer, P.; Weissinger, F. et al. "Gammadelta T cells for immune therapy of patients with lymphoid malignancies". *Blood* **2003**, *102*, 200-206.

Wolff, M.; Seemann, M.; Tse Sum Bui, B.; Frapart, Y.; Tritsch, D. et al. "Isoprenoid biosynthesis via the methylerythritol phosphate pathway: the (E)-4-hydroxy-3-methylbut-2-enyl diphosphate reductase (LytB/IspH) from Escherichia coli is a [4Fe-4S] protein". *FEBS Lett.*. **2003**, *541*, 115-120.

Wong, A.; Munos, J. W.; Devasthali, V.; Johnson, K. A.; Liu , H. W. "Study of 1-deoxy-D-xylulose-5-phosphate reductoisomerase: synthesis and evaluation of fluorinated substrate analogues". *Org. Lett.* **2004**, *6*, 3625-3628.

Woo, Y.-H. Studies of Non-Mevalonate isoprenoid Biosynthesis: The 1-Deoxy-D-xylulose-5-phosphate isomeroreductase (DXR) mediated reaction. In *Pharmacy*; Oregon state University: Corvallis, 2002; pp 140.

Yajima, S.; Hara, K.; Sanders, J. M.; Yin, F.; Ohsawa, K. et al. "Crystallographic structures of two bisphosphonate:1-deoxyxylulose-5-phosphate reductoisomerase complexes". *J. Am. Chem. Soc.* **2004**, *126*, 10824-10825.

Yin, X.; Proteau, P. J. "Characterization of native and histidine-tagged deoxyxylulose 5-phosphate reductoisomerase from the cyanobacterium *Synechocystis sp.* PCC6803". *Biochim. Biophys. Acta* **2003**, *1652*, 75-81.

Zhou, D.; White, R. H. "Early steps of isoprenoid biosynthesis in *Escherichia coli*". *Biochem. J.* **1991**, *273*, 627-634.

Zimmermann, F. T. S., A.; Schorken, U.; Sprenger, G. A.; Fessner, WD. "Efficient multi-enzymatic synhtesis of D-xylulose 5-phosphate". Tetrahedron: Asymmetry 1999, 10, 1643-1646.